MOLECULAR ANALYSIS OF THE ROLE OF YEAST MITOCHONDRIAL PROTEIN QCR7P IN *AGROBACTERIUM*-YEAST DNA TRANSFER

YANG QINGHUA

NATIONAL UNIVERSITY OF SINGAPORE

2013

MOLECULAR ANALYSIS OF THE ROLE OF YEAST MITOCHONDRIAL PROTEIN QCR7P IN *AGROBACTERIUM*-YEAST DNA TRANSFER

YANG QINGHUA

(*B. Sc. Biotech., B. Sc. Psychol.*)

A THESIS SUBMITTED

FOR THE DEGREE OF DOCTOR OF PHILOSOPHY

DEPARTMENT OF BIOLOGICAL SCIENCES

NATIONAL UNIVERSITY OF SINGAPORE

2013

Declaration

I hereby declare that this thesis is my original work and it has been written by me in its entirety. I have duly acknowledged all the sources of information which have been used in the thesis. This thesis has also not been submitted for any degree in any university previously.

ACKNOWLEDGEMENTS

I would like to express my sincere gratitude to Associate Professor Pan Shen Quan, my supervisor, for the patient guidance and useful critiques he provided in this research work. I would also like to thank Professor Wong Sek Man, Associate Professor Yu Hao, and Assistant Professor Xu Jian, for their valuable advice and generous assistance in keeping my research progress on track.

My grateful thanks are also extended to Mr. Li Xiaoyang, for the inspiring discussions and productive collaboration we have in the past years. I would also like to thank Ms. Tong Yan, Ms. Xu Songci, and Mr. Liu Xuguo for the important technical supports.

I wish to thank the following NUS Research Fellows who helped me a lot in discussions and techniques: Dr. Tu Haitao, Dr. Niu Shengniao, Dr. Gong Ximing, and Dr. Chu Huangwei. I would also like to extend my thanks to my laboratory members and friends for their help in different ways: Chen Zikai, Lim Zijie, Wang Bingqing, Wang Yanbin, Gao Ruimin, Wen Yi and Guo Song.

Finally, I gratefully acknowledge the financial support provided by National University of Singapore.

TABLE OF CONTENTS

SUMMARY

Agrobacterium tumefaciens has a unique capability to horizontally transfer DNA into host plants as well as non-natural recipients like yeast and fungal cells, which is useful to scientists in transgenic applications. Both the bacterium and host are important for this sophisticated transformation process. The virulence machinery of *A. tumefaciens* facilitating the DNA transfer has been intensively investigated, while the relevant host factors are less well understood. In this study, *Saccharomyces cerevisiae* was employed to investigate how host factors are involved in the process, due to its simplicity for handling and manipulations.

In this thesis, I show that a mitochondrial protein Qcr7p negatively regulates the transformation process. A knockout of Qcr7p in yeast enhanced the efficiency of *Agrobacterium*-mediated transformation. Experimental data show that this was due to an increase in the competency of the yeast to receive both T-DNA and virulence effectors. This implicates a role of mitochondria in the transformation process. Qcr7p may also have a role in the T-DNA integration process. Knocking out Qcr7p resulted in a decrease of non-homologous end joining ratio, suggesting that mitochondria also involves in DNA repair mechanisms of T-DNA integration.

To detect the virulence effectors received by yeast, a novel approach was established to visualize VirE2 molecules in recipient cells. In this study,

Agrobacterium-delivered VirE2 was, for the first time, visualized in both budding yeast *S. cerevisiae* and tobacco *Nicotiana benthamiana*. The data show that *Agrobacterium* is actually an efficient protein transporter besides a genetic engineer. With this new technique, visualization of VirE2 movement was also achieved. It enables molecular dissection of the intracellular trafficking pathway of VirE2 and T-complex as well as an exogenous molecule delivered by *Agrobacterium* biosyringe.

MANUSCRIPTS RELATED TO THIS STUDY

Li, X.[†], **Yang, Q.**[†], Tu, H. and Pan, S. Q. (2013). Direct visualization of *Agrobacterium*-delivered VirE2 in recipient cells (in submission)

[†] Equal contribution

Yang, Q., Tu, H., Li, X., Lim, Z. and Pan, S. Q. (2013). A yeast mitochondrial factor Qcr7p negatively regulates *Agrobacterium*-mediated transformation (in preparation)

LIST OF TABLES

LIST OF FIGURES

LIST OF ABBREVIATIONS

Amp	ampicillin	MCS	multiple cloning sites
AMT	*Agrobacterium*-mediated transformation	MS	Murashige and Skoog medium
AS	acetosyringone	NHEJ	non-homologous end joining
bp	base pair(s)	NLS	nuclear localization signal
BiFC	bimolecular fluorescence complementation	PAGE	polyacrylamide gel electrophoresis
BSA	bovine serum albumin	rpm	revolutions per minute
CFP	cyan fluorescent protein	s	second(s)
DMSO	dimethylsulfoxide	SDS	sodium dodecyl sulfate
g	gram(s)	ssDNA	single-stranded DNA
GFP	green fluorescent protein	T-DNA	transferred DNA
GUS	beta-glucuronidase	T4SS	typ IV secretion system
h	hour(s)	TBST	tris-buffered saline with tween
HR	homologous recombination	Ti	tumor inducing
HRP	horseradish peroxidase	Vir	virulence
kDa	kilodalton(s)	WT	wild type
Km	kanamycin	YFP	yellow fluorescent protein
LiAc	lithium acetate		

Chapter 1. Literature Review

The bacterium *Agrobacterium tumefaciens*, a soil borne phytopathogen, is the causative agent of plant crown gall disease (Smith *et al.* 1907). Under natural conditions, bacteria of the genus *Agrobacterium* are able to transfer a piece of single-strand T-DNA complexed with VirE2 and VirD2 proteins into plant cells and incorporate them into the host cell chromosomes (Alvarez-Martinez *et al.* 2009; Gelvin 2009). *A. tumefaciens* is therefore harmful to plants due to the genetic disturbation but useful to scientists for the same reason. Although plants are the natural hosts for *A. tumefaciens*, this bacterium can also transform a wide range of other eukaryotic species, from fungi to human cells(Lacroix *et al.* 2006). This DNA transfer represents the only known example of inter-kingdom transfer of genetic information (Pelczar *et al.* 2004). Hence, studying the mechanisms of this bacterium on its delivery of T-DNA into the cell is of great significance in the advances of gene engineering and development of gene therapy.

Early efforts have been directed to analyze pathogenic factors during *Agrobacterium* infection. Intensive research revealed a network of a series of virulence proteins which sense the signal from hosts construct a type IV secretary channel and prepare T-DNA strand and its associated translocators. As compared to the relatively clear knowledge on pathogenic factors, host factors are less explored. Only a couple of plant proteins involved in host defense response and the proteasomal degradation pathway has been identified

recently (Tzfira *et al.* 2001; Anand *et al.* 2007; Djamei *et al.* 2007). A major reason for the lagging research is that the plant, by nature, is not an ideal model for genome-wide identification of host factors.

To circumvent the limitation of plant hosts, a high throughput approach of *Agrobacterium*-mediated transformation of the yeast *Sacchromyces cerevisiae* has been established (Soltani *et al.* 2009; Tu 2010). A genome-wide screening study of yeast showed that mitochondria is actively participating in the *Agrobacterium*-yeast DNA transfer process (Tu 2010). However, there is no information about the interactions between mitochondria and DNA trafficking or DNA repair mechanisms, which are both needed for the final integration of foreign DNA into host genome. This study aims at exploring the connections of yeast mitochondrion and the fate of T-DNA.

In the next sections, a brief history of research on *Agrobacterium* will be presented, followed by detailed review of the known mechanisms of *Agrobacterium*-mediated transformation. Known host factors involved in this transformation will be included.

1.1. *Agrobacterium tumefaciens*: From a phytopathogen to a genetic tool

This part reflects several key experiments and discoveries that led to current knowledge and applications of *Agrobacterium*, which helps to determine the historical orientation of this study.

The first report on crown gall disease dates back to 1853, when such disease caused detrimental outcome in horticultural industry in both Europe and America (Galloway 1902). *Agrobacterium vitis* was the first strain identified as the causal agent of crown gall in grape, one of the other plant species kept unknown for one more decade. In 1907, bacterial origin of crown gall disease was confirmed, and designated firstly *Bacterium tumefaciens* (Smith *et al.* 1907), and later *Agrobacterium tumefaciens*. Thereafter, an era of *Agrobacterium* began.

In 1940s and 1950s, *Agrobacterium*-derived tumor-inducing principle (TIP) was proposed (Braun *et al.* 1948), based on the fact that only transient exposure to *A. tumefaciens* is sufficient to cause persisting tumor formation. Later, the finding of the exclusive existence of opines in affected tissues (Lioret 1956) enlightened the idea of a possible genetic nature of this kind of tumorigenesis. Later, attempts were made to isolate DNA contents from crown galls that were of bacteria origin or to employ DNA fractions of *Agrobacterium* to induce tumor formation. Though at that time lacking of modern techniques rendered these attempts non-productive, two important experiments found clues of the possible location of the tumor inducing information. One is the transferable nature of the tumor inducing capability of virulent strains to avirulents strains (Kerr 1969). This transferable nature suggested some sort of conjugal element, *e.g.* a plasmid, could be the information carrier. The other finding is the loss of virulence when culturing

the bacteria at 35 ℃(Hamilton *et al.* 1971), which was consistent with the cases that plasmids could get lost when culturing in an elevated temperature. Zaenen *et al.*, later in 1974, using gradient centrifugation and electron microscopy proved the existence of a large plasmid in *Agrobacterium*, only in virulent strains (Zaenen *et al.* 1974). Vanlareb *et al.*, also confirmed that a large "tumor inducing plasmid" (Ti plasmid) was responsible for the crown galls formation in the same year (Vanlareb.N *et al.* 1974). Refined region for this tumor inducing ability was then reported to be detected in the genome of crown gall tumors by southern blotting, which led to the discovery of transferred DNA, T-DNA (Chilton *et al.* 1977). This discovery became the landmark achievement in the history of *Agrobacterium* study. Since then, a potential application of this plasmid as a vector for genetic engineering tool in higher plant species became apparent (Chilton *et al.* 1977).

Utilization of *Agrobacterium* as a vector for genetic transformation requires several important works to be done. First of all, the tumor inducing information was to be removed from the T-DNA region (Zambryski *et al.* 1983). Second, a separation of *vir* genes and T-DNA region into two independent plasmids was proved possible, which made the editing of T-DNA easily accessible (Hoekema 1983). Finally, the transformed cells should be selectable with appropriate markers. A bacterial gene neomycin phosphotransferase *II* (*nptII*) was driven by the promoter of opine synthesis gene, to serve as the first selection marker (Fraley *et al.* 1983). This chimeric

gene conferred kanamycin resistance in plant cells and their progeny, and did not disrupt the ability of regeneration (Horsch *et al.* 1984), thus proved a suitable marker for transformation purpose. From then on, *Agrobacterium* have dominated the techniques for creating transgenic plants.

The successful utilization of *Agrobacterium* as a genetic vector has spurred the investigations of the mechanism behind this unique trans-kingdom DNA transfer process. The molecular basis of *Agrobacterium*-mediated transformation will be reviewed in detail in next section.

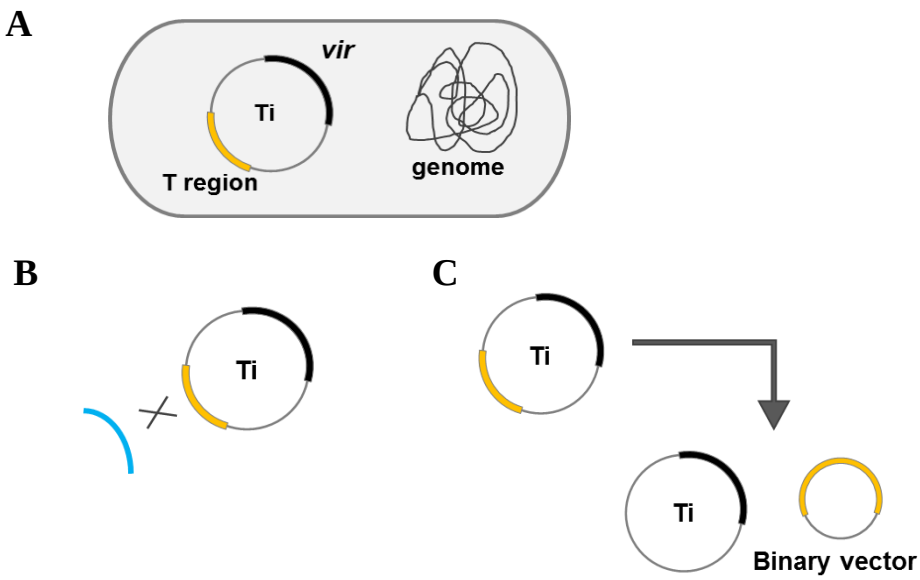

Figure 1. Schematic diagram of Ti plasmid and the modification strategies.

(A) *Agrobacterium* and Ti plasmid, *vir* represents *vir* genes, T region is the transferred DNA sequence. (B) T region can be replaced by other DNA sequence (blue).
(C) T region can be separated from Ti plasmid and carried by a smaller vector, binary vector.

1.2. Molecular basis of *Agrobacterium* mediated transformation

1.2.1. Activation of the *vir* genes and host attachment

vir genes, which are required for *Agrobacterium's* virulence, were identified outside T-DNA region (Klee *et al.* 1983; Stachel *et al.* 1986). The capability of transforming plant tissues to opine factory provides specific food for *Agrobacterium* growth. Albeit beneficial, this process is highly sophisticated and energetically demanding, therefore *vir* genes are under strict regulation. Activation of *vir* genes were reported to occur by culturing with plant cells (Stachel *et al.* 1986), except *virA* and *virG* which are constitutively expressed at basal level and induced in a feed-forward manner (Winans *et al.* 1988)..

virA and *virG* encode a two-component phosphor-replay system, in which VirG acts as intracellular regulator responds to the membrane-bound sensor VirA (Wolanin *et al.* 2002). Upon signal perception, VirA activates VirG through its histidine kinase activity; thereby VirG is phosphorylated and functions as transcription factor. The phosphorylation enables VirG to bind specifically to 12 bp DNA sequences of *vir* gene promoters, thus transcription is activated (Brencic *et al.* 2005).

The activation signals provided by plant cell culture are aldose monosaccharides, low PH, low phosphate, and phenolic compounds (Palmer *et al.* 2004; Brencic *et al.* 2005). By analyzing root exudates and leaf protoplasts, phenols like acetosyringone (AS) were identified as inducers of *vir* gene

expression (Stachel *et al.* 1985). And sugars were proved to sensitize VirA/VirG system to phenolic compounds at very low concentration and increase the response (Shimoda *et al.* 1990). Therefore, a glucose/AS combination has been used as induction condition in routine laboratory work.

Wound tissues are known to be hyper-active in phenylpropanoid pathway, and feature in low PH and sugars associated with cell wall synthesis. When *Agrobacterium* was pre-treated with these conditions provided in induction buffer, transformation can also occur in unwounded plants (Escudero *et al.* 1997). Therefore, *Agrobacterium* favors wounded plant tissue (Braun 1952), probably due to a chemotactic effect. Besides, the induction condition, the elevated activity in cell division required for wound repair also contributes to successful transformation (Braun 1952).

To transfer the genetic information and effector proteins, a close association is needed between the bacterium and the host cell surface. Although the secretion channel is a VirB/D4 type 4 secretion apparatus genetically encoded by Ti plasmid, the specific attachment of *Agrobacterium* to plant cells is not Ti plasmid dependent (Douglas *et al.* 1982; Neff *et al.* 1985). Chromosomal genes *chvA*, *chvB*, ans *pscA* which are involved in synthesis and localization of glucan components were reported to be involved in specific binding of *Agrobacterium* to plant cells (McCullen *et al.* 2006). Yet no direct receptor-like partners were identified to facilitate the attachment. However, genomic screening of mutant Arabidopsis lines has isolated several

mutants that are recalcitrant to *Agrobacterium* transformation, one of which the gene of a cell wall arabinogalactan protein is affected and result in poor bacteria binding (Zhu *et al.* 2003). By now, there is still a gap in the host cell recognition and physical attachment remains to be explored.

1.2.2. Translocation of T-DNA and Vir effectors

Upon induction, VirA/VirG system activates transcription of a series of Vir proteins, which participate in the transformation process in various aspects. VirD2 recognizes a pair of 25-nucleotide long repeats that flank the T-DNA region, nicks the T-DNA border and covalently attaches the 5'end of the T-DNA (Pansegrau *et al.* 1993). VirD2 is transported together with T-DNA into the plant cells, to facilitate the nuclear targeting and genomic integration (Gelvin 2003). VirE2 owns a non-specific single-stranded DNA (ssDNA) binding activity, and can coat the length of T-DNA strand *in vitro* (Christie *et al.* 1988; Citovsky *et al.* 1992). VirE2 is co-expressed with a bacterial chaperone VirE1, which binds to VirE2 tightly and thus prevent VirE2 from self-associating and block the ssDNA affinity sites when inside the bacterium (Deng *et al.* 1999; Dym *et al.* 2008).

VirD2-T-DNA, VirE2, and other effectors like VirD5, VirE3, VirF are delivered to host cells through a transporter complex formed by VirB proteins and VirD4. This complex belongs to the class of type 4 secretion system (T4SS), and forms a multi-subunit envelope-spanning structure (Christie *et al.*

2005). It penetrates across plasma membranes of the bacterium and the host cell, as well as the plant cell wall, and delivers virulence effectors into the host cells. In T4SS mediated plasmid transfer, the T4-pilus enables interaction between donor and recipient strains, followed by fusion of outer membranes in a mating junction (Schroder *et al.* 2005). Little is known on how VirB mediates transfer across host cell barriers. However, the large host range of *Agrobacterium* suggests that the specific host-pathogen interaction may not be needed for *Agrobacterium*-mediated transformation.

The recognition of translocation substrates by the T4SS apparatus was dependent on the C-terminal motifs. The C-terminal sequences of VirE2, VirE3, and VirF were reported to be sufficient in mediating transport of fusion proteins to plants (Vergunst *et al.* 2000). As short as 10 residues from the C-terminus of VirF were sufficient to direct protein translocation to plants, from which the minimal consensus sequence R-X(7)-R-X-R-X-R recognized by the VirB complex was deduced (Vergunst *et al.* 2005). C-terminal fusions of VirE2 blocked its translocation activity (Vergunst *et al.* 2000). A FLAG tag insertion at the C-terminus of VirE2, or a truncation of 18 amino acids at the C-terminal of VirE2, disrupts the virulence of *Agrobacterium*, whereas the capability to bind ssDNA is not affected (Simone *et al.* 2001). When constitutively expressing these VirE2 mutants in transgenic plants, these transgenic plants are susceptible to transformation by *A. tumefaciens virE2* strains, indicating that the disrupted virulence is due to the failure in

translocation (Bhattacharjee *et al.* 2008).

1.2.3. Nucleus import and chromosomal integration

After translocation, the T-DNA need to achieve nuclear localization before integrated into the chromosome. The proteins VirD2 and VirE2, which closely associate with T-DNA, contain Nuclear-Localization Signal (NLS) sequences. VirD2 contains two NLS sequences, and each of them is functional in directing a fusion protein into nucleus. But the C-terminal NLS may have biological importance in a steric consideration (Tinland *et al.* 1995). VirE2 contains two separate NLS regions, which can also target fusion protein in to plant nuclei (Citovsky *et al.* 1992; Citovsky *et al.* 1994). Deletion of VirD2 NLS caused a nearly complete loss of transformation (Rossi *et al.* 1993), but a double mutant *virE virD2*ΔNLS was able to form tumors on a transgenic tobacco exogenously expressing VirE2 (Gelvin 1998). This suggests that VirE2 may have a function in directing T-DNA into nucleus, but a natural level of VirE2 is not functionally redundant of VirD2. Although VirE2 has NLS sequences, a study of host protein VIP1 suggested a subversion of plant defense mechanism by VirE2, which utilized the nuclear localization activity of VIP1, rather than using its own NLS (Tzfira *et al.* 2001; Liu *et al.* 2010). This function of VIP1 is partially complemented by VirE3 (Lacroix *et al.* 2005).

Integration of T-DNA requires disassociation of T-complex to expose

T-DNA strand. The coating protein VirE2 undergoes proteasomal degradation with plant protein VIP1, which is triggered by the virulence effector VirF (Pitzschke *et al.* 2010). The integration mode is largely determined by the eukaryotic species. It is observed that transgenes integrate in the plant genome at fairly random positions with variable copy numbers, which suggests Non-Homologous End Joining (NHEJ) plays an important role in plant species (van Attikum *et al.* 2001). In yeast, T-DNA carrying homologous sequence to the genome preferably integrates by homologous recombination (HR) (Bundock *et al.* 1995; Risseeuw *et al.* 1996). Mechanism of integrating T-DNA into chromosomes after releasing from T-complex is relatively unclear. Since VirD2 is covalently attached to T-DNA, it is likely to have a function in T-DNA integration (Pansegrau *et al.* 1993). The integrated DNA sequence is always more precise in the 5' end (Tinland *et al.* 1995), maybe resulted from a protection effect provided by VirD2 capping. This also indicates that the detachment of VirD2 occurs very late in the transformation process, suggesting an involvement of VirD2 in during integration. Transient expression of T-DNA can be observed although it may not stably integrated into genome (Nam *et al.* 1997). This expression requires a double stranded form which is transcriptionally active (Narasimhulu *et al.* 1996), though T-DNA is delivered as a single-stranded DNA. Therefore, the double stranded form of T-DNA may be a possible substrate for chromosomal integration.

1.3. Host factors involved in *Agrobacterium*-mediated

transformation

T-DNA transfer process can also be affected by host factors. In the past decade, enormous efforts have been dedicated to understanding the T-DNA transfer process inside the eukaryotic host. Hitherto, many host factors that interact with virulent factors of *Agrobacterium* have been identified. Research of host factors was focused on plant hosts in the early beginning, and revealed a good number of plant factors involved in almost every stage of transformation. Ever since laboratory methods for *Agrobacterium*-mediated transformation of fungi were established, research interests have been changing from plants to a simpler model organism, yeast *Sacchromyces cerevisiae*.

1.3.1. Plant factors involved in *Agrobacterium*-mediated transformation

Several factors that directly interact with VirD2, the pilot protein of T-complex, were reported to have putative roles in nuclear import of T-complex. The *Arabidopsis* cyclophilins RocA, Roc4 and CypA showed physical interactions with VirD2 in the yeast two-hybrid assay. They may function as chaperones for T-complex transfer inside plant cells, in view of their peptidyl-prolyl isomerase activity. In addition, cycloporin A, an inhibitor of cyclophilins, can abort *Arobacterium*-mediated transformation of *Arabidopsis* and tobacco, indicating a role of cyclophilins in cytoplasmic transfer of T-complex (Deng *et al.* 1998). The *Arabidopsis* karyopherin α

KAPα specifically binds to VirD2 by the NLS in C-terminus both *in vivo* and *in vitro*. It mediates import of T-complex into nuclei of mammalian cells. While a VirD2 mutant with deletion of NLS failed to guide nuclear import of T-complex in mammalian cells (Ziemienowicz *et al.* 2001). The tomato DIG3, a type 2C serine/threonine protein phosphatase, also interacts with C-terminal region of VirD2. Overexpression of DIG3 in tobacco BY2 cells inhibited the nuclear import of a beta-glucuronidase-VirD2 fusion protein, suggesting DIG3 may affect VirD2 nuclear import (Tao *et al.* 2004).

Besides VirD2, VirE2 is also important in facilitating the nuclear import of T-complex. Yeast two-hybrid screens identified a VirE2 interacting protein from *Arabidopsis*, designated as VIP1 (Tzfira *et al.* 2001). The original function of VIP1 is to activate expression of PR-1, a pathogenesis related protein, upon bacterial infection. But its nuclear import activity is hijacked by *Agrobacterium*. When binding to VIP1, VirE2 takes advantage of its nuclear import activity to carry T-complex into host nuclei (Tzfira *et al.* 2004). VIP1 was also reported to interact with H2A, a histone protein of *Arabidopsis*, which is found to be necessary for tumorigenesis and stable genetic integration (Mysore *et al.* 2000; Yi *et al.* 2001). Recently an *Arabidopsis* protein VBF was found to be crucial for successful transformation, by facilitating the uncoating of VirE2 from the T-DNA strand in nuclei. VBF organizes the assembly of SCF complex, an E3 ubiquitin ligase, and VIP1, and mediates its ubiquitinization. When ubiquitinized VIP1 is recognized by proteasome, it will

be degraded through the proteasomal degradation pathway, together with the associated VirE2 (Zaltsman *et al.* 2010).

When T-DNA is successfully delivered into host nuclei, integration occurs presumably controlled by host machineries. The T-DNA integration into plant genome is predominantly through non-homologous end joining (NHEJ), even in the presence of long homologous region (Offringa *et al.* 1990). Research on Arabidopsis mutants by T-DNA insertion revealed that KU80, a key enzyme in NHEJ pathway, is related to the T-DNA integration. Mutations in KU80 showed decreased susceptibilities to *Agrobacterium*-mediated transformation, indicating the importance of NHEJ in the T-DNA integration process (Friesner *et al.* 2003).

The above reviews show a rough picture of the trafficking and integration of T-DNA inside host cells. We can see that research on host factors of *Agrobacterium*-mediated transformation was mainly focused on plant hosts. This strategy inevitably suffers from the disadvantages of the plant study *per se*, that is gene redundancy and relatively low throughput. The redundancy of the plant genome may cover the effects of single gene mutations. Low throughput, due to the long life cycle of plant cells and whole individuals, is also a limiting factor that prevents the acquisition of a genome-wide profile of host factors involved in *Agrobacterium*-mediated transformation. We have reason to believe that more cellular mechanisms in host cells may be proven to participate in this DNA transfer process, when a high-throughput approach is

available for a global study of host factors

1.3.2. Yeast factors involved in *Agrobacterium*-mediated transformation

In answer to the global study, it was proposed to use yeast, the simplest eukaryotic organism, as the host for *Agrobacterium*-mediated transformation in the last decade. Unlike plant hosts, the yeast *Sacchromyces cerevisiae* has a very small genome with about 4800 non-essential genes and 800 essential ones. Furthermore, *S. cerevisiae* can proliferate in both haploid and diploid forms. With deletion of a single gene in a haploid strain, the genetic and phenotypic background becomes remarkably clear-cut compared with other higher eukaryotes. A high-throughput method for screening yeast genome with *Agrobacterium*-mediated transformation has been developed recently (Soltani *et al.* 2009; Tu 2010). Such work, for the first time, exhibited a genome-wide response of a yeast deletion library to *Agrobacterium*-mediated transformation, and paved the way for research on novel pathways which had been kept unknown before.

It was reported that deletion of genes for histone acetyltransferase, *GCN5*, *NGG1*, *YAF9* and *EAF7*, will greatly enhance the transformation efficiency; while deletion of genes for histone deacetylase, *HDA2*, *HDA3* and *HST4*, shows the opposite effect, confirming the integral role of histone modification in *Agrobacterium*-mediated transformation (Soltani *et al.* 2009). Glycosylation was also found to be important. Deletion of *OST3*, a subunit of

the oligosaccharyltransferase complex, greatly decreases the transformation efficiency. Since oligosaccharyltransferase catalyzes asparagine-linked glycosylation of newly synthesized proteins (Karaoglu *et al.* 1995; Knauer *et al.* 1999), OST3 may play its role through downstream proteins that are destined for glycosylation (Tu 2010). The reported pathways also include ATP generation, chromatin modification, nuclear envelope, RNA processing and DNA repair *etc.* (Soltani 2009; Tu 2010). These findings have revealed a number of cellular processes involved in *Agrobacterium*-mediated transformation, most of which have not been reported. Thus new directions are readily available for further research.

Quite interestingly, mitochondria were also reported to play a role (Tu 2010). Among its important functions is the ATP generation. A study of grape proteomics upon *Agrobacterium* challenge also found that ATP generation activities have been greatly suppressed (Zhao *et al.* 2011). All these findings directed to an important role of energy metabolism in *Agrobacterium*-mediated transformation. Considering that both T-DNA trafficking and integration should be energy-consuming processes, it is not surprising that alteration of ATP generation contributes to T-DNA transfer. It is logical to think that more ATP supply will be helpful to the successful transformation. Controversially, according to the existing findings, it is defect in ATP generation that promotes transformation process. This phenomenon lacks a reasonable interpretation based on current knowledge. The controversy

between these energy consuming processes and down-regulation of ATP generation remains to be explained. It is unlikely that the shortage of energy will facilitate nuclear import of T-complex, or T-DNA integration. Chances are T-complex is in favor of other effects associated with suppression of ATP generation for its final integration into the host genome. Therefore, it is of interest and great importance to investigate how ATP generation metabolism is involved in *Agrobacterium*-mediated transformation

1.4. Objective and Scope

As described in above reviews, yeast *Sacchromyces cerevisiae* is an ideal model to study the unique case of trans-kingdom delivery of genetic information performed by *Agrobacterium* (Soltani 2009; Soltani *et al.* 2009; Tu 2010). Previous studies by genome-wide screening have suggested a role of mitochondria in this transfer process (Soltani 2009; Tu 2010). But the exact mechanism remains unknown. This thesis, in order to answer such a question, is aimed at achieving the following goals:

a. To screen the single-gene mutations at the genes involved in the Electron Transport Chain (ETC), which is the most important pathway of a mitochondrion where ATP is generated. A five-fold difference in transformation efficiency compared to the wild type is set as the cut-off so that the selected mutant(s) for study would have a significant effect.

b. To develop detecting methods to track VirD2, VirE2 and T-DNA strand, respectively. T-DNA is transferred in the form of T-DNA complex, which comprises VirD2, VirE2 and T-DNA strand. Association, disassociation and movement of these components are thereof important for understanding how T-DNA complex is trafficking inside yeast cells. This event represents a good model for nucleoprotein trafficking in eukaryotic cells, which would shed a light on anti-infection strategies.

c. To determine the pattern of T-DNA integration in selected mutant(s). Genomic integration occurs to form stable transformants, after successful *Agrobacterium*- mediated transformation of yeast. Different integration patterns, namely homologous recombination (HR) and non-homologous end joining (NHEJ), employ different DNA repair machineries and have distinct efficiencies. A possible shift between these two patterns is expected in the selected mutant(s), and such a change is of tremendous importance as it determines chromosomal integrity and is related to many human diseases.

d. To study the connections of how mitochondria and T-DNA trafficking and integration are related. The tendency of pathogens to target and subvert host mitochondrial functions has been reported in many cases (Rudel *et al.* 2010). The A*grobacterium*-yeast DNA transfer process has a high degree of similarity to other bacterial and viral infection, in terms of injecting exogenous proteins and foreign DNAs. So the attempt of deciphering the cross talk between mitochondria and other cellular processes which help T-DNA trafficking and integration, may provide useful insights to other research fields.

In this study, *A. tumefaciens* and *S. cerevisiae* were employed to perform

the *Agrobacterium*-yeast DNA transfer. Other species of *Agrobacterium* and yeast was not involved. The yeast mutants were from a yeast knock out (YKO) library generated from strain BY4741, which is commercially available by Open Biosystems. Due to the limit of YKO library, only non-essential nuclear gene mutants are tested. Essential nuclear gene mutants and mitochondrial gene mutants are beyond the scope of this study.

Chapter 2. Materials and Methods

2.1. Strains and plasmids

Yeast strains and culture conditions

The collection of *S. cerevisiae* haploid deletion strains in BY4741 (***MAT****a his3Δ0 leu2Δ0 met15Δ0 ura3Δ0*) (Brachmann *et al.* 1998) were obtained from Open Biosystems. Stains used in this study are listed in Table 1. Yeast cells were grown in liquid YPD medium, or in synthetic defined (SD) minimal medium with appropriate dropout supplements. All strains were grown at 30 ℃ in a 200 rpm orbital shaker.

Bacterial strains and culture conditions

Bacterial strains used in this study are also listed in Table 1. *A. tumefaciens* was cultured in MG/L (Garfinkel *et al.* 1980) at 28 ℃, and *E. coli* was cultured in Luria-Bertani (LB) broth at 37 ℃, both in a 200 rpm orbital shaker.

Plasmids

Plasmids used in this study are listed in Table 2 with relevant features. Binary vectors are included here, and further described in respective transformation methods.

Table 1. Strains used in this study

Strains	Relevant characteristics	Source
Saccharomyces cerevisiae		
BY4741	**MAT***a his3*Δ1 *leu2*Δ0 *met15*Δ0 *ura3*Δ0	Open Biosystem
*cor1*Δ	**MAT***a his3*Δ1 *leu2*Δ0 *met15*Δ0 *ura3*Δ0 *cor1::KanMX4*	Open Biosystem
*rip1*Δ	**MAT***a his3*Δ1 *leu2*Δ0 *met15*Δ0 *ura3*Δ0 *rip1::KanMX4*	Open Biosystem
*cyt1*Δ	**MAT***a his3*Δ1 *leu2*Δ0 *met15*Δ0 *ura3*Δ0 *cyt1::KanMX4*	Open Biosystem
*qcr2*Δ	**MAT***a his3*Δ1 *leu2*Δ0 *met15*Δ0 *ura3*Δ0 *qcr2::KanMX4*	Open Biosystem
*qcr6*Δ	**MAT***a his3*Δ1 *leu2*Δ0 *met15*Δ0 *ura3*Δ0 *qcr6::KanMX4*	Open Biosystem
*qcr7*Δ	**MAT***a his3*Δ1 *leu2*Δ0 *met15*Δ0 *ura3*Δ0 *qcr7::KanMX4*	Open Biosystem
*qcr8*Δ	**MAT***a his3*Δ1 *leu2*Δ0 *met15*Δ0 *ura3*Δ0 *qcr8::KanMX4*	Open Biosystem
*qcr9*Δ	**MAT***a his3*Δ1 *leu2*Δ0 *met15*Δ0 *ura3*Δ0 *qcr9::KanMX4*	Open Biosystem
*qcr10*Δ	**MAT***a his3*Δ1 *leu2*Δ0 *met15*Δ0 *ura3*Δ0 *qcr10::KanMX4*	Open Biosystem
*cyc1*Δ*cyc7*Δ	**MAT***a his3*Δ1 *leu2*Δ0 *met15*Δ0 *ura3*Δ0 *cyc1::KanMX4* *cyc7::URA3*	this study
Agrobacterium tumefaciens		
EHA105	Wild-type, nopaline strain containing pTiBo542, disarmed	(Chen *et al.* 1991)
EHA105 *virE2*	EHA105, *virE2* mutant strain with CDS knockout	this study
EHA105 *virE2::GFP11*	EHA105, *virE2* fused with GFP11 at +162	this study
MX243	A348, *virB::Tn3-HoHol*	lab collection
A348	wild-type chromosomal background of strain C58 and contains pTiA6	(Sciaky *et al.* 1978)

Table 2. Plasmids used in this study

Plasmids	Relevant characteristics	Source
pQH02	Yeast expression vector, 2μ origin, *LEU2*, Amp^R, *AHD1* promoter and terminator	this study
pQH02-*QCR7*	pQH02, bearing *QCR7* with upstream and downsteam sequence from yeast genome	this study
pQH04	Yeast expression vector, 2μ origin, *HIS3*, Amp^R, *AHD1* promoter and terminator	this study
pQH04-*S1-10*	Yeast expression vector, 2μ origin, *HIS3*, expressing GFP1-10	this study
pQH213	*CEN/ARS*, *HIS5* from *Schizosaccharomyces pombe*, *URA3* modified to insert two 11 bp direct repeats with a stop codon trap in between	this study
pCB301	Binary vector, *nptIII*	(Xiang *et al.* 1999)
pQH302	Binary vector for yeast, *URA3*	this study
pQH303	Binary vector for yeast, *URA3* flanked by homologous arms cloned from *LYS2*	this study
pQH304	Binary vector for yeast, *URA3*, 2μ origin	this study
pQH305	*GFP1-10* driven by an *AHD1* promoter is inserted into pQH303 downstream of URA3	this study
pBI121	Binary vector for plants, nptIII, KanR, *35S::GUS*	(Chen *et al.* 2003)
pQH121	Derivative from pBI121, with *GUS* substituted by a multiple cloning site	this study
pQH122	pQH121 backbone, *35S::DsRed*	this study
pQH308	Binary vector for plants, *nptIII*, Bar^R, Hyg^R, *35S::GFP1-10*, *35S::DsRed*	this study
pQH308a	Binary vector for plants, *nptIII*, Kan^R, *Pmas::GFP1-10*, *35S::DsRed*	this study
pYES2	Yeast expression vector, 2μ origin, *GAL1* promoter, *CYC1* terminator, URA3, Amp^R	Invitrogen
pYES2-*GFP*	pYES2 backbone, expressing GFP upon galactose induction	lab collection
pYES2-*GFP:virD2*	pYES2 backbone, expressing GFP-VirD2 upon galactose induction	lab collection
pEx18Tc	Counter-selectable plasmid carrying sacB, oriT, $Tetracycline^R$	(Hoang *et al.* 1998)
pEx18TcKm-*virE1-virE2::GFP1-10*	pEx18Tc backbone, *nptIII* inserted to confer $Kanamycin^R$, fusion gene *virE2::GFP11* with upstream virE1 was inserted into MCS	this study

2.2. *Agrobacterium*-mediated transformation of yeast

2.2.1. Protocol

Agrobacterium-mediated transformation (AMT) of *S. cerevisiae* has been established for over fifteen years (Bundock *et al.* 1995; Piers *et al.* 1996). The protocol used in this study was based on previous publications with modifications that simply the handling and produce repeatable results (Figure 2). Medium and solutions used in this part are listed in Table 3. The detailed procedure was described as follows. *A. tumefaciens* cells were grown overnight in MG/L with appropriate antibiotics. After 1:50 subculture dilution, allow the culture growing for additional 6~7 hours to reach OD_{600}=1. The cells were pelleted, resuspended in 10 ml of IBPO4 with appropriate antibiotics and 200 μM acetosyringone (AS) for induction, and harvested 16~18 h later. 3×10^8 cells were collected for cocultivation. A single colony on a fresh YPD plate was inoculated into 2 ml of YPD broth. The cells were grown overnight at 30 ℃ with shaking. The cells were then diluted ~20 fold with fresh YPD medium and grown for extra 3~4 h, usually at OD_{600}=0.350. 1×10^6 cells were collected for cocultivation. The cocultivation of bacteria and yeast was initiated by mixing mentioned quantity of cells respectively, resuspended in 100 μl IBPO4, and drop onto a cocultivation medium (CM) plate. The cocultivation mixture was left in the laminar flow hood for 20 min, or until when the mixture is dry out on the plate. Then incubate the CM plate for 24 h at 20 ℃ in complete darkness.

The cocultivated cells were washed off the plate with 1 ml of PBS. 100 µl of the washoff suspension was plated on SD plates with appropriate dropout for selection of transformants and with cefotaxime to kill bacteria. Remaining suspension was subject to $1:10^4$ dilution, and plate 100 µl on synthetic complete (SC) plate for recovery. The plates were incubated at 30 ℃, and the colonies were counted after 3-4 days.

Table 3. Media and solutions

Medium/Solution	Recipe	Reference
A. tumefaciens		
MG/L	LB, 500 ml; mannitol, 10 g; sodium glutamate, 2.32 g; KH_2PO_4, 0.5 g; NaCl, 0.2 g; $MgSO_4 \cdot 7H_2O$, 0.2 g; biotin, 2 µg; pH 7.0	Cangelosi *et al.*, 1991
20 × AB salts	NH_4Cl, 20 g; $MgSO_4 \cdot 7H_2O$, 6 g; KCl, 3 g; $CaCl_2$, 0.2 g; Fe $SO_4 \cdot 7H_2O$, 50 mg	Cangelosi *et al*, 1991
20 × AB buffer	K_2HPO_4, 60 g; NaH_2PO_4, 23 g; pH7.0	Cangelosi *et al.*, 1991
$IBPO_4$ (Induction Medium)	20 × AB salts, 50 ml; 20 × AB buffer, 1 ml; 62.5 mM KH_2PO_4 (pH 5.5), 8 ml; 30% glucose, 18g; autoclave separately	Piers *et al.*, 1995
CM (Cocultivation medium)	$IBPO_4$; histidine,20 µg/ml; leucine 60 µg/ml; methionine 20 µg/ml; uracil 20 µg/ml	Piers *et al.*, 1996

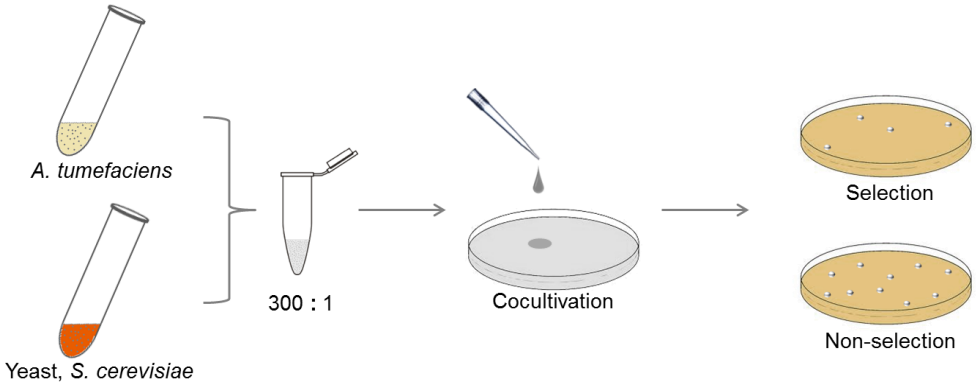

Figure 2. *Agrobacterium*-mediated transformation of yeast.

The bacteria culture is induced with AS in IBPO4 for 16 hours, and mixed with early log-phase yeast cells at 300:1. The mixture is dropped onto cocultivation medium (CM) plate, and dried in a laminar flow hood. The plate is incubated at 20℃ in total darkness for 24 hours. After cocultivation the mixture is washed off and spread onto selection or non-selection plate with proper dilution.

2.2.2. Binary vectors

Three derivatives of *A. tumefaciens* strain EHA105 were used in the yeast transformation study: One carries the binary vector pQH302 which contains a *URA3* yeast expression cassette in its T region (Figure 3A). The second one carries the binary vector pQH303 which can generate a T-DNA that harboring a *URA3* cassette flanked by two sequences homologous to *LYS2* locus (Figure 3B). And the third one carries the binary vector pQH304 which was constructed by inserting a yeast 2μ origin in the T-DNA region of pQH302 (Figure 3C).

These three strains represent three different types of stable existence of T-DNA in transformants' genome. Two adjacent sequences from genomic *LYS2* locus were cloned into pQH303, with 1.3 kb placed upstream of *URA3* and 2.0 kb downstream. Therefore, the T-DNA generated from pQH303 will be targeted into *LYS2* locus though homologous recombination (HR). 2μ origin contains an autonomous replication sequence together with related genes. Existence of a 2μ origin should make the T-DNA from pQH304 self-maintained in recipient yeast cells by cyclization. pQH302 carries neither homologous sequences nor 2μ replication origin, thus can only be randomly inserted into the genome through non-homologous end joining (NHEJ).

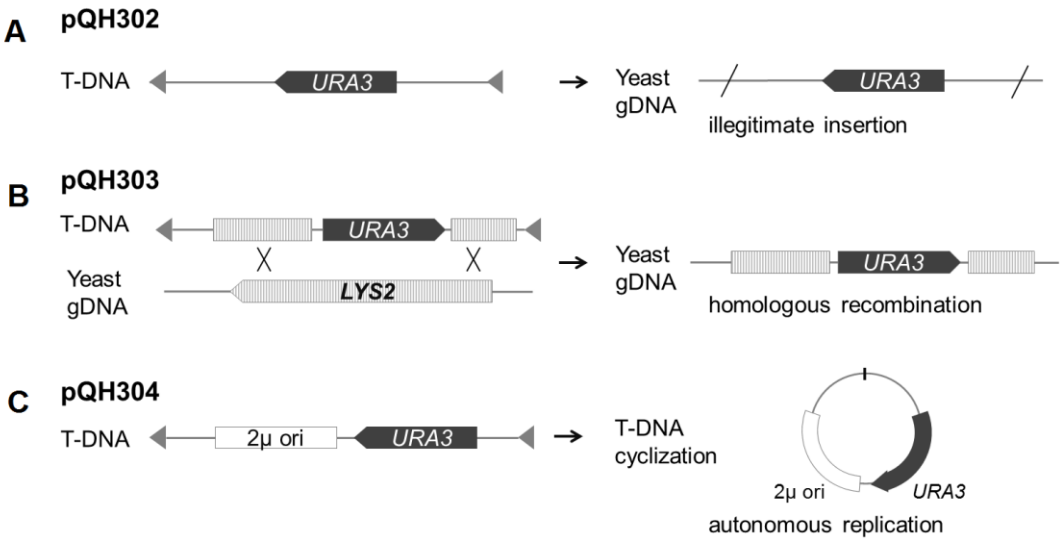

Figure 3. Binary vectors used in transformation of *S. cerevisiae*.

The binary vectors used in this study are based on mini binary vector pCB301.
(A) pQH302 generates a T-DNA sequence containing a *URA3* marker, which can only be randomly inserted into yeast genome through NHEJ.
(B) pQH303 generates a T-DNA sequence in which *URA3* is flanked by homologous arms cloned from *LYS2* locus, 1.3 kb and 2.0 kb, respectively; this type of T-DNA can be targeted into *LYS2* locus through HR.
(C) pQH304 generates a T-DNA sequence containing a 2μ origin besides *URA3* marker, which is capable of self-maintaining in yeast after cyclization.

2.3. Agroinfiltration

2.3.1. Protocol

2 ml Agrobacteria culture was grown overnight with appropriate antibiotics, and subcultured with 1:50 dilution for additional 6~7 hours until OD_{600} reaches 1. The bacteria cells were pelleted by centrifuging 3 minutes at 4000 g, and then resuspended in 10 ml infiltration buffer (10mM $MgCl_2$, 10mM MES, PH 5.5), OD_{600}≈0.2-0.4. This bacteria suspension was then placed in a syringe, without a needle. The tip of the syringe was pressed against the abaxial side (lower side) of a fully expanded leaf from a 6-8 weeks old *Nicotiana benthamiana*, while applying gentle counter-pressure to the other side with an index finger. The bacteria suspension was then push-injected into the airspaces inside the leaf through stomata, or through tiny incisions caused by the syringe tip. Transient expression can be optimally visualized 3~5 days after infiltration.

2.3.2. Binary vectors

The binary vector pQH308 was used in the visualization of VirE2 in plant cells. It was constructed on the basis of pHB (Mao *et al.* 2005). DNA coding *GFP1-10* was purchased from American Peptide Company Inc., and cloned downstream of 35S promoter of pHB. A plant expression cassette *35S::DsRed* was inserted downstream of *rbcS* PolyA sequence.

pQH308a was derived from pBI121. *GUS* was replaced by *DsRed* coding sequence, and a plant expression cassette *Pmas::GFP1-10* was inserted upstream of 35S promoter. This vector was designed to carry out the same function of pQH308, and was supposed to circumvent promoter interference happened when using pQH308 for stable transformation.

T-DNA features of pQH308 and pQH308a were shown in Figure 4.

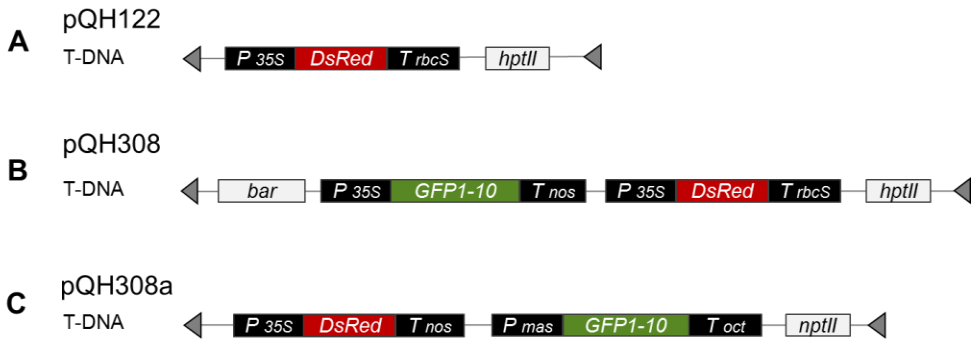

Figure 4. Binary vectors used in agroinfiltration of *N. benthamiana*.

T-regions of binary vectors are shown above. (A) pQH122 has a pBI121 backbone, with *GUS* replaced by *DsRed*. (B) pQH308 is derived from pHB (Mao *et al.* 2005). *GFP1-10*, encoding GFP big fragment, is driven by CaMV 35S promoter. A 35S driven *DsRed* is inserted in a *cis* position downstream of *GFP1-10*. (C) pQH308a is a reconstructed version based on pBI121 to execute functions of pQH308, with *GFP1-10* driven under a *mas* promoter.

2.4. Markerless gene replacement

In this study, genetic modifications were introduced into *A. tumefaciens* strain EHA105. In order to maintain the bacterium's genetic integrity, a markerless gene replacement was performed. This method is based on a two-step homologous recombination, whereby the first recombination introduces the vector into genetic context by one homologous arm and the second recombination releases the vector off with the other homologous arm to realize double crossover. The first recombination was selected with appropriate antibiotics according to the vector used, while a suicide gene on this vector backbone was used for counter-selection in the second recombination.

To substitute *virE2* with *virE2::GFP1-10*, a suicide vector pEx18TcKm was employed to carry out the replacement. pEx18TcKm was modified from the suicide vector pEx18Tc (Hoang *et al.* 1998), by inserting an *nptIII* cassette downstream of MCS to confer a kanamycin resistance (EHA105 is tolerant to tetracycline, Tc). *Bacillus subtilis sacB* gene that confers sucrose sensitivity (Pelicic *et al.* 1996) was encoded in the backbone of pEx18TcKm for counter-selecting the vector in the second recombination. *virE2::GFP1-10* was inserted into the MCS, together with the upstream *virE1* gene, generating pEx18TcKm-*virE1-virE2::GFP1-10*. The cloned fragment was identical to the corresponding sequence on pTiBo542, except that *virE2* was fused with *GFP1-10*. Therefore, there was about 500 bp upstream of *GFP1-10* and 1.4 kb

downstream, which are sufficient for crossover events (Tymms *et al.* 2001).

pEx18TcKm-*virE1-virE2::GFP1-10* was introduced into EHA105 by electroporation (Lin 1994). Bacteria culture was spread on a LB kanamycin plate to select the first recombination transformants, and incubated at 28 ℃ for 2 days. A single colony of transformant was streaked on a LB plate with 5% sucrose, and incubated 28 ℃ for 2~3 days until colonies coming out. These colonies would possess two genetic backgrounds: one accomplished double crossover to achieve gene replacement, and the other one stored to WT due to repeated involvement of the same homologous arm in two rounds of recombination. Colony PCR was performed to examine the genotype of each colony. The genetic changing during this process was illustrated in Figure 5.

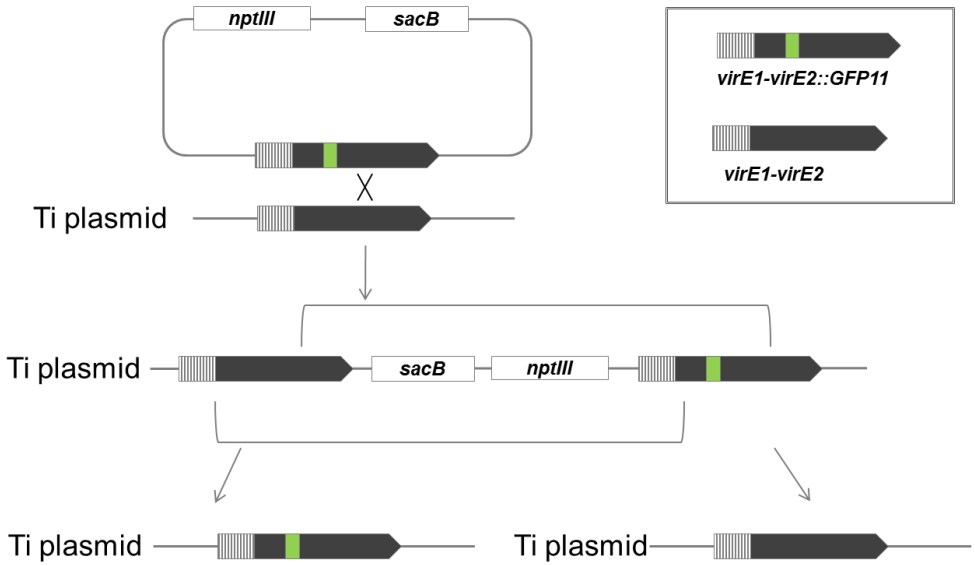

Figure 5. Replacement of *virE2* with fusion gene *virE2::GFP11*.

The fusion gene *virE2::GFP11* was carried by the sucrose suicide vector pEx18TcKm, together with *virE1* as an extended upstream homologous region. The first recombination occurred either at upstream or downstream region of *GFP11* coding sequence. The first recombination was selected through kanamycin resistance conferred by *nptIII*. In the second recombination, a loss of pEx18TcKm backbone occurred. The *sacB* on backbone was counter-selected with LB sucrose medium. Two genotypes can be selected, and the replaced strains were identified with PCR.

2.5. Tumorigenesis

2.5.1. Leaf tumorigenesis on *Kalanchoe daigremontiana*

A. tumefaciens strains harboring a tumor inducing T-DNA can cause crown galls in *K. daigremontiana* leaves. The virulence of genetically modified *Agrobacterium* was examined by such tumorigenesis capability. The protocol was described by Guo *et al.* previously (Guo *et al.* 2007), with modifications that enable it to measure the virulence of a non-tumor-inducing strain. *virE2* of the tumor inducing strain A348 was deleted using the method described in 2.4. A348 *virE2* thus provided only VirD2-T-DNA in tumorigenesis. Experimental strain EHA105 *virE2::GFP1-10* and its control strains were all T-DNA incompetent strains. Co-infiltration of A348 *virE2* and EHA105 strains would complement the latter with tumor inducing ability. The level of this acquired ability was subject to different VirE2 backgrounds of testing strains.

All strains were cultured in 1 ml MG/L to mid-log phase, pelleted by centrifugation, and resuspended in 10 ml MilliQ water, $OD_{600} \approx 0.1$. Linear wounds were introduced by gently streak a needle on a fully expanded *K. daigremontiana* leaf. A348 *virE2* suspension was mixed 1:1 with other testing strains, namely EHA105, EHA105 *virE2::GFP1-10*, EHA105 *virE2*. 5 μl mixed bacteria were applied to each wound. The plant was then placed in ordinary growth conditions for 4 weeks for tumor formation.

2.5.2. Root segment tumorigenesis on *Arabidopsis thaliana*

Arabidopsis seeds were sterilized, and germinated on an MS plate at 23℃ in 16 h photoperiod. Roots of 10 days seedlings were collected, and cut into 0.5 mm segments. *A. tumefaciens* strain A348 was grown in MG/L overnight, and subcultured with 1:50 dilution for additional 6~7 h until OD_{600} =1. The cells were pelleted and resuspended in MS medium, with final concentration at OD_{600} =0.1. About 50 root segments were dipped into 1 ml bacteria suspension, and spread onto a plain MS plate for 2 days cocultivation at 23℃ in complete darkness. The infected root segments were transferred and aligned neatly onto an MS plate containing cefotaxime to kill bacteria. The plate was kept at 23℃ in complete darkness at least 3 weeks for tumor formation.

2.6. Real-time PCR detection of T-DNA

Real-time PCR was employed to detect cellular T-DNA level in recipient cells. Primers were designed to amplify DNA fragments from *URA3*, *virE2*, and *PMP3*, representing the abundance of T-DNA, agrobacteria, and yeast cells, respectively. The primers designed for this assay were listed in Table 4. DNA extracted from induced agrobacteria was used to establish a correlation of T-DNA (including T region) versus agrobacteria by making a standard curve. And this standard curve was used for deducting contaminant proportion from total detected T-DNA levels. The efficiency of three primer pairs were

tested, and listed as follows: *URA3* 103%, *virE2* 93%, *PMP3* 103%.

Cocultivated yeast cells were washed off from the CM plate. Majority of the bacteria were removed by repeated differential centrifugation. Total DNA was extracted from the yeast cells by lyticase digestion/phenol:chloroform extraction/ethanol precipitation. In this study, KAPA SYBR fast universal qPCR kit was used to carry out real-time PCR reaction. [94 ℃ 10 s – 55 ℃ 30 s]×40 cycles was performed on Bio-Rad CFX384, followed by melting curving checking.

Since the primer efficiency was close to 100% for all three pairs, the algorism can be approximately simplified to a traditional $2^{-\Delta\Delta Ct}$ method. A modification of algorism was made to deduct the contaminant proportion of T-DNA data: Ct*virE2* was converted into corresponding value of Ct$URA3^{virE2}$ according to aforementioned standard curve. Relative amount of *URA3* and $URA3^{virE2}$ was obtained by normalizing Ct*URA3* and Ct $URA3^{virE2}$ with Ct*PMP3*. Therefore, the T-DNA amount and its contaminant proportion were transformed into the same linear coordinate system, thus can directly execute deduction. Net cellular T-DNA level was obtained for subsequent comparison between strains.

Table 4. Primers used in real-time PCR

Primer	Sequence
URA3INF	5’--TCCTGTTGCTGCCAAGCTAT-3’
URA3INR	5’--AATGTCTGCCCATTCTGCTA-3’
VirE2seqF	5’--CATAGAGGAAATGAGCGGCAGTC-3’
VirE2seqR	5’--AACTTCCGTTCGGGTAGGGCT-3’
PMP3F	5’--ATGGATTCTGCCAAGATCATTAAC-3’
PMP3R	5’--TTAATCTTGTAGGACAATGTACAAGG-3’

2.7. Automated Fluorescent Microscopy

The movement of VirE2 in *N. benthamiana* leaves was captured with time lapse fluorescent imaging. Samples were cut from an agroinfiltrated leaf, as described in 2.3. A 5 mm × 5 mm piece of leaf tissue was placed on a concave slide and sealed in 2% low melting agarose under a coverslip. The motorized system microscope Olympus BX61 was employed for time lapse imaging. FITC (Ex488Em520), TxRed (Ex560Em620) filters were used to detect GFP and DsRed signals, respectively. The leaf epidermal cells can be clearly visualized with 10×, 20× and 40× lenses. For detecting movement, a larger viewing field was needed to monitor multiple cells. Therefore, a 10× lens was chosen for time lapse imaging. The light intensity was set in such way that 100 ms exposure would give enough signal strength, usually at 10%

power. Multiple sites of observation were marked with the appropriate focus. 5~7 focal planes spanning 25~40 μm were set for each observation site. The minimal interval of timing was subject to the number of focal planes and observation sites. For 1 site of 7 focal planes, 30 s was the minimal requirement; For 8 sites of 7 focal planes, 3 min was needed for a complete turn of all frames. The recording time was less than two hours: too short would result in fragmented information; too long would result in signal bleaching in later part.

2.8. SDS-PAGE and Western blot

Crude extraction of proteins were separated with sodium dodecyl sulfate polyacrylamide gel electrophoresis (SDS-PAGE) as described previously by Laemmli (Laemmli 1970). Discontinuous SDS-PAGE with a stacking gel (0.125 M Tris-HCl pH 6.8, 0.1% SDS and 5% acrylamide/Bis solution) and separating gel (0.375 M Tris-HCl pH8.8, 0.1 % SDS and 15% acrylamide/Bis solution) was performed in 1 × SDS running buffer (20 mM Tris Base, 200 mM glycine, 0.1 % SDS) at 70 volts for 20 minutes and followed by 200 volts.

The protein samples were then transferred onto an Immun-Blot^{TM} PVDF membrane (Bio-Rad) by electrophoresis using an Electro-Blot Unit (Scie-Plas, EB10). The PVDF membrane was soaked in methanol for 1 min before covering onto the protein gel. Bubbles in between were carefully removed. Transfer was performed at 200 mA constant current for 2 hours. The blotted

membrane was then blocked in 3% BSA in TBST (20 mM Tris pH 7.4, 154 mM NaCl, 0.1% Tween 20) for 1 hour, washed in TBST for 10 min and repeat twice. The membrane was then incubated with primary antibody (1:5000) for 1 hour with mild shaking, washed in TBST for three times, 10 min each time. The PVDF membrane was then incubated with secondary antibody (HRP IgG antibody) for 1 hour with mild shaking. After three times washing as described above, the membrane was treated with Supersignal® West Pico Chemiluminescent Substrate. Fluorescent signals were detected by BioMax XAR films and developed with an X-ray developer.

Chapter 3. A knockout of Qcr7p affected *Agrobacterium*-mediated transformation of yeast

3.1. Introduction

A mitochondrion is an important organelle that are membrane-enclosed and found in most eukaryotic cells (Henze *et al.* 2003). Mitochondria implement multiple critical functions in a cell, the most prominent one of which is to produce the major energy currency molecule of the cell, ATP (Dahout-Gonzalez *et al.* 2006). Other functions include regulation of the membrane potential (Voet *et al.* 2006), calcium signaling (Gyorgy *et al.* 2006) and apoptosis (Green 1998). Since mitochondria undertake so many fundamental roles of maintaining the proper functions of a cell, it becomes a major target of many pathogen infection cases (Rudel *et al.* 2010; Ohta *et al.* 2011). Therefore, it intrigues a very interesting question whether mitochondria also play a role in the *Agrobacterium*-mediated transformation process.

Genome-wide screening studies of yeast knock-out mutants have linked mitochondrial components to *Agrobacterium*-mediated transformation efficiency (Soltani *et al.* 2009; Tu 2010), among which the Electron Transport Chain (ETC) has been articulated. The ETC consists of a series of spatially separated reduction-oxidation reactions, in which electrons are transferred from donor molecules to receptor molecules driven by Gibbs free energy. A trans-membrane proton electrochemical gradient between inter-membrane

space and mitochondrial matrix is formed as a result of redox reactions along ETC (Murray *et al.* 2003). According to the chemiosmotic coupling hypothesis, the ETC is coupled with oxidative phosphorylation by this proton gradient across the inner mitochondrial membrane. Influx of protons through mitochondrial inner membrane enables ATP synthase work, converting mechanical energy into chemical energy in the form of ATP production (Mitchell 1961). Another critical role of ETC is associated with cytochrome c, a highly conserved protein across the spectrum of species. Cytochrome c is localized solely in the mitochondrial inter-membrane space under normal conditions (Neupert 1997). When cytochrome c is released from mitochondria to the cytosol, it activates the caspase family of proteases, leading to the onset of apoptosis (Kroemer *et al.* 1998). Critical roles of ETC sparkles the initial interest of this study to explore the mechanism for which the efficiency of *Agrobacterium*-mediated transformation has been altered in ETC mutants of yeast.

In this chapter, ETC mutants of yeast knock-out library are screened, hunting for appropriate candidate of research. Selected mutant, *qcr7Δ*, is analyzed at the molecular level for its contribution to hyper-susceptibility of *Agrobacteirum*-mediated transformation.

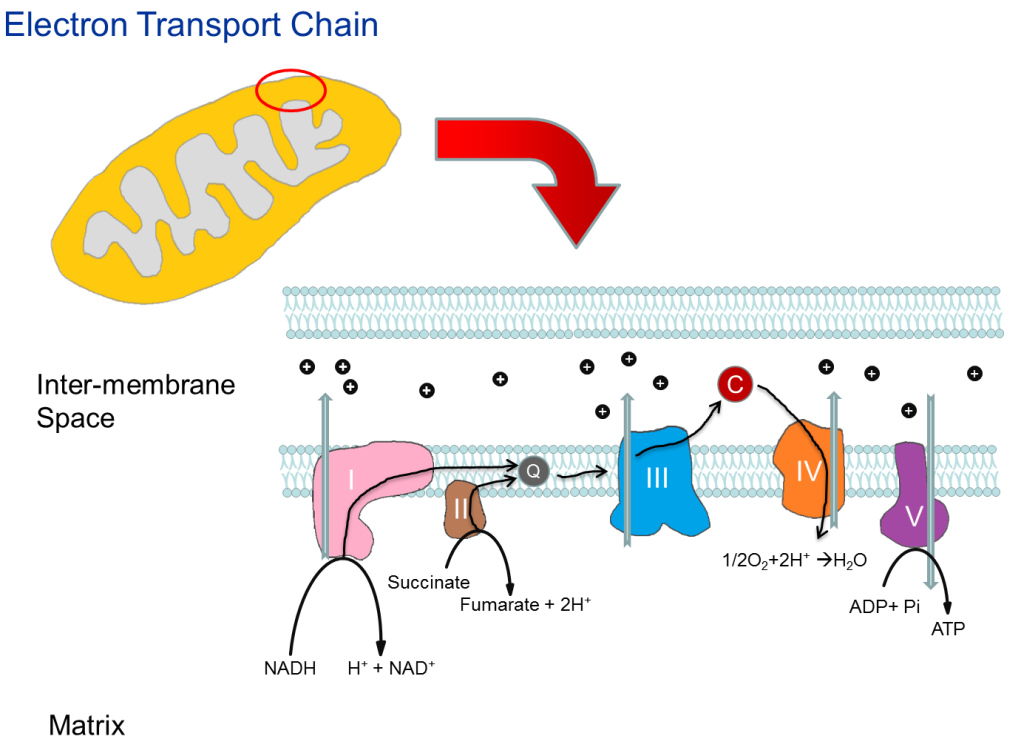

Figure 6. Schematic representation of Electron Transport Chain.

(I). NADH dehydrogenase; (II). succinate dehydrogenase;
(III). ubiquinol cytochrome c oxidoreductase; (IV). cytochrome c oxidase;
(V). ATP synthase; (Q). ubiquinone, co-enzyme Q; (C). cytochrome c.

3.2. A knockout of Qcr7p affected *Agrobacterium*-mediated transformation of yeast

At the mitochondrial inner membrane, the redox reaction is carried out through a series of membrane-embedded complexes (Figure 6). Complex I (NADH dehydrogenase) accepts electrons from electron carrier NADH, and passes them to coenzyme Q (ubiquinone, Q), which also receives electrons from complex II (succinate dehydrogenase). Complex III (ubiquinol cytochrome c oxidoreductase) receives electrons from Q and passes them to cytochrome c (C). C passes electrons to Complex IV (cytochrome c oxidase), where molecular oxygen obtains the electrons to be reduced to water (Belevich 2007).

Peptide components and subunits of these complexes are encoded in nuclear genome as well as mitochondrial genome. In this research, the yeast knockout library only contains mutants for nuclear genes. Thus only nuclear gene mutants were assayed with yeast AMT protocol in this study.

3.2.1. Mutation in some complex III components of Electron Transport Chain enhanced the efficiency of *Agrobacterium*-mediated transformation

As described previously, T-DNA will be maintained in yeast cells with three different fates, namely non-homologous end joining (NHEJ), homologous recombination (HR), and cyclization (Hooykaas *et al.* 1994). Binary vectors carrying out these three fates were described in Chapter 2.

Under the same experimental condition, transformation efficiency of these three fates was shown in Figure 7A. Although NHEJ dominates the T-DNA integration events in plant species (van Attikum *et al.* 2001), in *S. cerevisiae* HR plays a more important role (van Attikum *et al.* 2003). Correspondingly, NHEJ events (pQH302) were hardly detected in this experimental setting. Considerable amounts of transformants were obtained by HR with pQH303. Due to the existence of a 2μ origin in the T-DNA region of pQH304, T-DNA cyclization was easily formed through DNA repair, making the highest transformation efficiency.

Among all the complexes assayed, including UQ and cyt c, complex III mutants showed an overall trend of enhanced transformation efficiency. Complex III in *S. cerevisiae* consists of three catalytic subunits Cobp, Rip1p, and Cyt1p, and seven additional subunits: Cor1p, Qcr2p, Qcr6p, Qcr7p, Qcr8p, Qcr9p, and Qcr10p (Brandt *et al.* 1994; Hunte *et al.* 2003). All, but Cobp, are encoded by the nuclear genes. Fold changes of AMT efficiency of these nine mutants are shown in Figure 7B and 7C. Plasmid pQH302 was not included in the screening because of the extremely low efficiency. The results show that mutation in some complex III components enhanced the transformation efficiency, suggesting a negative regulation by complex III to AMT. This trend triggered a question of whether blocking ETC would result in an enhanced AMT efficiency. To address this question, a cytochrome c mutant was tested for its AMT susceptibility. Complete knockout of cytochrome c was achieved

by deleting *CYC1* and *CYC7*, in which both isoforms of cytochrome c were eliminated (Dumont *et al.* 1990). Although cytochrome c null mutant also suffers from ETC disruption, which leads to a slower proliferation rate, it was not more susceptible to AMT (Figure 8B). This result demonstrates that the enhanced transformation efficiency of complex III mutants cannot be simply attributed to ETC blockage.

3.2.2. A knockout of Qcr7p enhanced *Agrobacterium*-mediated transformation efficiency

Among complex III mutants, *qcr7*Δ was the most remarkable by enhancing the transformation efficiency over five folds (Figure 8A), though Qcr7p does not execute any catalytic functions. When complemented *qcr7*Δ with a yeast expression vector carrying *QCR7*with its genomic context (pQH02-*QCR7*), the enhanced transformation efficiency of *qcr7*Δ was partially rescued (Figure 8C). This result confirmed that a knockout of Qcr7p indeed contributed to an enhanced AMT efficiency.

Qcr7p is a ubiquinone binding protein that is essential for assembly and activity of complex III (Schoppink *et al.* 1989). It forms, together with Cor1p and Qcr2p, a large domain that extends into the mitochondrial matrix (Hunte *et al.* 2003). Genetic study suggests that Qcr7p plays a role in proton uptake of the complex (Lee *et al.* 2001) . There is no evidence that Qcr7p and T-DNA complex can associate with each other. Therefore, the altered AMT efficiency

by *qcr7*Δ could be a result of an overall change of cellular conditions that favored by AMT process.

To test whether mutation of *QCR7* also leads to enhanced efficiency to other transformation approaches, I performed a well characterized LiAc method, to transform yeast with PCR amplified T-DNA region of pQH303 and pQH304. LiAc method is a physicochemical approach to transform yeast *S. cerevisiae* with alkaline cations with a history of 30 years (Ito *et al.* 1983). It is widely used for different purposes for yeast molecular biology (Gietz *et al.* 2001). Therefore, a connection of AMT to LiAc transformation could help to analyze the reason of enhanced AMT in *qcr7*Δ.

In this study, LiAc transformation was performed as described previously (Gietz *et al.* 2007). Yeast strains were transformed with amplified from T-DNA region of pQH303 and pQH304. Transformation efficiency was calculated and shown in Figure 8D. LiAc transformation of yeast with DNA fragments showed a lower efficiency of *qcr7*Δ compared to WT; this different from what we observed from AMT results. This suggests that *Agrobacterium*-mediated transformation is a pathway different from LiAc transformation; the effect of Qcr7p is specific to *Agrobacterium*-mediated transformation.

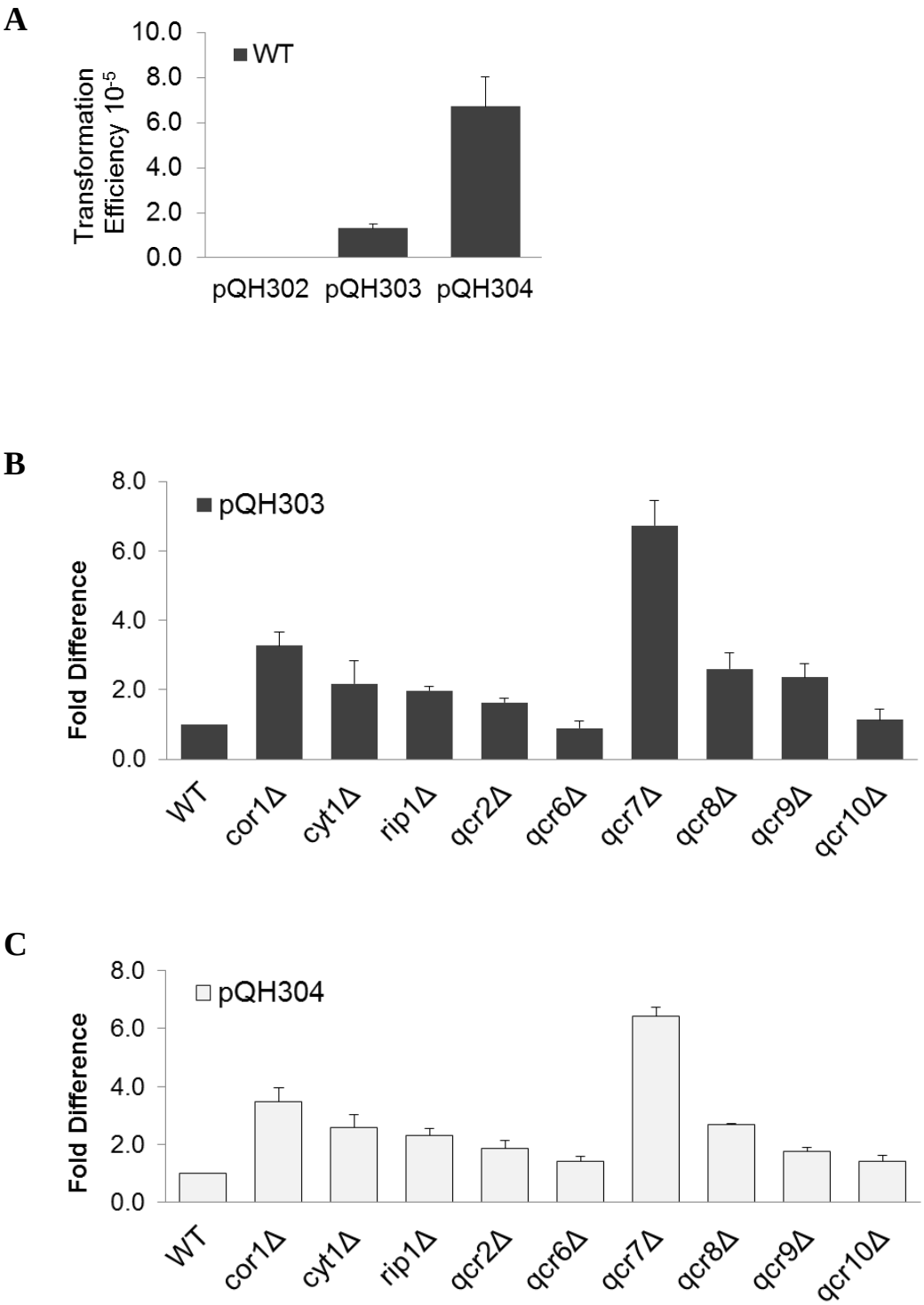

Figure 7. Mutation in some complex III components enhanced *Agrobacterium*-mediated transformation efficiency.

(A). Typical AMT efficiencies with three binary vectors used in this study;
(B-C). Fold changes of complex III mutants in AMT with pQH303 and pQH304, respectively. Mean value of three independent experiments is shown with standard deviation.

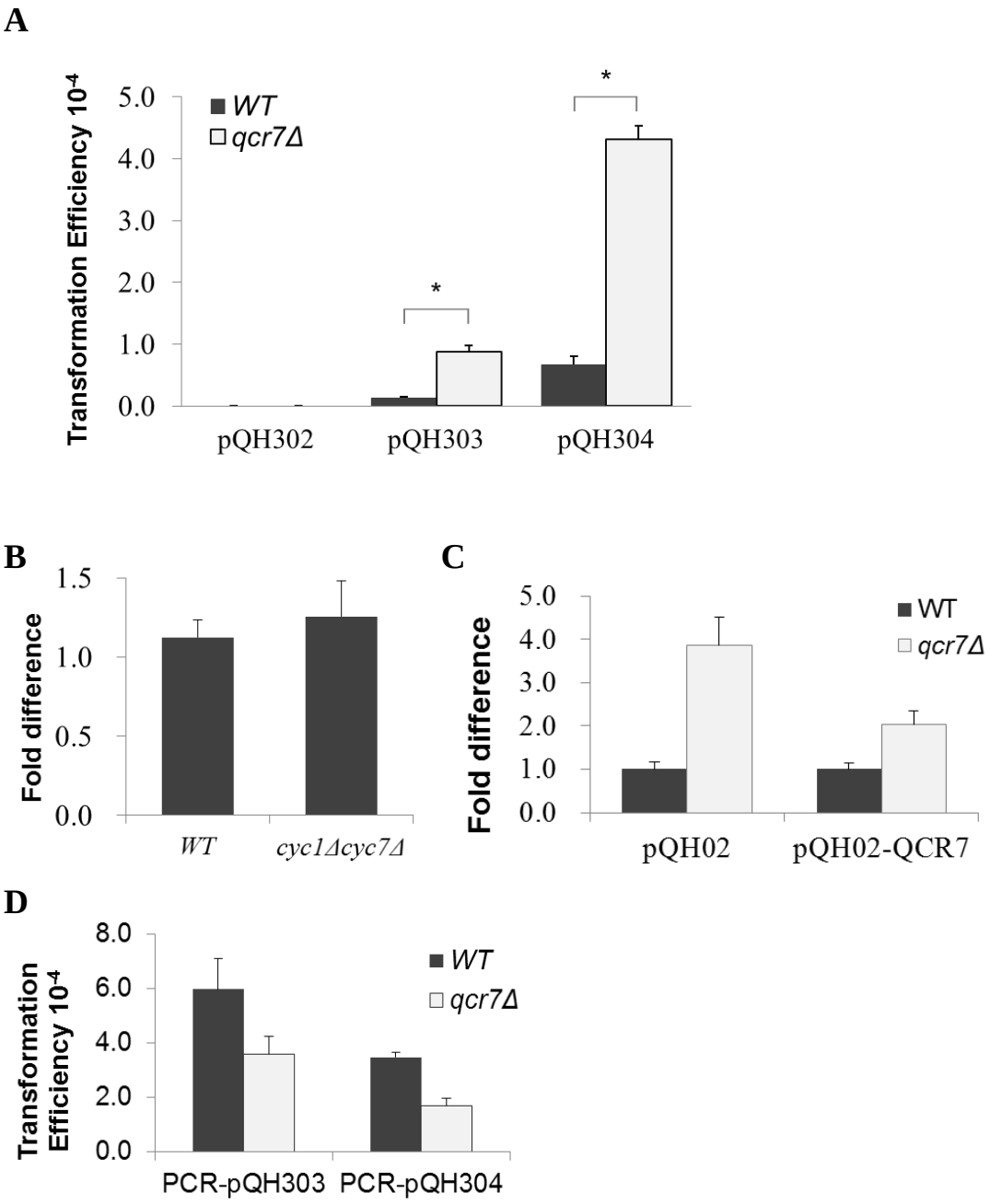

Figure 8. A knockout of Qcr7p enhanced *Agrobacterium*-mediated transformation efficiency.

(A). AMT efficiency of *qcr7*Δ with three constructs, * $P < 0.05$; (B). Fold difference of a knockout of both cytochrome c isoforms; (C) Fold difference of AMT efficiency of *qcr7*Δ complemented with genomic *QCR7* sequence; (D). Transformation efficiency of *qcr7*Δ in LiAc transformation, DNA for transformation was PCR-amplified T region. Mean value of three independent experiments was shown with standard deviation.

3.2.3. A knockout of Qcr7p showed decreased Non-Homologous End Joining in *Agrobacterium*-mediated transformation

As described in Chapter 2, transformation of yeast by pQH303 relies on successful crossover of homologous arms flanking the *URA3* cassette with *LYS2* locus. After integration through HR, *LYS2* should be knocked out with *URA3* knocked in. Therefore, the transformants are supposed to acquire Ura+ phenotype at the expense of becoming lysine auxotrophic. Unexpectedly, in the transformation practice, a small proportion of transformants showed Ura+ Lys+, which represented integration through NHEJ wherewith *URA3* got integrated and *LYS2* was not knocked out. These transformants were easily selected with a double drop-out medium (Figure 9A). Surprisingly, the proportion of Ura+ Lys+ transformants in *qcr7*Δ was much lower compared with WT (Figure 9B), indicating a decrease in NHEJ/HR ratio when T-DNA was integrated. To test whether this is due to a general shift of NHEJ/HR activity in Qcr7p knockout, I tested the yeast strains with a competitive plasmid repair assay. A specially designed plasmid pQH213 was employed in this assay (Figure 10A), which carries two direct repeats in *URA3* coding sequence with two stop codon traps in between. A BamHI site is to cleave this plasmid in the middle of stop codon traps. The linearized plasmid would be cyclized by the DNA repair mechanisms of yeast, either by a recombination between two direct repeats (HR events), or by a direct end joining (NHEJ events) (Wilson 2002). His+ confirmed the acquisition of pQH213 in

transformant colonies. HR events would ensure a restored function of *URA3* thus showing an Ura3+ phenotype; while if NHEJ happened, the corresponding transformants were not able to survive on uracil dropout medium. As can been seen from Figure 10B, there was no statistical difference between *qcr7*Δ and WT, indicating that the NHEJ/HR ratio of *qcr7*Δwas not altered in the plasmid repair conditions.

The integration of T-DNA may not solely rely on host DNA repair mechanisms Virulence effectors of *Agrobacterium* could also be involved, for example, VirD2 which is covalently attached to the T-DNA strand. To date, the integration substrate of AMT has not been elucidated; it is possible that the T-DNA integration is through an ssDNA form which favors different mechanism of DNA repair from what was utilized in the competitive plasmid repair assay. Therefore, this interesting phenomenon of decreased NHEJ ratio in *qcr7*Δ is specific to AMT, and remains to be elucidated in the future.

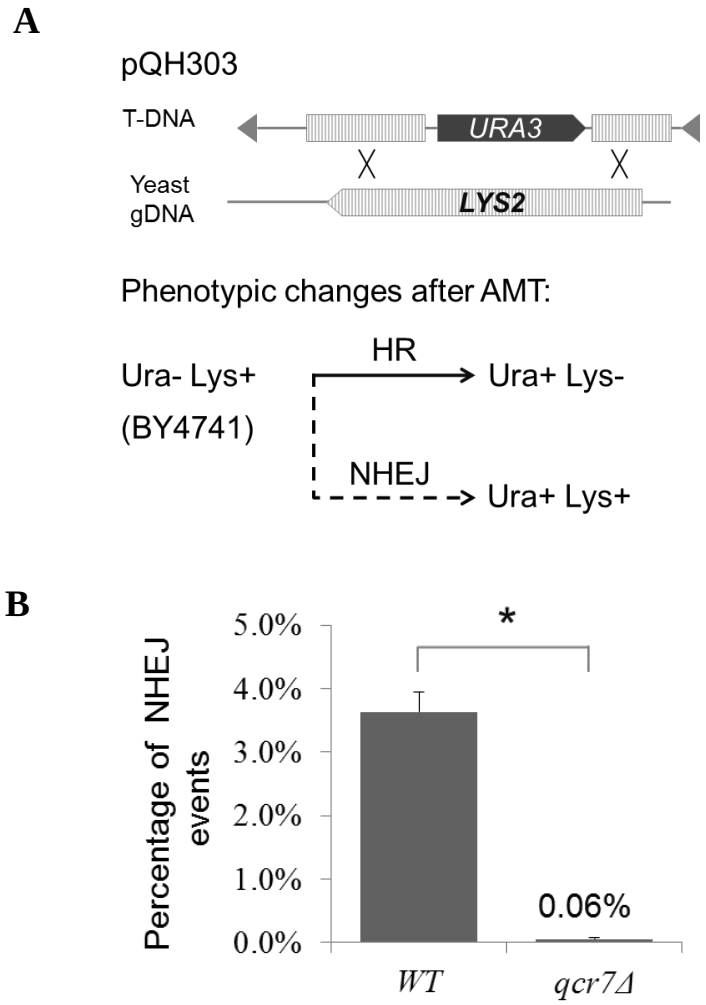

Figure 9. A knockout of Qcr7p showed decreased NHEJ ratio in AMT.

(A). Schematic diagram of the T-DNA integration with pQH303, a homologous recombination design; (B). Percentage of NHEJ events in overall transformants: The NHEJ events were selected with a –Ura –Lys double dropout medium, overall transformants were selected with a –Ura dropout. Mean value of three independent experiments was shown with standard deviation. * $p < 0.05$.

A

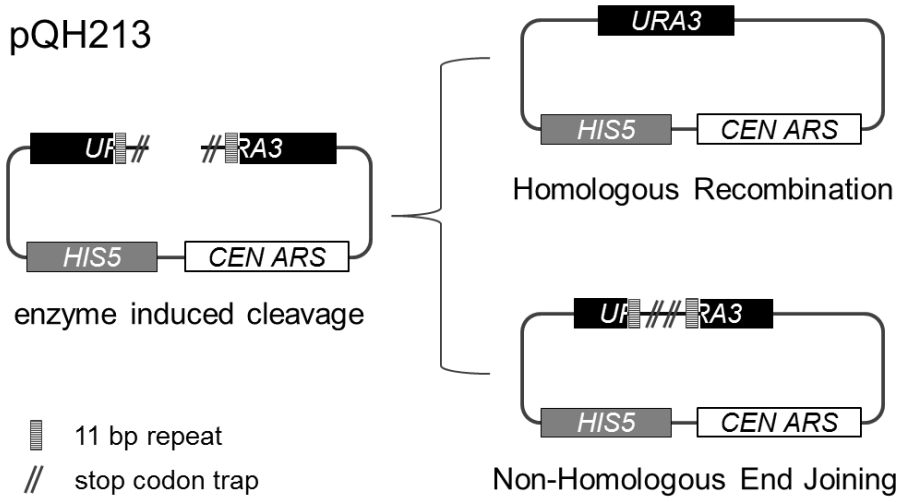

B

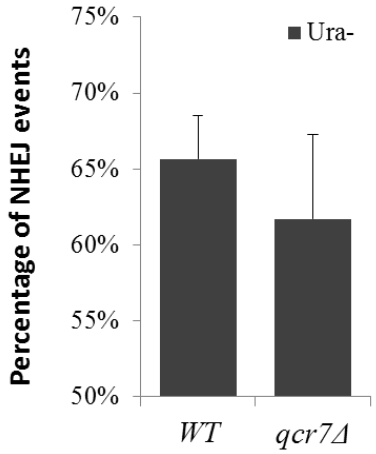

Figure 10. NHEJ/HR ratio as determined by competitive plasmid repair assay.

(A). Schematic diagram of competitive plasmid repair assay: specially designed pQH213 carries two 11 bp repeats and a stop codon trap in between. When a cleavage is introduced as designed, DNA repair will occur with two forms, 1) to restore a functional *URA3* by HR, or 2) to join the cleavage by NHEJ, therefore *URA3* is not functional.
(B). Percentage of NHEJ events in overall transformants: total transformants were selected with –His dropout medium, and the colonies were then transferred to a –Ura dropout medium. Ura+ colonies were identified as HR events, the rest were NHEJ events. Presented are a percentage of NHEJ events. Mean value of three independent experiments was shown with standard deviation.

3.3. A knockout of Qcr7p did not affect VirD2 nuclear localization activity

A quite distinct aspect of AMT from LiAc methods is the involvement of a series of virulent proteins (reviewed in Chapter 1). They actively participate in the formation, trafficking and integration of T-DNA along this trans-kingdom journey. Among those, VirD2 is a crucial player by introducing single-strand-specific nick in border repeats of T-DNA region and forming a covalent phosphodiester bond to 5'end of the nicked T-strand (Filichkin *et al.* 1993; Scheiffele *et al.* 1995). VirD2 contains two distinct functional nuclear localization signals (NLSs), so it is postulated to facilitate the movement of the T-complex and target it to the nucleus of recipient cell (Howard *et al.* 1992; Rossi *et al.* 1993).

To detect a possible change of motility of VirD2 in *qcr7*Δ, which might in turn lead to an altered AMT efficiency, a time course study of VirD2 localization assay was performed. Yeast strains were transformed with pYES2-*GFP:virD2*, an galactose inducible expression vector encoding GFP:VirD2 fusion protein (Figure 11A). Upon induction, GFP:VirD2 was expressed in cytoplasm and subsequently localized into nucleus. By observing the in-nucleus signal percentage in a time course manner, the motility of VirD2 in yeast strains was reflected. Control experiments were conducted with the same vector expressing GFP only, pYES2-*GFP*. Time course study of GFP expression ruled out the possibility of discrepant expression ability by *qcr7*Δ

and WT (Figure 11D), justifying the comparison of nuclear signal percentage of GFP:VirD2 between the two strains. Figure 11B shows the nuclear localization of VirD2:GFP upon galactose induction. Along with the time post induction, cells with illuminated nucleus increased due to accumulation effects. Two accumulating curves are comparable as shown in Figure 11C, which implies that the localization ability of VirD2 protein was not elevated or disturbed by knocking out of Qcr7p.

Although VirE2 also contains nuclear localization signals (NLS) that facilitate import of the T-complex into the nucleus (Zupan *et al.* 1996; Citovsky *et al.* 1997; Ziemienowicz *et al.* 2001), it fails to localize into nucleus in non-plant species (Tzfira *et al.* 2001). Therefore, in this study, an analogous experiment on VirE2 was not performed.

A


P gal1
GFP
virD2
T cyc1

B

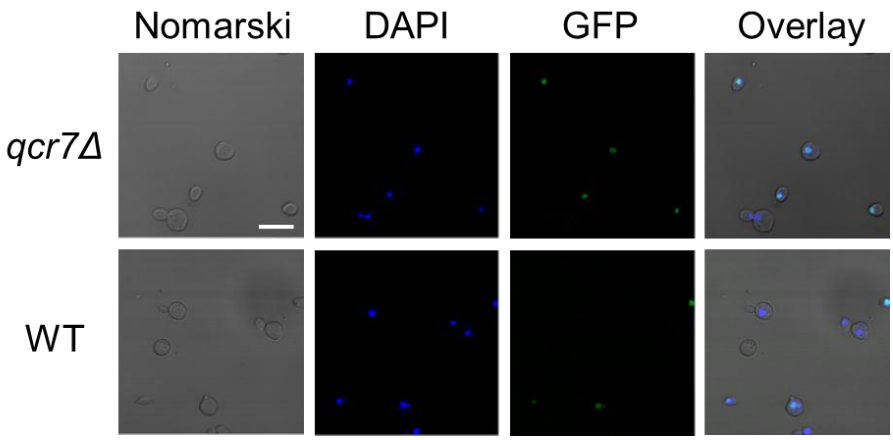
Nomarski
DAPI
GFP
Overlay
qcr7Δ
WT

C

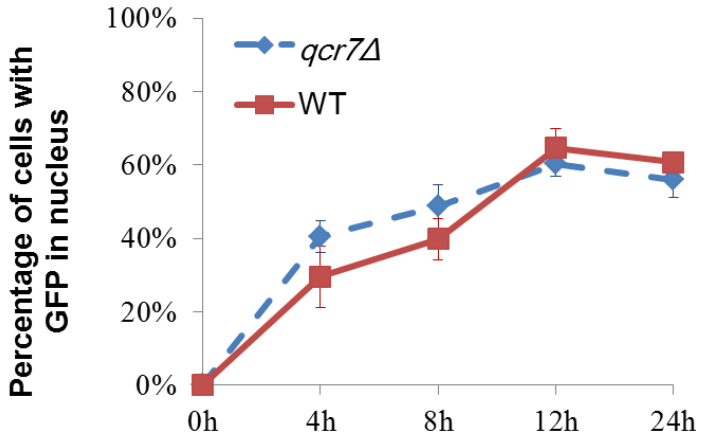
Percentage of cells with GFP in nucleus
100%
80%
60%
40%
20%
0%
qcr7Δ
WT
0h
4h
8h
12h
24h

D

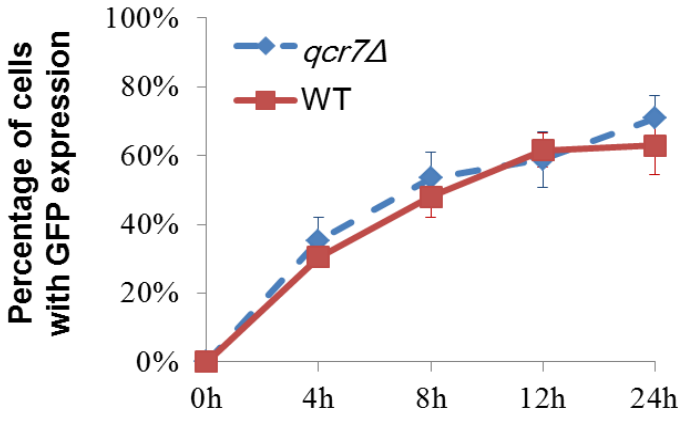
Percentage of cells with GFP expression
100%
80%
60%
40%
20%
0%
qcr7Δ
WT
0h
4h
8h
12h
24h

Figure 11. A knockout of Qcr7p did not affect VirD2 nuclear localization activity.

(A). *GFP* was fused with *virD2* at N terminus. The fusion gene was cloned into pYES2, downstream of a galactose inducible promoter. This construct was used in subsequent time course study.
(B). Nuclear localization of GFP-VirD2. Bar, 10 μm.
(C). Percentage of cells with GFP in nucleus, when expressing GFP:VirD2. Yeast cells were cultured overnight in a non-inducible medium, and subcultured in a galactose medium to induce expression of fusion protein.
(D).The control experiment expressed only GFP in yeast strains. Percentage of GFP positive cells is shown in a time course. For (C-D), at least 6 random fields were captured, and a total number over 100 cells were counted at each time point. Mean value of three independent experiments is shown with standard deviation.

3.4. A knockout of Qcr7p showed an increased competency to *Agrobacterium*-mediated delivery of T-DNA and VirE2

3.4.1. A knockout of Qcr7p showed an increased competency to *Agrobacterium*-mediated delivery of T-DNA

To analyze the reasons for enhanced transformation efficiency, the trans-membrane delivery of T-DNA was the first aspect to investigate. Thus, T-DNA amount was detected in cocultivated yeast cells. In order to examine the delivery, T-DNA is not supposed to replicate in recipient yeast cells. Therefore, EHA105(pQH302) was employed for cocultivation. The extremely low efficiency of this construct ensures that the T-DNA has little chance of integration, so that the PCR detected T-DNA is delivered by *Agrobacterium*.

Before quantifying the amount of T-DNA received in yeast cells, cocultivated mixtures were subject to repeated differential centrifugation to remove majority of agrobacteria. Because of the nature of *Agrobacterium*-host attachment by the T4SS apparatus (Lippincott *et al.* 1977), contaminant agrobacteria can never be completely eliminated. Therefore, DNA sequence from Ti plasmid was also quantified to provide a control of contamination.

Total DNA samples were prepared as described (Looke *et al.* 2011). PCR was conducted with three pairs of primers detecting Ti plasmid (VirE2seqF, VirE2seqR), T-DNA (URA3INF, URA3INR), and yeast genome (PMP3F, PMP3R), respectively. PCR cycles were determined in such way that Ti products were under detection limit, and yeast genome amplicons were

detected but not saturated. In this study, with a template amount of 100 ng DNA, practical cycle numbers were around 25-28. As can be seen in Figure 12A, the band for T-DNA detected from cocultivated *qcr7*Δ was much stronger than that from wild type. Quantification was later performed by real-time PCR, which showed an over five folds increase of T-DNA level in *qcr7*Δ than in WT (Figure 12B). For physicochemical transformation, like LiAc and electroporation, exogenous DNA must pass through the cell wall and plasma membrane and be delivered in the cytosol to reach the nucleus. Regardless of the pathways that make the nucleus accessible to exogenous DNA, the amount of input DNA makes a remarkable difference to transformation efficiency. Under the same experimental setting, transformation efficiency of WT yeast appeared positively correlated with DNA input. When the DNA amount was increased five folds, transformation efficiency rose with an even higher proportion (Figure 12D). These results revealed a direct cause of enhanced transformation efficiency – an elevated cellular T-DNA level.

It should be noticed that T-DNA level detected in yeast cells was a balance of delivery from the bacterium and degradation in yeast. So an immediate question would be: which part, delivery or degradation, contributed to the elevated T-DNA level in *qcr7*Δ? As commonly believed, T-DNA strand is coated with VirE2 and covalently attached with VirD2 at the 5’ end. Equipped well as a T-complex, the T-DNA should be relatively stable in recipient cells, especially in non-plant species yeast which lacks corresponding

degradation mechanisms (Tzfira *et al.* 2001; Lacroix *et al.* 2005). To test the stability of delivered T-DNA in yeast cells, cocultivated yeast samples were resuspended in $IBPO_4$ after removing the bacteria and incubated at 20 ℃ for another 24 h. During this period, no delivery was continuing, and the existing T-DNA was only subject to degradation. Samples underwent anther 24 h were marked as Day 2, while wash-off samples were marked Day 1. DNA of yeast samples at both time points were extracted for qPCR analysis. T-DNA quantity of Day 2 was normalized by that of Day 1, presented in percentage. When suspended in $IBPO_4$ at 20 ℃, yeast growth was limited. Thus, the decrement largely reflected the degradation activity. In this experiment, *qcr7*Δ showed a level of about 70% T-DNA was remaining, and nearly 80% in WT (Figure 12C), with no statistical difference between these two. This result demonstrates that degradation did not play a major role in the intracellular T-DNA level. Therefore, it was unlikely a cause of discrepancy between *qcr7*Δ and WT. Taken together, the elevated level of T-DNA in *qcr7*Δ was most probably due to enhanced delivery of T-DNA, which finally contributed to the enhanced AMT efficiency.

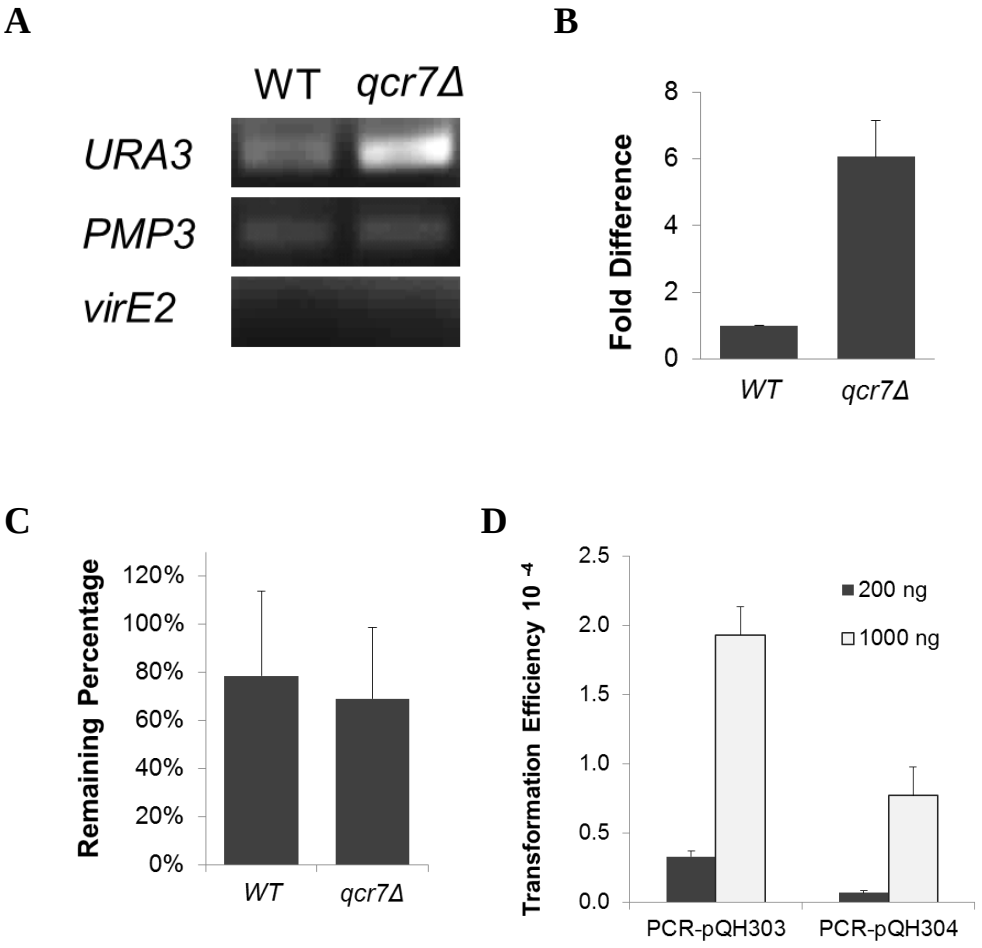

Figure 12. A knockout of Qcr7p led to increased competency to T-DNA transfer.

(A). Semi-quantitative PCR analysis of T-DNA delivery, *URA3*: T-DNA, *PMP3*: loading control for yeast genomic DNA, *virE2*: contaminant DNA control from Ti plasmid.
(B). real-time PCR analysis of T-DNA delivery. (C). Cellular T-DNA level remains after 24 hours prolonged incubation without agrobacteria, reflecting the yeast degradation effect to T-DNA. (D). LiAc transformation of WT yeast with different amounts of PCR amplified T region. Mean value of three independent experiments is shown with standard deviation.

3.4.2. A knockout of Qcr7p showed an increased competency to *Agrobacterium*-mediated delivery of VirE2

The T4SS of *Agrobacterium* does not only delivers T-DNA, but also secrets effector proteins into host cells interacting with numerous host factors to facilitate T-complex transport and T-DNA integration (reviewed in Chapter 1). Hence, the increased T-DNA delivery intrigues a question that whether the same situation applies to the effector proteins. Among those, VirE2 is the most abundant protein translocated into recipient cells (Citovsky *et al.* 1988), making it a preferable candidate for delivery study. In the past decade, a Cre recombinase assay for translocation (CRAfT) method was developed for quantification of translocated Vir proteins (Vergunst *et al.* 2000). CRAfT utilizes Cre recombinase as a reporter protein. Cre (343 aa) is a member of the integrase family of site specific recombinase, which catalyses the site specific recombination between a pair of short target sequences called the LoxP sequences. Cre-LoxP recombination is widely used to carry out deletions, translocations and inversions in the DNA of cells (Sauer 1987). In CRAfT, LoxP flanked (floxed) *URA3* was integrated into yeast genome first, Cre was fused with a series of vir proteins at the N terminal and expressed by agrobacteria. Successful translocation of fusion virulent effectors leads to excision of floxed *URA3*from genome, making the recipient survival through 5-FOA selection (counter-selection reagent for *URA3*). With this method, the delivery efficiency of each Cre-vir fusion proteins was calculated. The

reported efficiency of Cre:VirE2 delivery in yeast is at 10^{-2} (Schrammeijer *et al.* 2003). It would be quite interesting to know whether knockout of Qcr7p also resulted in an alteration of VirE2 delivery. However, CRAfT requires the fusion protein Cre:VirE2 localize in nucleus to carry out the recombinase activity, which is a downstream event of trans-membrane delivery. This requirement inevitably involves other processes in the reported delivery, making the result complicated. In addition, positive events rely on an enzymatically active fusion. Disruption to functions of either CRE or virulence effectors will lead to an artifact of reported delivery. Thus, an instant and precise approach for measuring VirE2 delivery would be able to generate more useful data about the bacterium-delivered VirE2

To instantly detect the bacterium-delivered VirE2 in yeast, we developed a novel approach with minimal disruption to the function of VirE2 and visualize it *in vivo*. This technique involves a split GFP system. With an only 16-residue peptide (GFP 11) inserted into a permissive site (Pro54) near N-terminus of VirE2, the virulence of VirE2 maintained intact. A non-florescent GFP1-10, the big fragment of GFP, was expressed in recipient cells, i.e. yeast. Upon delivery of GFP11 tagged VirE2, GFP1-10 would spontaneously bind to the exposed tag of VirE2::GFP11 fusion protein, whereby the florescence of GFP was restored. With this method, the percentage of yeast cells that received VirE2 can be easily visualized and calculated.

The *virE2* gene on Ti-plasmid (pTiBo542) was replaced by *virE2::GFP11* through a markerless gene replacement as described in Chapter 2, making a GFP11 tagged strain EHA105 *virE2::GFP11*. This strain was tested for its virulence as exhibited in AMT. Although VirE2 is not absolutely necessary for yeast transformation, with its existence the transformation efficiency was apparently higher. The tagged strain showed a full virulence as compared with its wild type EHA105 (Figure 13). VirE2::GFP11 is hereby a good representative of VirE2 in this study.

Expressing GFP1-10 in yeast can be easily achieved with a yeast expression vector, but the possible influence of selection marker on yeast growth should preferably be excluded. To circumvent this problem, a binary vector pQH305 was constructed by inserting a *Padh1:GFP1-10* cassette downstream of *URA3*. Therefore, the GFP1-10 expression cassette, together with *URA3*, is flanked by homologous arms derived from LYS2 *locus*. When transforming yeast with EHA105 (pQH305), the *Padh1:GFP1-10* cassette will be targeted into *LYS2* locus by HR. Thus the subsequent VirE2 delivery assay can be performed with the same condition as described for AMT of yeast previously. Figure 14A shows the complemented split GFP signal in yeast generated by the bacterium-delivered VirE2. The signals were cytoplasmic inside the yeast cell, without having to be in nucleus. Given extended observation time, the VirE2 kept still, suggesting a lack of host factors to facilitate its nuclear import (Tzfira *et al.* 2001). GFP positive cells were

counted among multiple microscopic fields for each strain. *qcr7*Δ showed a remarkably higher percentage of GFP positive cells (Figure 14B). Like what was discussed in the previous section, this observed percentage only reflected the balance of delivery and degradation of VirE2. Degradation must be properly evaluated before making any conclusion on the delivery aspect. In order to evaluate the contribution of degradation to this result, the cocultivated yeast (Day1) was resuspended in IBPO4 after removing bacteria by repeated differential centrifugation. This suspension was incubated at 20 ℃ for another 24 hours (Day 2). The GFP positive percentage at Day 2 was normalized by that was observed at Day 1, resulting in a remaining percentage showing how much GFP positive was remaining after 24 hours incubation (Figure 14C). Both *qcr7*Δ and WT showed near 80% signal remaining, and no statistical difference was detected between the two. This result suggests degradation was not a major player in this VirE2 visualization assay. To sum up, knockout of Qcr7p generally led to an enhanced delivery of VirE2 into yeast recipients.

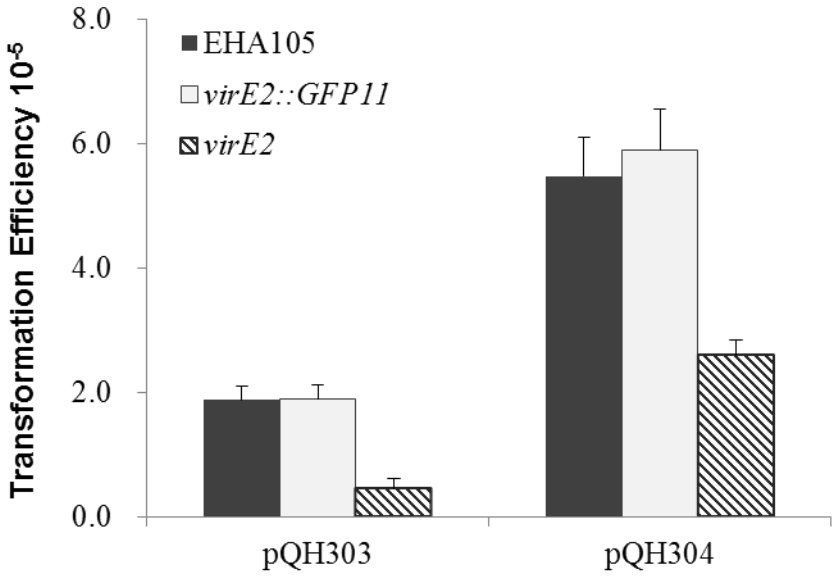

Figure 13. Fusion protein VirE2::GFP11 was functional in AMT.

The tagged strain EHA105 *virE2::GFP11* was compared with its wild type strain EHA105 and a VirE2 knockout strain EHA105 *virE2* in terms of the transformation efficiency. WT yeast was transformed with above strains carrying either pQH303 or pQH304.

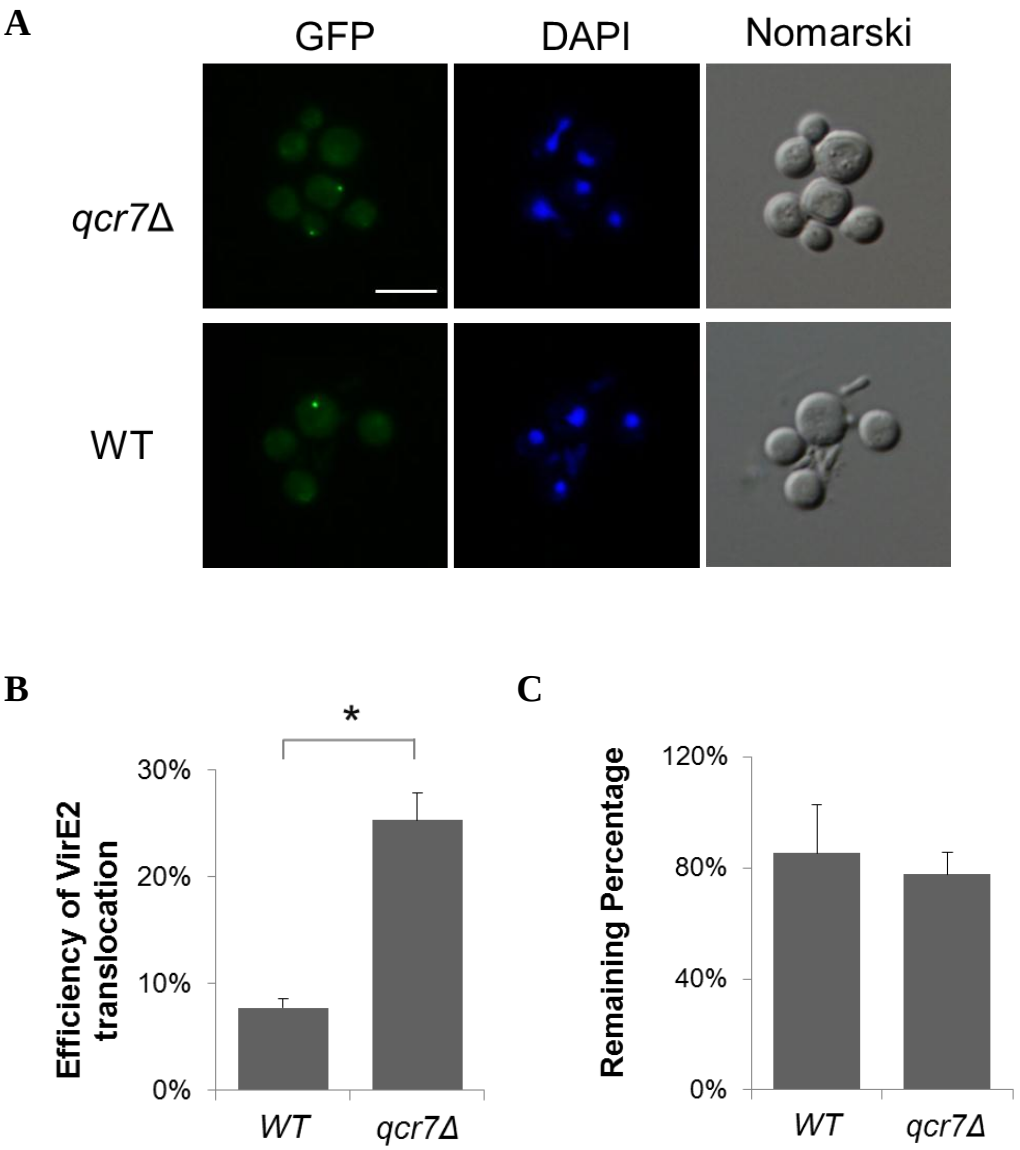

Figure 14. A knockout of Qcr7p led to increased competency to VirE2 transfer.

(A). VirE2 signals visualized in yeast cells. Yeast strains bearing pQH04-*S1-10* were cocultivated with EHA105 *virE2::GFP11*using the method as described in yeast AMT protocol. pQH04-*S1-10* enabled constitutive expression of GFP1-10 in yeast. GFP1-10 can recognize and bind to GFP11 tag, to restore green fluorescence. Bar, 10 μm.
(B). Efficiency of VirE2 translocation: percentage of VirE2 positive cells. At least 6 fields were randomly captured, with a total number of 500 cells counted. Mean value of three independent experiments is shown with standard deviation. * $p < 0.05$.
(C). VirE2 signal remains after 24 hours prolonged incubation without agrobacteria, reflecting the yeast degradation effect to VirE2. Mean value of three independent experiments is shown with standard deviation.

3.5. Analysis of an *Arabidopsis* mutant of Qcr7p homolog

AMT represents a favored approach to introduce genetic information into plants. But many commercially important species remain recalcitrant to transformation (Gelvin 2003). Analysis of the genetic background that makes plant species resistant or susceptible to AMT, hereby, is always the focal point. The role of Qcr7p in AMT would be more meaningful if the findings obtained from yeast can be expanded to plant species. Qcr7p belongs to the family of ubiquinol-cytochrome c reductase complex 14kD subunit (UQCRB family), and is conserved across eukaryotes. Figure 15 shows an alignment of Qcr7p homologs in several typical eukaryotic species, where two *Arabidopsis* homologs are listed, namely QCR71 (*AT4G32470*) and QCR72 (*AT5G25450*). So, it is of interest to know whether knockout of QCR71 or QCR72 can alter AMT efficiency of *Arabidopsis*.

In order to test loss-of-function mutants, T-DNA insertion lines were obtained from ABRC seed collection. Only *QCR71* has insertion mutant available (labeled 792), confirmed with RT PCR detection of mRNA (Figure 16A). So I firstly examined the susceptibility of *qcr71* mutant with a root segment tumorigenesis assay. Root samples were collected from 10 days seedlings geminated and grown on MS plates. The roots were harvested and cut into <5 mm segments. These segments were cocultivated with a tumor inducing strain A348 in darkness for two days. Then the segments were transferred into new MS plates (with cefotaxime to kill the bacteria) and

incubated up to 4 weeks in room temperature for tumor formation (Figure 16B). 66.7% of root segments from 792 developed tumors, very close to that of Col-0: 61.8% (Figure 16C). This result shows that *qcr71* is not more susceptible to AMT compared with the wild type Col-0. However, due to the existence of another homologous locus, whether Arabidopsis QCR7 is involved in transformation still remains unknown. For a better understanding of this question, both homologs are to be knocked down in future analysis.

Figure 15. Qcr7p is conserved across eukaryotes.

Alignment was made by Uniprot (http://www.uniprot.org/)
ARATH: *Arabidopsis thaliana.* FASHE: *Fasciola hepatica* (Liver fluke). HUMAN: *Homo sapiens.*
MOUSE: *Mus musculus*. SOLTU: *Solanum tuberosum* (Potato). YEAST: *Saccharomyces cerevisiae*.
SCHMA: *Schistosoma mansoni* (Blood fluke). BOVIN: *Bos taurus*

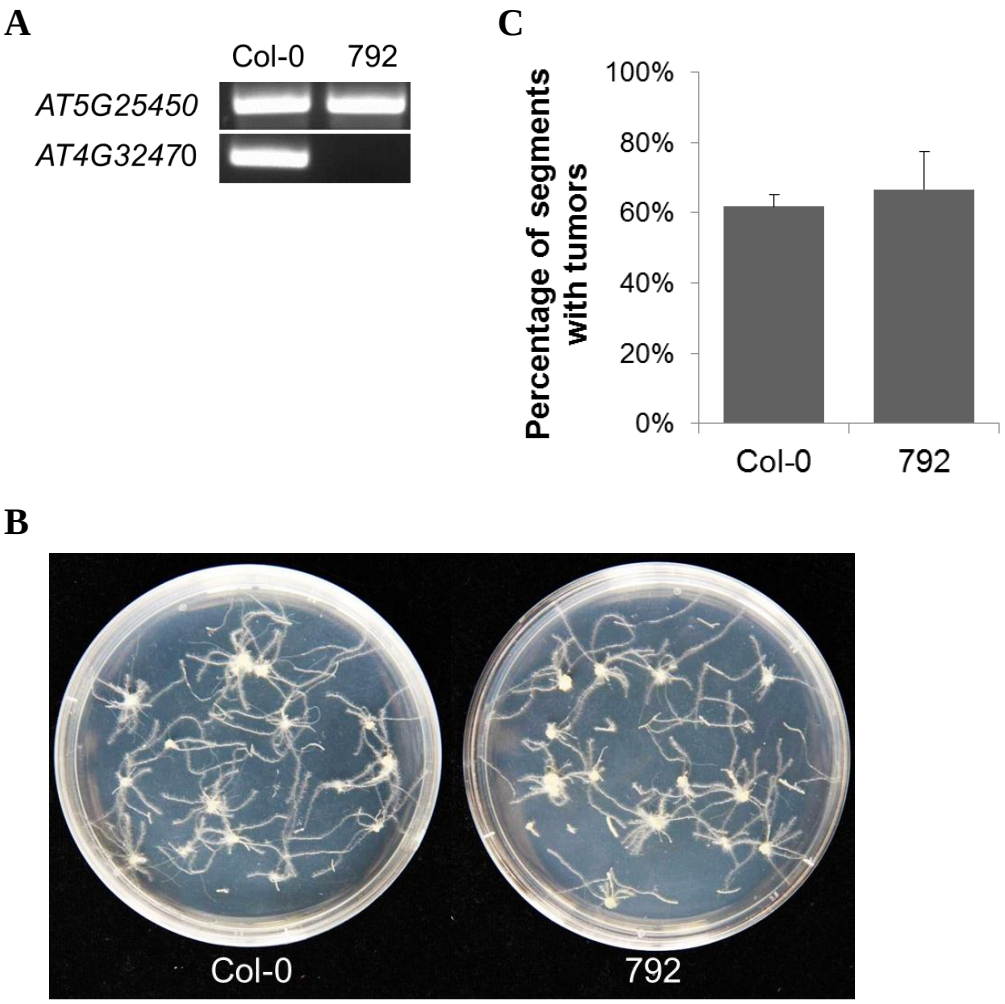

Figure 16. Root segment tumorigenesis of an *Arabidopsis* mutant in Qcr7p homolog.

(A). RT-PCR confirmation of *QCR7* mRNA in an *Arabidopsis* mutant line.
(B). Tumorigenesis assay. The roots were collected from 10 days seedlings, and cut into <5 mm segments. These segments were cocultivated with a tumor inducing strain A348 for two days on an MS plate, and then transferred onto an MS cefotaxime plate for 4 weeks incubation at dark.
(C). Percentage of root segments with tumors formed in total population.

3.6. Discussion

During the past decade, tremendous endeavors were done to elucidate the T-DNA trafficking process inside eukaryotic hosts. One of those was to identify and characterize the host factors that affect AMT (reviewed in Chapter 1). Although plant species are the natural host of *Agrobacterium*, their genome sizes are diversified and variable from species to species. And plant genomes contain a large percentage of repetitive sequences. These features made plant species unfavorable for this study. Nevertheless, *Agrobacterium* has been found capable of transferring genetic information to a very wide spectrum of species, including the very basic form of eukaryotic life, yeast. This led to the development of transformation techniques in yeast species, such as *S. cerevisiae*. These techniques paved the way for studying this unique transformation process in unicellular organisms which possess a compact yet essential genetic background.

Soltani developed a high throughput transformation method, with which he screened the genome of diploid deletion pool of BY4743 based knockout library (Soltani 2009). Tu conducted a similar research with haploid mutants from BY4741 knockout library (Tu 2010). Both research revealed several important pathways, and both included mitochondrial components. To achieve genome-wide screening, throughput was made very high so that reliability was inevitably sacrificed. Therefore, this research began with a standard AMT protocol and screened several mitochondrial mutants. Mitochondrion is critical

not only as a bio-energy reactor, but also participates in signaling of cell death. This makes mitochondrion a prime target for pathogenic apoptosis-modulating factors and for the signaling cascades influenced by pathogenic infection (Bohme *et al.* 2009; Rudel *et al.* 2010).

This work showed that mutation in some complex III components of mitochondrial ETC enhanced the transformation efficiency of yeast, especially when Qcr7p was knocked out. By dissecting the transformation process, we roughly segment this interactive process into three steps: T-DNA translocation (trans-membrane delivery), intracellular movement and T-DNA integration (in yeast, integration includes cyclization of T-DNA to form a plasmid). Therefore, exploration of the reasons for enhanced transformation efficiency was conducted according to the above aspects.

In this research, a higher level of T-DNA and VirE2 was detected in *qcr7*Δ. With examination of corresponding degradation effects, both elevated levels were proved to be dominated by delivery rather than degradation. Hereby, I conclude that the enhanced transformation efficiency was most probably caused by an increased competency to T-DNA and VirE2 delivery. To date, reported mechanisms of *Agrobacterium*-host interaction largely focused on the trafficking and integration mechanism whereby the plant immune system was subverted and hijacked to facilitate the nuclear import and integration of T-DNA(Tzfira *et al.* 2001; Lacroix *et al.* 2005; Djamei *et al.* 2007; Zaltsman *et al.* 2010). Little is known regarding the delivery. Therefore,

the finding in this study adds knowledge to this transformation process in a new perspective.

Possible alteration in trafficking was also examined in *qcr7*Δ. VirD2 has an NLS sequence and functions as a pilot protein covalently attached to T-DNA. Therefore examination of the nuclear localization activity of VirD2 can provide useful information of T-DNA nuclear import. VirD2 localization assay on time course basis did not show evidence of altered nuclear localization activity of VirD2. VirE2, another protein closely associated with T-DNA, was proved immobile by newly established split GFP assay. Attempts of detecting T-DNA with FISH was also done, but failed to give out useful signals (data not shown). Based on the above evidence, no explanation can be made from the perspective of intracellular trafficking.

When T-DNA integration was analyzed, Qcr7p knockout showed a surprisingly decreased NHEJ ratio in total transformants by EHA105 (pQH303). Although this result clearly indicates a shift between NHEJ/HR activities, a competitive plasmid repair assay failed to show a similar effect in cyclization of a linearized plasmid DNA. This specific effect in AMT therefore intrigues a question whether T-DNA utilizes a special mechanism to achieve chromosomal integration.

Since complex III functions in the inner membrane of a mitochondrion, its connection to changes happen at the outer part of a cell will be indirect. Mitochondrion is one important partner in energy production, ROS generation

and membrane potential regulation. These roles might help mitochondria be involved in AMT through general changes in cellular chemical or physical conditions. Detailed mechanism remains to be explored in future endeavors.

Although the method for VirE2 visualization was developed to meet the need of detecting the efficiency of VirE2 delivery, it turned out to be strikingly powerful by proving that *Agrobacterium* achieved such a high ratio of protein delivery. In this research, 8% of the wild type yeast received VirE2 under predetermined transformation parameters, several hundred folds higher than genetic transformation efficiency (at a level of 10^{-4} in this study). Much higher efficiency (>50%) was obtained under optimized condition (unpublished data). This finding subverted the knowledge of *Agrobacterium* being a genetic engineer, and proved it as an excellent protein transporter. In the following section of this thesis, application of this promising method in plant species will be described.

Chapter 4. Direct visualization of *Agrobacterium*-delivered VirE2 in *N. benthamiana*

4.1. Introduction

A number of bacterial pathogens evolved specialized secretion machinery for delivering effectors to the cytosols of plant or mammalian host cells during infection. The T4SS of *A. tumefaciens* is known to translocate diverse macromolecule substrates into recipient cells. Besides T-DNA strand, a series of virulence proteins are also translocated, including VirD2, VirD5, VirE2, VirE3, and VirF (Citovsky *et al.* 1992; Howard *et al.* 1992; Schrammeijer *et al.* 2003; Tzfira *et al.* 2004). These proteins are virulence effectors, which interact with host factors in recipient cells to facilitate transformation.

Among these effectors, VirE2 was the most abundant protein delivered in to recipient cells (Engstrom *et al.* 1987). It may help in allowing passage of the T-DNA complex by forming a pore in the plant plasma membrane (Duckely *et al.* 2005) and coats the T-DNA strand in the plant cytoplasm to protect it against nucleolytic attack (Rossi *et al.* 1996). It can also interact with plant VIP1, which relocalizes into nucleus upon phosphorylation, and several importin α isoforms, suggesting a role to mediate nucleus targeting of T-DNA (Tzfira *et al.* 2001; Djamei *et al.* 2007; Bhattacharjee *et al.* 2008). In addition, VirE2 was reported to mediate integration of T-DNA through association with

host VIP2(Anand *et al.* 2006). Information on localization, structure, and interaction of this protein can provide key insights into its functions. Therefore, visualization of VirE2 will make a great impact by directly revealing this critical information. However, neither the DNA nor protein molecules have been directly visualized in a bacterium-delivery manner. The subcellular localization of VirE2 also remains controversy, as both cytoplasmic and nuclear localization of VirE2 has been reported (Citovsky *et al.* 1994; Zupan *et al.* 1996; Ziemienowicz *et al.* 2001; Bhattacharjee *et al.* 2008). These studies artificially introduce VirE2 into the plant cells either by directly uptake or transgenic expression, which may differ from what happens during natural AMT process. Moreover, VirE2 is a "vulnerable" protein that is sensitive to protein tagging. Full-length GFP protein tagged at either the C-terminus or N-terminus will block its translocation activity (Zhou *et al.* 1999; Simone *et al.* 2001; Christie 2004), making it difficult to track VirE2 protein by natural translocation. Here, we adapted a recently developed split-GFP system (Cabantous *et al.* 2005) and successfully visualized the VirE2 in host cells during natural transformation process.

The achievement of direct visualization of bacterium-delivered VirE2 illuminated the hope of tracking T-DNA complex in the recipient cells, especially in plant species where natural transformation occurs. In this part, the method for VirE2 visualization was successfully implemented into a plant species. Delivery efficiency, localization and intracellular trafficking of

bacterium-delivered VirE2 in *N. benthamiana* were observed.

4.2. Development of the method for visualization of *Agrobacterium*-delivered VirE2

Visualization of a protein of interest is usually achieved by fusing this protein with fluorescent reporters. But it may exhibit altered processing (Bertens *et al.* 2003) or mis-folding (Waldo *et al.* 1999). Moreover, the fusion partner inevitably enlarges the protein size, and may also compromise certain original activities due to steric hindrance.

The endeavor of visualizing VirE2 has been a common interest for a decade. Lacroix *et al*. co-expressed GFP:VirE2 and other interaction partners in plant cells, revealing the coorperation mechanism of VirE2 nuclear import (Lacroix *et al.* 2005). Exogenously expressed YFP:VirE2 was also reported never to be in nucleus in localization study, and a BiFC (Citovsky *et al.* 2006) approach was also employed in this research for visualization of interaction activities (Bhattacharjee *et al.* 2008). Despite of these attempts, all visualization information was obtained through exogenous expression, which suffered from a giant gap from the true transformation scenario. In this case, expressing tagged VirE2 in *Agrobacterium* is a necessary endeavor. But, addition of peptides or proteins to either N-or C- terminus of VirE2 resulted in a loss of protein function (Zhou *et al.* 1999). Despite the finding that a functional VirE2:YFP fusion complemented the virulence of a *virE* mutant

Agrobacterium strain when expressed in transgenic plants, it failed to implement its function when expressed by the bacterium (Bhattacharjee *et al.* 2008), suggesting a possible disruption to the translocation activity of VirE2. Zhang in Purdue University tried to capture images in a bacterium-delivery manner: a peptide aptamer fragment of VirE2–VirE2 interaction domain was fused with N terminal fragment of Venus (nVenus) and expressed in *Arabidopsis* roots; *Agrobacterium virE2* mutant strain expressing cCFP (83 residues) tagged VirE2 (VirE2i–cCFP) was used to infect aforementioned roots. Interaction of VirE2i-cCFP with the aptamer would bring together N-terminal and C-terminal fragments of the split-YFP derivatives, and the roots fluoresced yellow (Gelvin 2010). This interesting attempt was only documented in Gelvin's review, and was not published independently as a research article. In this work, yellow signals from VirE2 were visualized in a diffusion pattern all over root cells, which cannot be easily explained with current knowledge.

In summary, the visualization of *Agrobacterium*-delivered VirE2 by now has been proven extremely difficult. The ideal tagging system for VirE2 should overcome two technique obstacles: not to obstruct the translocation activity, and not to disturb the virulence function.

Here I show that a split GFP system best fulfilled the requirements. It is a pair of self-associating fragments of modified GFP molecule that can be employed to tag either soluble or insoluble proteins in living cells. In this

system, the protein of interest is fused to a small GFP fragment (β-strand 11, residues 215–230), with a linker sequence if possible. The large, complementary GFP fragment (β-strands 1–10, residues 1–214) is expressed separately. Either part alone does not produce fluorescence. When encountered, the small and large GFP fragments combine spontaneously, resulting in GFP folding and generation of the fluorophore (Cabantous *et al.* 2005). The tagging partner GFP11 is a 16-residue peptide, which is much shorter than fragmented parts in BiFC. A smaller tag greatly raised the probability of non-perturbing insertion to possible tolerant sites. Zhou *et al.* reported a permissive site for short peptide insertion, which was discovered through transposon mutagenesis of VirE2 (Zhou *et al.* 1999). The reported tolerance is 31 residues, which is nearly twice as long as the proposed GFP11 tag. This site is located between Pro38 and Thr39 of octopine-type pTiA6NC, whereas in this study an *A. tumefaciens* strain bearing pTiBo542 was employed. Thus, we aligned amino acid residue sequences of VirE2 in both Ti plasmids, and determined Pro54 as the permissive site for our work.

We inserted the coding sequence of GFP11 into the permissive site of VirE2, resulting in *virE2::GFP11*. Gene substitution was done with an markerless gene replacement method as described previously (Hoang *et al.* 1998). The fusion gene *virE2::GFP11*, together with an upstream *virE1* (to provide a longer homologous arm), was cloned into a gene replacement vector pEx18TcKm, a modified version of pEx18Tc with an insertion of an *nptIII*

cassette. The fusion gene was targeted to pTiBo542 to substitute the native *virE2*. *GFP1-10* was cloned into plant expression vector downstream of 35S promoter (pQH308), or driven by an *AHD1* promoter when used in yeast (pQH04-*S1-10*). Before agroinfection, GFP1-10 was expressed separately in recipient cells; *Agrobacterium* strain EHA105 *virE2::GFP11* was induced at 25 ℃ for 16 hours with AS. Omission of induction process is possible for plant infection. For visualization in *S. cerevisiae*, yeast strain bearing pQH04-*S1-10* was cocultivated with EHA105 *virE2::GFP11*, as described for AMT of yeast; for visualization in *N. benthamiana*, EHA105 *virE2::GFP11* (pQH308) was used to perform agroinfiltration. A schematic representation of this method is shown in Figure 17.

To demonstrate that VirE2::GFP11 fulfilled the function of native VirE2, virulence of EHA105 *virE2::GFP11* was compared with wild type EHA105 in a tumorigenesis assay as described (Guo *et al.* 2007). Since EHA105 is disarmed and cannot cause tumor formation in infected plant tissues, a tumor inducing strain A348 was mixed with testing strains to provide hormone-encoding T-DNA. As shown in Figure 18, tumors caused by A348 + EHA105 *virE2::GFP11* was identical in size compared to those caused by A348 + EHA105, suggesting that VirE2::GFP11 functions similarly to VirE2 in plant species. This is consistent with the virulence test performed in earlier section (Figure 13), demonstrating that VirE2::GFP11 fulfilled the function of native VirE2 to our knowledge.

To visualize VirE2 in *N. benthamiana* leaf cells. Overnight culture of EHA105(pQH308) and EHA105 *virE2::GFP11* were mixed at 1:1, and infiltrated into a fully expanded leaf of a 4~6 week old plant. Images were taken three days post infection, to provide sufficient period for both expression and delivery. GFP signals were successfully detected, with DsRed outlining the cell shape as shown in Figure 19.

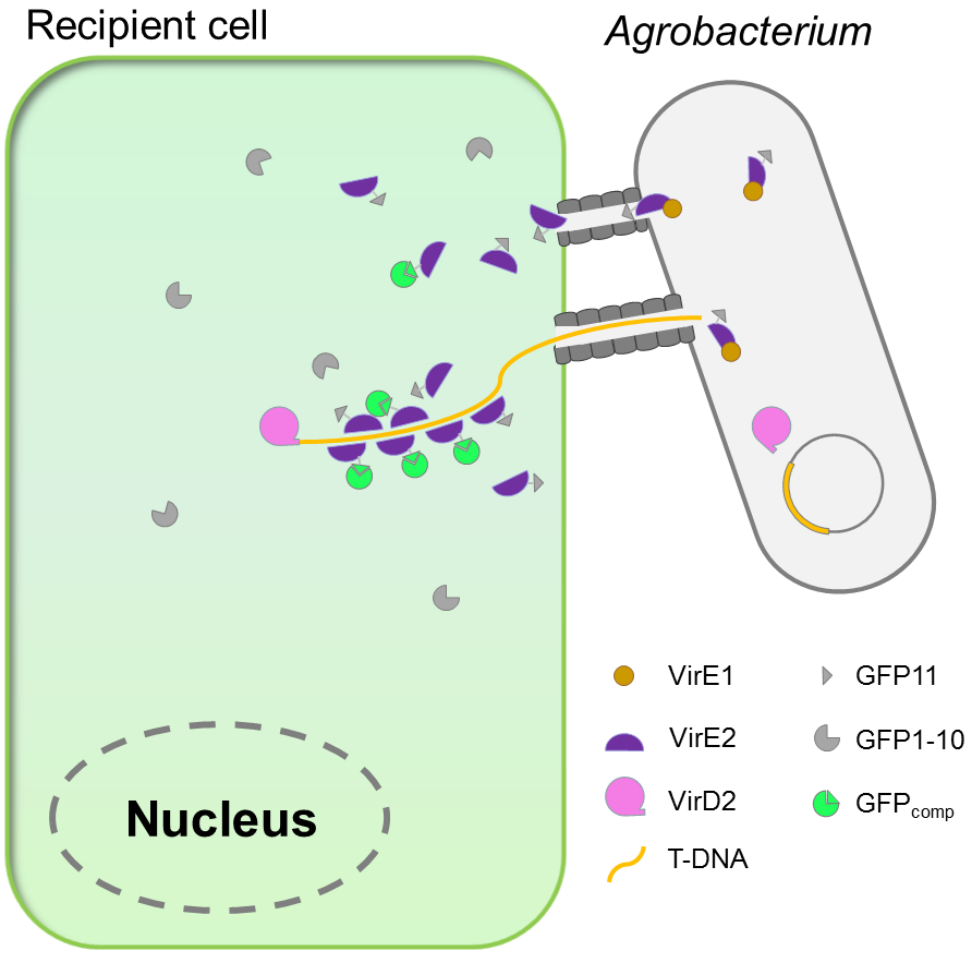

Figure 17. Schematic representation of visualizing VirE2 with a split GFP system.

VirE2was fused with GFP11 at Pro54, a reported permissive site. Native *virE2* was substituted with *virE2::GFP11* through markerless gene replacement. GFP1-10 was expressed in the recipient cell. Upon translocation of VirE2::GFP11, GFP1-10 will spontaneously recognize and bind to the small tag GFP11, and thus the green fluorescence was restored. The self-assembly nature of VirE2 or the formation of T-complex made the signals generated by VirE2 strong enough to be detected.

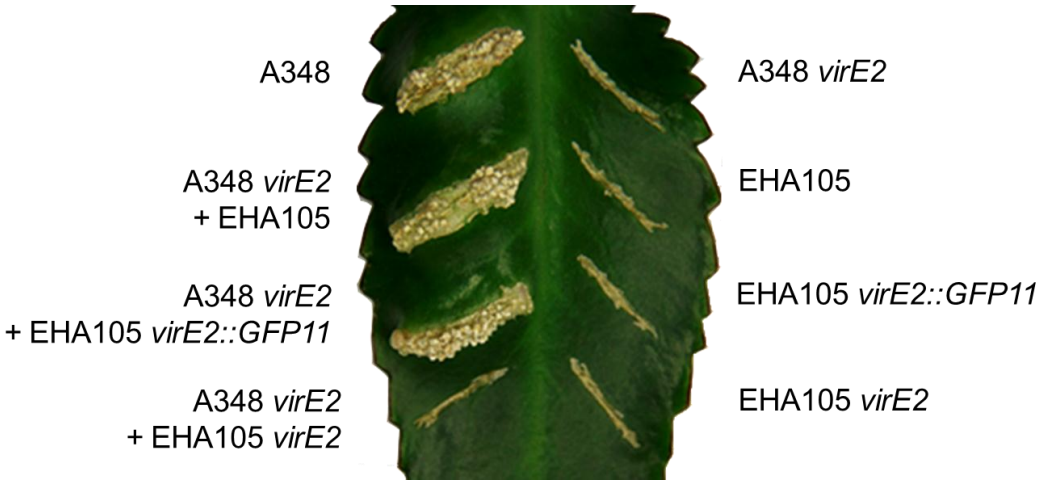

Figure 18. Fusion protein VirE2::GFP11 was functional in a leaf tumor assay.

A fully expended leaf from *Kalanchoe* was scraped with a needle to introduce physical wounds. 10 μl bacteria culture was applied to the wound site. Tumors would form in 4 weeks when infected with a tumor inducing strain. A348 is a tumor inducing strain that can independently cause tumor formation. Without VirE2, the virulence of A348 was almost completely compromised. A mixture of A348 *virE2* with an EHA105 strain restored the virulence with VirE2 delivered by EHA105. When A348 *virE2* was mixed with EHA105 *virE2::GFP11*, the tumor formation ability was comparable with A348 alone or A348 *virE2* + EHA105.

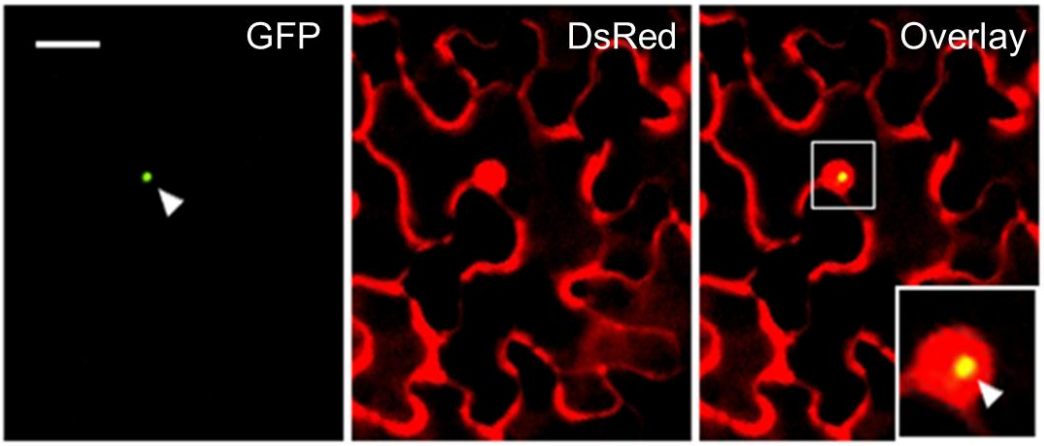

Figure 19. Visualization of VirE2 inside *N. benthamiana* leaf cells.

A. tumefaciens strain EHA105 *virE2::GFP11* (pQH308) was infiltrated into *N. benthiamiana* leaves by a syringe. The leaf tissues were observed at 3 d after infiltration under a fluorescent microscope BX53 (Olympus) with a Digital Camera DP72 (Olympus). The GFP signal (arrowed) was detected inside plant nucleus. DsRed was expressed from T-DNA transferred into plant cells so that cellular locations were indicated. Bar: 20 μm.

4.3. Localization of VirE2 in *N. benthamiana* leaf cells

Since the T-strand is principally coated with VirE2 molecules, the localization of VirE2 became an important issue for uncovering T-DNA behavior. *Agrobacterium* biologists have long been interested in its localization in various hosts for recent two decades. By fusing with reporters, such as GUS and GFP, the localization of VirE2 was reported to be in the nucleus in certain plant species (Citovsky *et al.* 1992; Citovsky *et al.* 1994; Tzfira *et al.* 2001), and be cytoplasmic in yeast or mammalian cells (Guralnick *et al.* 1996; Rhee *et al.* 2000; Tzfira *et al.* 2001). But due to aforementioned technical problems, these reports were only based on exogenous expression of fusion protein in the observed cell types. Thus the reported information remains unauthentic until *Agrobacterium*-delivered VirE2 was observed, however this has been extremely challenging.

With development of the new method for visualizing bacterium-delivered VirE2, we were able to observe its localization in accordance with the natural behavior during transformation process. In line with previous findings, we observed nuclear localization of VirE2 in leaf cells of *N. benthamiana* with the split GFP assay (Figure 19). While in yeast cells the localization was cytoplasmic (Figure 14A). Difference in localization may reflect that specific host factors were involved, which is in consistent with the findings of MAPK-VIP1 nuclear targeting mechanism (Tzfira *et al.* 2001; Djamei *et al.* 2007).

4.4. Efficient delivery of VirE2 was observed in N. benthamiana leaves

Visualization of VirE2 not only showed its localization, but also revealed the delivery efficiency. When the N. benthamiana leaves were infiltrated with *A. tumefaciens* strain EHA105(pQH122) which transfers an T-DNA encoding *35S::DsRed*, a very large percentage of transient expression in infiltrated tissues was observed , nearly 100% as demonstrated in Figure 20A. On the contrary, when infiltrated with EHA105 *virE2*(pQH122) the transient expression was almost totally abolished (Figure 20A). This result was in consistent with the previous report that when VirE2 is absent, transient expression is abolished or lowered (Nester *et al.* 1993). Herein lies a fact that VirE2 must have been efficiently delivered so that transient expression efficiency can achieve at a high level.

Previously, Vergunst *et al.* reported a delivery efficiency of Cre::VirE2 to *Arabidopsis* root segments at 20/300 and 25/325 (calli/explants), determined by CRAfT (Vergunst *et al.* 2000). It was for the first time that translocation of VirE2 had been detected. However, CRAfT requires nuclear localization of the fusion protein Cre:VirE2 to carry out the recombinase activity, thus representing a retarded reporter system. In this way, downstream processes of trans-membrane delivery were inevitably involved, making it more complicated. In addition, the fusion significantly enlarged the protein size, which may introduce spatial hindrance to certain important activity centers of

VirE2. It could be possible reasons why the delivery of VirE2 has been underestimated. With the newly developed method, we were able to observed VirE2 with more faithful delivery efficiency. As can be seen from Figure 20B, almost every cell in the microscopic flied received at least one VirE2 signal, which may truly reflect the powerful capability of *A. tumefaciens* as an excellent protein transporter. In addition, such a high efficiency also made analysis on VirE2 behavior easier by providing multiple signals within one microscopic field.

A

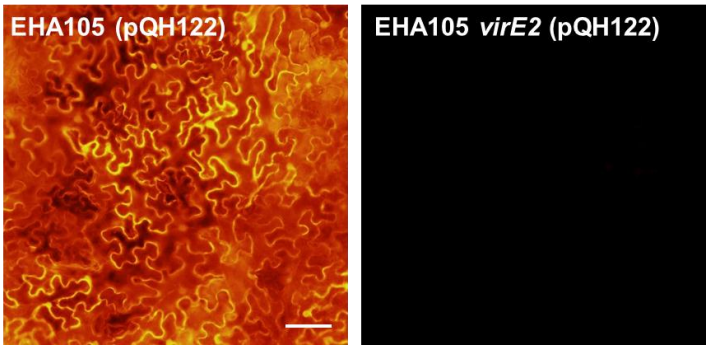

B

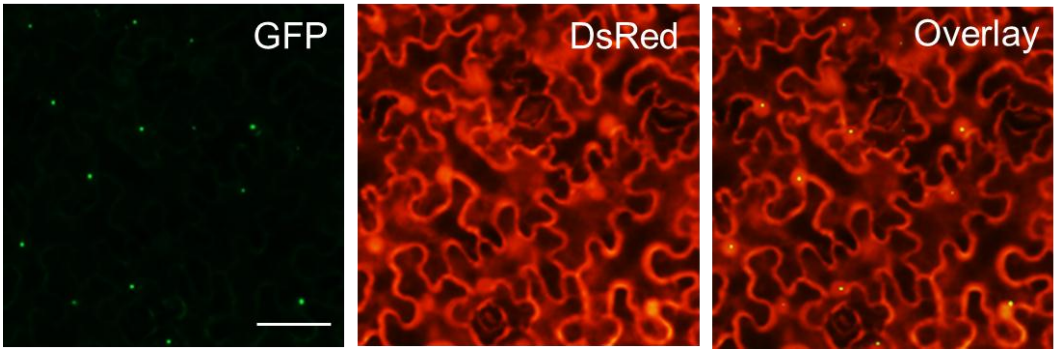

Figure 20. VirE2 was efficiently delivered in *N. benthamiana* leaf cells.

(A) Agroinfiltration of *N. benthamiana* leaves with EHA105(pQH122) to transiently express DsRed, and with EHA105 *virE2*(pQH122) to test the necessity of VirE2 in transient expression. (B) EHA105 *virE2::GFP11* (pQH308) was infiltrated into *N. benthiamiana* leaves by a syringe. The leaf tissues were observed at 3 d after infiltration under a fluorescent microscope BX53 (Olympus) with a Digital Camera DP72 (Olympus). DsRed was expressed from T-DNA transferred into plant cells so that cellular locations were indicated. Bar: 50 μm.

4.5. Intracellular trafficking of VirE2

4.5.1. Agroinfiltration caused inhibition to subsequent infection within the infiltrated zone

To describe the process of intracellular trafficking of VirE2, ideally the observation should start from the formation of complemented GFP signal when VirE2 molecules just pass through plasma membranes. For such reason, I attempted to perform a sequential agroinfiltration, whereby the GFP1-10 was expressed in advance with the first agroinfiltration of EHA105(pQH308) and VirE2::GFP11 would be expressed and delivered by *Agrobacterium* in a subsequent agroinfiltration of EHA105 *virE2::GFP11* three days later. This sequential infiltration aimed at ensuring the pre-existence of GFP1-10, so that when VirE2::GFP11 was delivered the signal would be visualized in the very beginning.

In contrast to what was expected, very few signals were detected (data not shown). Physical damages to the leaf tissue or certain host responses initiated by the first agroinfiltration could be responsible for this problem. I hereby tested the hypothesis by performing the second agroinfiltration with EHA105(pQH122) to transiently express DsRed as an indicator. If there was any suppression caused by the first agroinfiltration, the expression of DsRed by the second infiltration would be lowered or abolished.

In the first agroinfiltration, individual leaves were infiltrated with *E. coli*, an T-DNA-competent strain EHA105(pQH302), MX243 (A348 *virB*), or

infiltration buffer only. The second agroinfiltrated was done two days later within the infiltration zone of the first agroinfiltration. Thereby, the suppression effect can be reflected from the intensity of DsRed signal three days after second agroinfiltration. As can be seen in Figure 21A, when pretreated with EHA105(pQH302), the leaf exhibited an suppression effect on subsequent transient expression. Neither *E. coli* nor MX243 exerted any influence on the second agroinfiltration. This result suggests that the suppression effect was specifically initiated by a pathogenic strain of *A tumefaciens*. This finding is in consistent with early reports, in which first inoculum of *Agrobacterium* would inhibit the symptom of subsequent infection of *Pseudomonas* or TMV (Robinette *et al.* 1990; Pruss *et al.* 2008; Rico *et al.* 2010). This is an unfavorable phenomenon as it invalidated the proposed sequential agroinfiltration approach. The only choice is to infiltrate two strains together, whereby the suppression was released (Figure 21B). But more conveniently, considering the full function of VirE2::GFP11, the roles of EHA105(pQH308) and EHA105 (*virE2::GFP11*) can be merged into one strain─ EHA105 *virE2::GFP11*(pQH308). This is how visualization of VirE2 was achieved in Figure 19 and 20B.

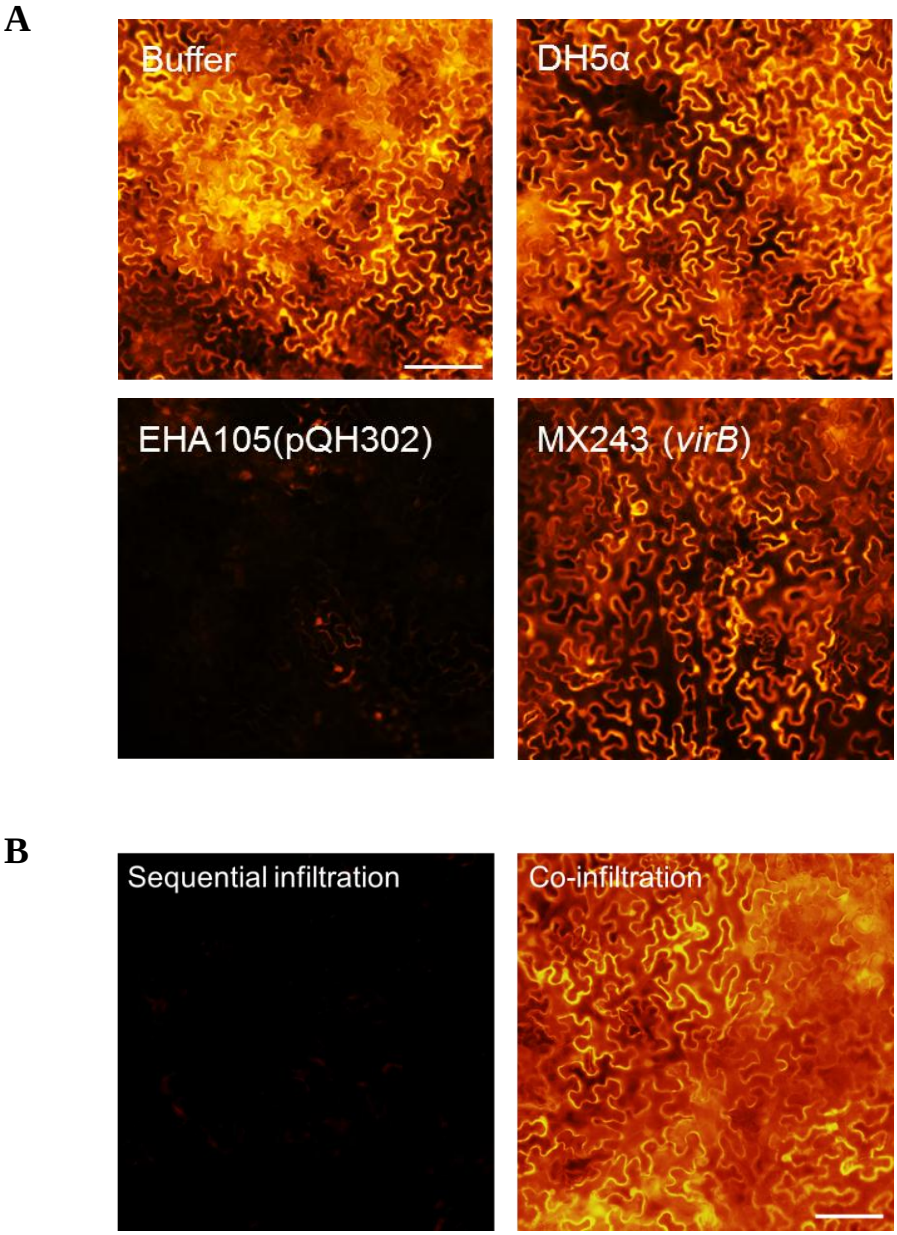

Figure 21. The first agroinfiltration caused a suppression effect on the subsequent infiltration.

(A). Strains used in the first agroinfiltration are indicated. A second infiltration with EHA105(pQH122) was performed in the previous infiltrated zones. Leaves were observed 3 days after the second agroinfiltration. The expression levels of DsRed for different experimental settings were shown.
(B). Sequential infiltration indicated the strategy used in (A), EHA105(pQH302) and EHA105(pQH122) were used as the first strain and the second strain, respectively. The image was taken 3 days after the second infiltration. Co-infiltration was to mix these two strains and infiltrate them together. The image was taken three days later.

4.5.2. Intracellular trafficking of VirE2 by time lapse imaging

As discussed in last section, the final approach was made by using one strain to transfer the T-DNA for GFP1-10 expression and to deliver VirE2::GFP11. Due to the time requirement for sufficient expression, images were only able to be taken three days after agroinfiltration. This time window has masked the early stages of VirE2 delivery and movement, so that the signals we observed were predominantly localized into the nucleus. However, some cytoplasmic localized VirE2 can occasionally be captured, indicating that there was still a small portion of active delivery continued. Albeit occasional, it still made the observation of VirE2 trafficking possible. An automated fluorescent microscope, Olympus BX61, was employed to record this movement. The signals for VirE2 were usually generated two days post infection. However, it took longer of DsRed to illuminate the cell and the nucleus. In this study, the practical time for observation was around 2.5 days to 3 days post infection.

Here I show a time lapse series of images showing VirE2 forming at the plasma membrane, intracellular trafficking, and entering the nucleus (Figure 22). The intensity of a VirE2 signal was gradually intensified, along with a growing size, suggesting the accumulation of VirE2 molecules at the plasma membrane. When reached a certain size, the VirE2 cluster detached from the membrane, and migrated towards the nucleus. In this specific series, the whole process lasted about 30 min. Because the trafficking was relatively

straightforward to the nucleus, it triggered an interesting question that of VirE2 followed a paved way to nucleus rather than a random motion?

In another series, the VirE2 signal bypassed the nucleus rather than entering it (Figure 23). At the beginning of observation, VirE2 signal was already in the process of intracellular trafficking. The movement of VirE2 tended to be along the plasma membrane, possibly implying a certain degree of membrane affinity of VirE2. When it came to a very close position near the nucleus, the VirE2 signal continued on the moving direction without entering the nucleus. This observation represents another scenario different from what was observed in Figure 22. Therefore, the answer to the previous question became obscured. More information is to be obtained to provide clues for future analysis of its intracellular trafficking.

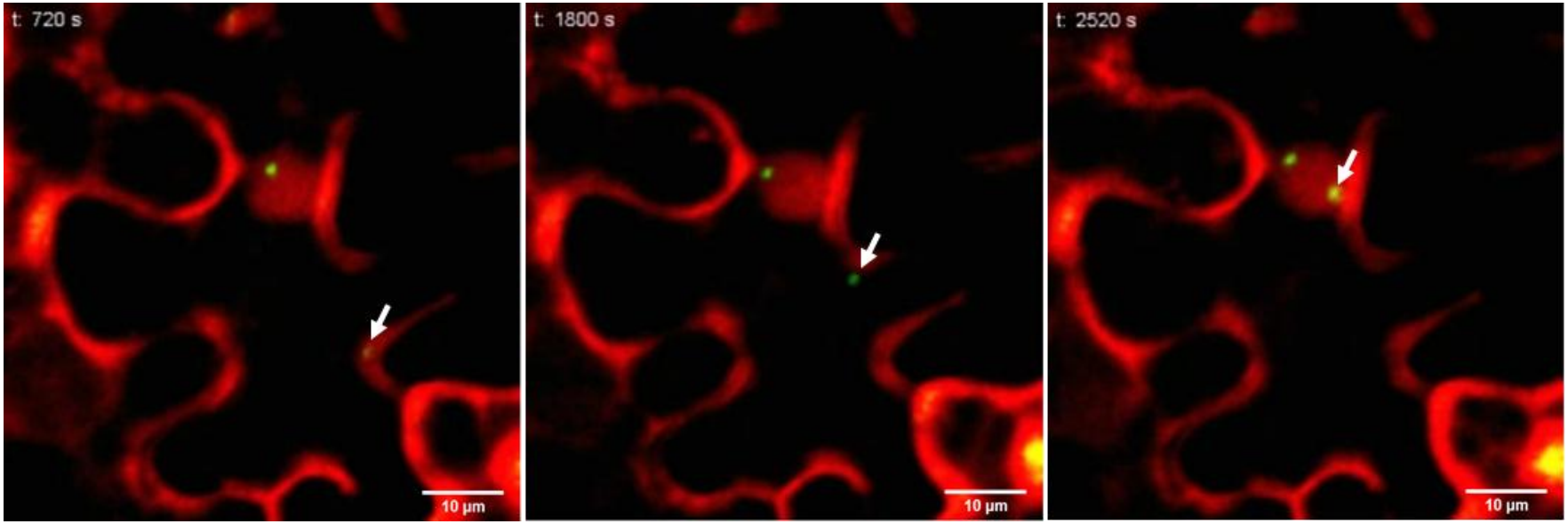

Figure 22. A VirE2 signal moved towards the nucleus.

A time lapse imaging series were taken with Olympus BX61 as described in Chapter 2. The VirE2 signal (arrowed) was observed from forming at plasma membrane, intracellular movement, to the final nuclear localization. Time axis was indicated at top left, with the starting point corrected several minutes before VirE2 was detected. The signal moved straight forward into the nucleus within 30 min. Bar, 10 µm.

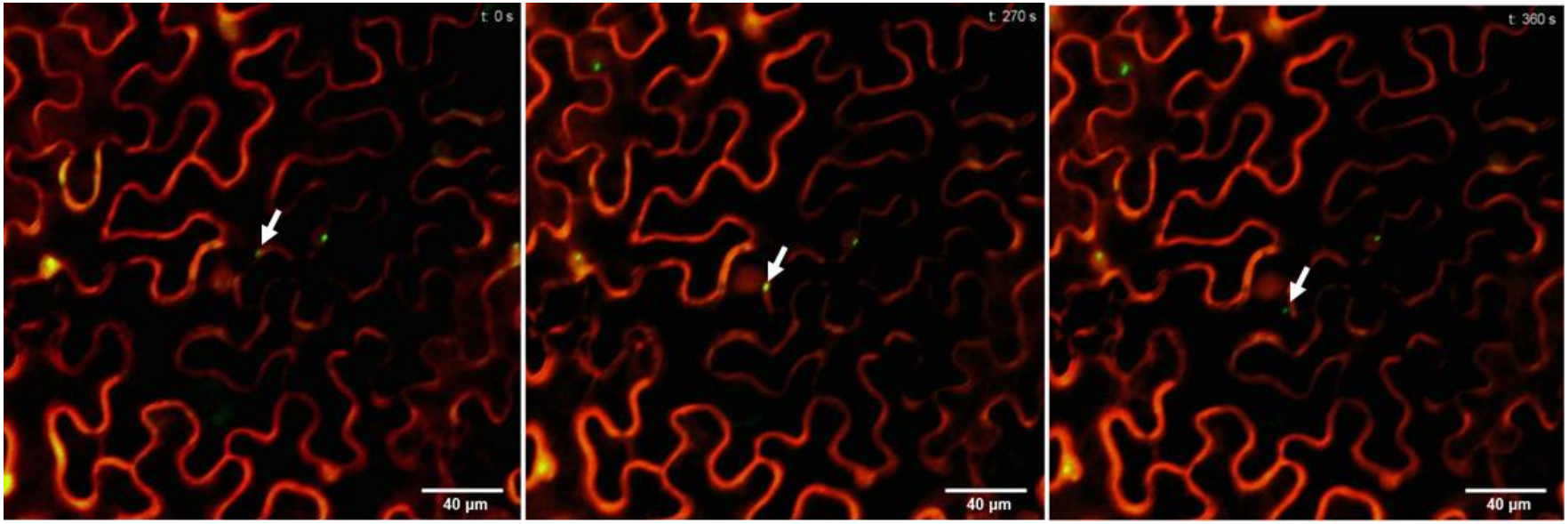

Figure 23. A VirE2 signal bypassed the nucleus.

A time lapse imaging series were taken with Olympus BX61 as described in Chapter 2. The VirE2 signal was moving as observation started. Time axis was indicated at top right, with the starting point exactly overlapping with when observation started. The VirE2 signal bypassed the nucleus without entering it. Over 1hour's movement was recorded; only early part with a close reference to nucleus was shown. Bar, 40 µm.

4.6. Regeneration of transgenic *N. benthamiana* for constitutive expression of GFP1-10

As described in previous sections, an agroinfiltration of T-DNA competent strain caused suppression to the subsequent agroinfiltration. This phenomenon prevented visualizing VirE2 at the early stage of delivery. Therefore, the minimal time required for the earliest detection was kept unknown. Moreover, though with current "one strain" method a whole process was still successfully captured (Figure 22), the probability was so low that hundreds of cells were monitored only to get one successful image series. This made collecting movement information of VirE2 challenging. To address this issue, a transgenic *N. benthamiana* to constitutively express GFP1-10 was preferred.

Leaf disc transformation and regeneration was performed as described (Barton *et al.* 1983; Gallois *et al.* 1995), resulting transgenic *N. benthamiana*, Nb-T308 (Figure 24A). Unexpectedly, when infiltrated with EHA105 *virE2::GFP11*, Nb-T308 plants (different regenerated individuals) failed to produce complemented GFP signals, though DsRed was detectable (Figure 24B). Western blot was performed to examine the expression of GFP1-10 with an anti-GFP polyclonal antibody in the transgenic plants. As shown in Figure 24C, GFP components were under detection in Nb-T308, but easily detectable in agroinfiltrated leaf tissues. The poor expression of GFP1-10 in Nb-T308 was unexpected, given that agroinfiltration of the same strain was always

successful. This was probably due to the interference between multiple 35S promoters within the same construct. Coincidentally, a group in New Zealand also experienced poor expression of GFP when driving two genes with two separate 35S promoters (The New Zealand Institute for Plant & Food Research Limited). I thereby reconstructed pQH308, in which *GFP1-10* is cloned downstream of a mannopine synthase promoter (*P mas*) and *DsRed* is driven by 35S promoter, resulting in pQH308a. A new transgenic *N. benthamiana* transformed by pQH308a may help to tackle the problems mentioned at the beginning of this section.

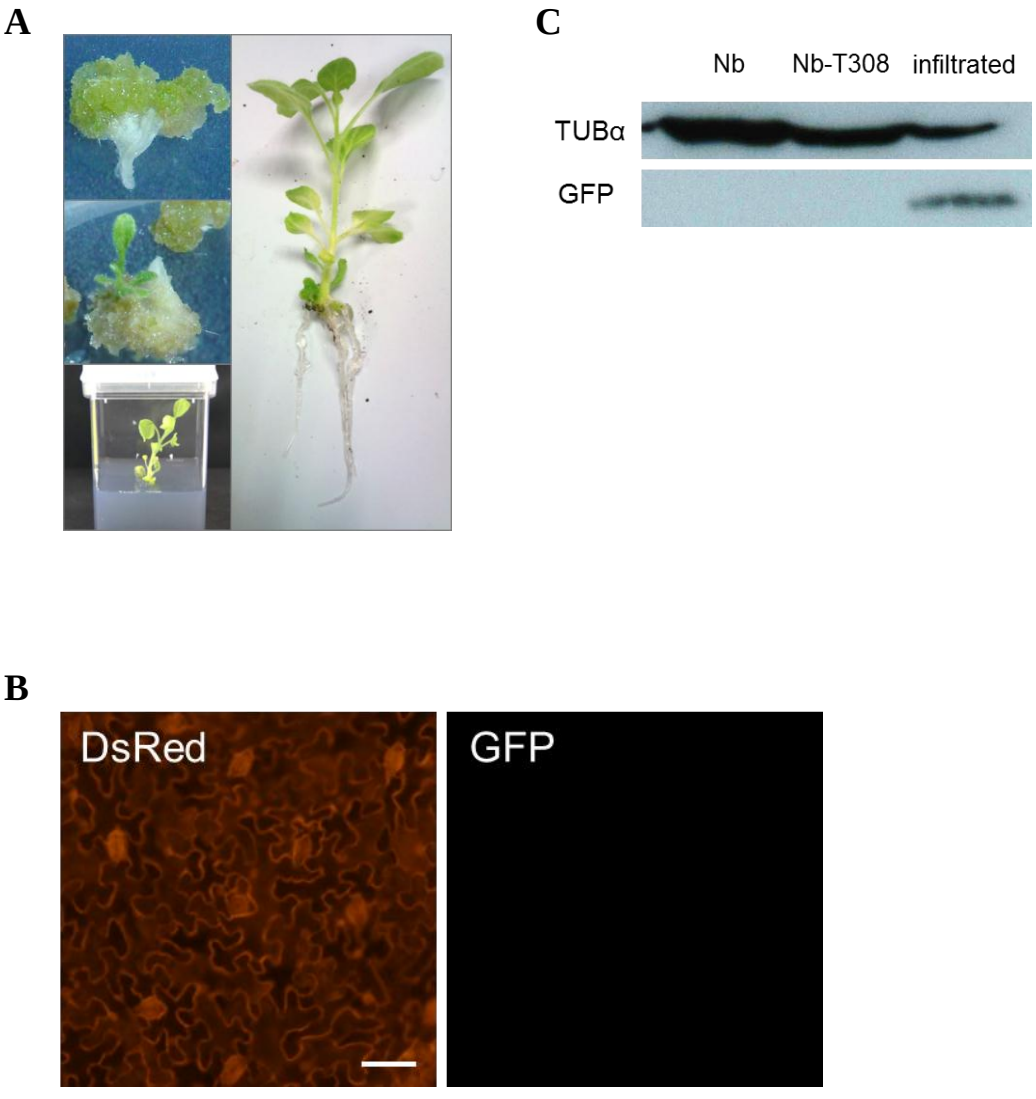

Figure 24. Regeneration of a transgenic *N. benthamiana*.

(A). Regeneration of EHA105(pQH308) transformed leaf discs into a transgenic plant, Nb-T308. (B). Infiltrate a fully expanded leaf of Nb-T308 with EHA105 *virE2::GFP11*. Bar 50 μm. (C) Western blotting. Nb: wild type *N. benthamiana*, Nb-T308 transgenic line by pQH308, infiltrated: wild type infiltrated with EHA105(pQH308). Polyclonal GFP antibody was used to detect the expression of GFP1-10.

4.7. Discussion

It was the first time that Agrobacterium-delivered VirE2 was directly visualized

The VirE2 protein, the most abundant virulence protein in *Agrobacterium* (Engstrom *et al.* 1987), protects T-DNA by coating it with numerous molecules (Tzfira *et al.* 2002). It was calculated that about every 19 bases of T-DNA is coupled with one molecule of VirE2 (Citovsky *et al.* 1997). Thus, a 2 kb T-DNA easily attracts 100 molecules of VirE2. In addition, the VirE2 protein can also assemble without T-DNA, to form homodimers and solenoids (Dym *et al.* 2008). Based on its abundance and the nature of aggregation, the detection of it was expected to be easier than that of other virulence proteins.

Tagging VirE2 with different fluorescent proteins was done in various studies (Bhattacharjee *et al.* 2008; Grange *et al.* 2008; Aguilar *et al.* 2010). But none of these fluorescent protein-tagged VirE2 successfully translocated into recipient cells, probably because the enlarged size or certain barrel structure of these fusion proteins plugged the channel of T4SS (Vergunst *et al.* 2003; Aguilar *et al.* 2010). Therefore, a better tagging method was needed for visualization of VirE2 translocation. The novel design of a split GFP system (Pedelacq *et al.* 2006) answered this imperative demand. It cleaved the 11^{th} β strand off a GFP molecule, resulting in a 16-residue peptide (GFP11) as the tag part, while the remaining 215 residue fragment (GFP1-10) can spontaneously bind to the small one upon recognition. Being a very small tag,

GFP11 greatly reduced the possibility of perturbing functions of the tagged protein. An important finding of a permissive site for short peptide insertion in VirE2 (Zhou *et al.* 1999) was equally critical. We were able to tag the VirE2 with GFP11 at this permissive site, without compromising its virulence and translocation activity.

In this work VirE2, originating from the bacterium, was visualized for the first time. This technique enabled us to observe the localization of VirE2 in recipient cells in a way with close approximation to the natural process, allowed us to assess delivery efficiency of VirE2 into recipient cells, and paved the way for the study of host factors affecting protein delivery by T4SS, and so on.

VirE2 localized in nucleus of N. benthamiana leaf cells

Nuclear import of VirE2 was reported to occur only in the plant cells of some species (Citovsky *et al.* 1992; Citovsky *et al.* 1994; Tzfira *et al.* 2001), but not in yeast or mammalian cells (Guralnick *et al.* 1996; Rhee *et al.* 2000; Tzfira *et al.* 2001). Visualization of its localization was mainly achieved by exogenous expression of a fusion of VirE2 to reporters (Citovsky *et al.* 1992; Citovsky *et al.* 1994; Tzfira *et al.* 2001; Lacroix *et al.* 2005; Grange *et al.* 2008). The reported localization of VirE2 is still controversial, as different reporter fusion generated different results even in the same species.

Visualizing localization of VirE2, originating from the *Agrobacterium*,

has been extremely challenging and produced little results (Grange *et al.* 2008). In this study, we successfully visualized the subcellular localization of VirE2 in recipient cells, generated by *Agrobacterium*. In line with some previous findings, we observed nuclear localization of VirE2 in the cell of *N. benthamiana* leaves, and cytoplasmic localization in yeast.

VirE2, as a major player in T-DNA transport, cooperatively binds to the T-DNA strand, protects it from nuclease activity, maintains it in a transportable form, and mediates its nuclear import (Tzfira *et al.* 2000; Ward *et al.* 2001). Thus, cellular localization, nuclear or cytoplasmic, of VirE2 may delineate the disparity between natural hosts and non-natural hosts. It is probable that the T4SS of *Agrobacterium* is highly promiscuous and does not distinguish, at least between yeast and plant, recipient types. And the only difference of natural and non-natural hosts could be made after uptake of VirE2 into the cytoplasm, *i.e.* whether VirE2 migrates into the nucleus or not. This difference determines how active the T-DNA is transported into the nucleus, and in turn contributes to the final integration. From such a perspective, natural hosts should be those species whose cellular mechanisms have been hijacked by *Agrobacterium* to help the nuclear import of VirE2.

Agrobacterium is an efficient protein transporter

Agrobacterium has been, for a long time, well-known for its ability of transferring DNA into wide variety of plants, which makes it of significant

importance to the agriculture industries (Moore *et al.* 1997). In the past two decades the host range has been greatly expanded, from plants to fungi and to mammalian cells. The expansion of its host range was based on a simple idea that the host is a certain species that can be genetically transformed by *Agrobacterium*. This historical viewpoint rooted, from the very beginning, in the tumor inducing mechanisms of *Agrobacterium,* and excited enormous studies on the mechanisms of T-DNA transfer. Yet it may lead to ignorance of another great ability of *Agrobacterium*—protein delivery. In order to facilitate final integration of T-DNA, *Agrobacterium* delivers several virulence proteins into host cells. Therefore, *Agrobacterium* should be deemed as a good protein transporter, as well as a biological DNA-deliver device.

In 2000, Vergunst *et al.* monitored protein transport from *Agrobacterium* to plant cells, with the Cre Recombinase Assay for Translocation (CRAfT), and reported the delivery efficiency of virulence proteins into *Arabidopsis* root explants(Vergunst *et al.* 2000). Later, the transport efficiency for yeast cells as the recipient was obtained with the same assay. 1% of yeast cells received Cre:VirE2 fusion protein (Schrammeijer *et al.* 2003). This is remarkably high, in view of a relatively low transformation efficiency at 10^{-5} (Soltani *et al.* 2009). According to the findings of Vergunst *et al*., no translocation can be detected for a Cre-GFP-virF37C fusion protein, though Cre-virF37C was successfully transported (Vergunst *et al.* 2003). This could be attributed to the highly folded structure of GFP that blocked translocation of such fusion

proteins. Considering the size of Cre (343 residues), the function of VirE2 may have been compromised in the Cre:VirE2 fusion, which brought in artifacts to the results of CRAfT. In this study, we were able to introduce a 16-residue peptide at the permissive site of VirE2, which minimized the possible perturbation. Thus the delivery efficiency was much more faithful. In this study, a very high efficiency was observed *N. benthamiana* leaf cells. Under optimal conditions, over 50% of yeast cells got GFP signals (Li and Yang *et al.* unpublished data), which is strikingly surprising for a non-plant species. By now, such high efficiency of VirE2 delivery by *Agrobacterium* has only been detectable with the spilt GPF assay. The studies of genetic transformation using *Agrobacterium* for variety of species have awarded this insatiable bacterium the fame of promiscuity (Kado 1994; Lacroix *et al.* 2006). And our results suggest that the promiscuous nature of *Agrobacterium* should be more highlighted from the perspective of protein delivery.

Intracellular trafficking of VirE2

The technique developed in this research also made it possible to record the intracellular trafficking of VirE2. Current knowledge of the intracellular transport of proteins and nucleoproteins were mostly derived from research of the infectious pathways of mammalian viruses. Nevertheless, it was reported that an “animalized” VirE2 can be actively delivered along a reconstituted microtubule network (Salman *et al.* 2005), suggesting that the intercellular

transport system of the host may also be hijacked for the transport of its T-DNA complex. However, *in vivo* study of the intracellular transport of VirE2 has been lacking of practicable approaches, as exogenous expression and conventional tagging failed to simulate the natural transport process. Successful observation of VirE2 with the split GFP assay made it possible to record the intracellular movement of VirE2 in a time lapse manner. It marks the beginning of a real time study of VirE2 intracellular trafficking.

Chapter 5. General conclusion and future prospects

5.1. General Conclusion

This study is part of the interest of identifying eukaryotic host factors involved in *Agrobacterium*-mediated transformation. This study started on the basis of Tu's forward genetic screening of deletion strains that exhibited altered AMT efficiencies, in which mitochondrial was suggested a role in this biological transformation process. Therefore, components of the most critical pathway, oxidative phosphorylation, were examined using BY4741 haploid deletion pool of *S. cerevisiae*. Downstream of Crebs cycle (TCA cycle), the oxidative phosphorylation pathway transfers electrons from electron donors generated from Crebs cycle to electron acceptors such as oxygen in redox reactions, and store the released energy into ATP molecules. This study mainly focused on the process upstream of ATP synthesis, *i.e.* Electron Transport Chain (ETC). Knockout mutants of some components in ETC complex III showed enhanced transformation efficiencies of yeast. A knockout of Qcr7p was chosen for later analysis as it made the highest transformation efficiency among tested mutants. Trans-membrane delivery, intracellular trafficking and chromosomal integration made the three major parts of analyses. Uptake of T-DNA and VirE2 by yeast was quantified respectively with qPCR and newly established split GFP essay. Both T-DNA and VirE2

exhibited a higher level in *qcr7*Δ than in WT, suggesting an increased competency of *qcr7*Δ to T4SS secretion. Intracellular trafficking and integration were also analyzed, and no difference was detected between *qcr7*Δ and WT. Therefore, the enhanced transformation efficiency of *qcr7*Δ was most probably grounded on increased competency to T4SS secretion.

Previous investigations mainly emphasized on the intracellular trafficking and integration. Relatively little research activity was focused on trans-membrane delivery. The finding in this study provided knowledge on alteration in macromolecules delivery between *Agrobacterium* and yeast when mitochondria malfunction. The mitochondrion is involved in many cellular functions, such as ATP generation, ROS production, calcium homeostasis, and cell fate determination. Considering the spatial apartness of mitochondria and the cell membrane, their connection in AMT might be an indirect one through a cellular condition like the concentration of ions, ROS etc. A changing caused by knocking out Qcr7p may result in a favorable cellular condition that makes the yeast cell more accessible to bacterial T4SS secretion.

Since yeast is a unicellular organism that lacks intercellular organizations and structures which multicellular organisms have, this finding can be made more useful when this phenotype is consistent in the plant species. Therefore, *Arabidopsis* mutants in Qcr7p homologs or other ETC components should be carefully tested of the susceptibility to AMT.

In an analysis of integration patterns with the strain EHA105(pQH303) designed to generate transformants through HR, *qcr7*Δ showed a much lower NHEJ ratio (0.06%) compared with WT (3.6%). This result suggested a shift of NHEJ/HR ratio when Qcr7p was knocked out, which made the recombination more accurate. But this shift was not observed with a competitive plasmid repair assay, possibly because of different DNA repair mechanisms of the two. The integration mechanism of T-DNA was not well elucidated, with two very important questions unknown: 1) which is the substrate for integration, ss-DNA or ds-DNA? 2) whether VirD2 involves in the T-DNA integration? Therefore, this result may provide a new perspective for the exploration of the mechanism of T-DNA integration.

This study made another impact by directly visualizing bacterium-delivered VirE2 in the recipient cells. This method was developed to meet the need of quantifying VirE2 delivery. But its success realized the long lasting wish of monitoring intracellular trafficking of VirE2. As a critical virulence effector closely associate with T-DNA, VirE2's trafficking largely reflects the behavior of T-DNA in the host, which is important for understanding the transformation process. This has been proved extremely difficult for years. VirE2 translocates from the bacterium to the recipient through T4SS channels, protects T-DNA by binding to it with an ss-DNA affinity center, aggregates to form solenoid structure, interacts with plant immune factors, and targets the

nucleus. These multiple characteristics make VirE2 vulnerable to proteins fusion. Previous attempts abolished the virulence of *A. tumefaciens* by disrupting one or some of these functions, so that reported studies exogenously expressed VirE2 fusion in the recipient.

In this research, this problem was conquered by exploiting a split GFP system, whereby VirE2 was tagged with a genetically encoded 16-residue peptide sequence, at a reported permissive site for short peptide insertion. Thereby, *Agrobacterium*-delivered VirE2 was visualized for the first time. This technique revealed the high efficiency of VirE2 delivery, giving *A. tumefaciens* the credit of an excellent protein transporter. This technique also made it possible to record VirE2 movement in *N. benthamiana* leaf cells. With an automated fluorescent microscope, intracellular trafficking of VirE2 was recorded in a time lapse manner. This work marks the beginning of a real time study of VirE2 trafficking in plant cells. The trafficking of VirE2 is to be further characterized with more observations.

5.2. Future prospects

Although the enhanced transformation efficiency in a knockout of Qcr7p was contributed by the increased competency to both T-DNA and VirE2 delivery, exact connections between this increased competency and mitochondria functions still remains unknown. Some efforts were spent in ATP concentration, ROS generation, and cell dividing in search of possible

clues. However, no useful information was obtained. The future study could try to tackle this issue in other aspects, such as the cell wall integrity and cellular ion strength.

The approach for visualizing bacterium-delivered VirE2 is a promising technique. In this study a real time study of VirE2 trafficking was achieved with this technique. Yet, a lot of questions remain to be answered with more sophisticated utilization of this technique. For instance, by now we cannot determine whether the visualized signal represents T-complex or simply a VirE2 cluster. We do not know whether or not the movement of VirE2 follows a microtubule structure. In future study, proper markers can be incorporated into this technique to provide more information on VirE2 trafficking. A transgenic plant may also be needed to bring forward the time window of observation, so that the recording will be made much easier and productive. Some ambiguous observations, such as different competency to stable transformation and transient expression (Lee *et al.* 2012), may also find an answer from the perspective of VirE2 delivery.

Bibliography

Aguilar, J., Zupan, J., Cameron, T. A. and Zambryski, P. C. (2010). *Agrobacterium* type IV secretion system and its substrates form helical arrays around the circumference of virulence-induced cells. *Proc Natl Acad Sci U S A* **107**(8): 3758-3763.

Alvarez-Martinez, C. E. and Christie, P. J. (2009). Biological diversity of prokaryotic Type IV secretion systems. *Microbiol Mol Biol R* **73**(4): 775-808.

Anand, A., Krichevsky, A., Schomack, S., Lahaye, T., Tzfira, T., Tang, Y. H., *et al.* (2007). *Arabidopsis* VIRE2 INTERACTING PROTEIN2 is required for *Agrobacterium* T-DNA integration in plants. *Plant Cell* **19**(5): 1695-1708.

Anand, A., Tzfira, T., Citovsky, V. and Mysore, K. S. (2006). Characterizing the functional role of VIP2 - a VirE2 interacting protein 2 in genetic transformation of plants by *Agrobacterium tumefaciens*. *Phytopathology* **96**(6): S5-S5.

Barton, K. A., Binns, A. N., Matzke, A. J. and Chilton, M. D. (1983). Regeneration of intact tobacco plants containing full length copies of genetically engineered T-DNA, and transmission of T-DNA to R1 progeny. *Cell* **32**(4): 1033-1043.

Belevich, I. (2007). Proton translocation coupled to electron transfer

reactions in terminal oxidases. *University of Helsinki,*.

Bertens, P., Heijne, W., Van der Wel, N., Wellink, J. and Van Kammen, A. (2003). Studies on the C-terminus of the Cowpea mosaic virus movement protein. *Arch Virol* **148**(2): 265-279.

Bhattacharjee, S., Lee, L. Y., Oltmanns, H., Cao, H., Veena, Cuperus, J. and Gelvin, S. B. (2008). IMPa-4, an *Arabidopsis* importin alpha isoform, is preferentially involved in *Agrobacterium*-mediated plant transformation. *The Plant cell* **20**(10): 2661-2680.

Bohme, L. and Rudel, T. (2009). Host cell death machinery as a target for bacterial pathogens. *Microbes Infect* **11**(13): 1063-1070.

Brachmann, C. B., Davies, A., Cost, G. J., Caputo, E., Li, J. C., Hieter, P. and Boeke, J. D. (1998). Designer deletion strains derived from *Saccharomyces cerevisiae* S288C: a useful set of strains and plasmids for PCR-mediated gene disruption and other applications. *Yeast* **14**(2): 115-132.

Brandt, U., Uribe, S., Schagger, H. and Trumpower, B. L. (1994). Isolation and characterization of QCR10, the nuclear gene encoding the 8.5-kDa subunit 10 of the *Saccharomyces cerevisiae* cytochrome bc1 complex. *J Biol Chem* **269**(17): 12947-12953.

Braun, A. C. (1952). Conditioning of the host cell as a factor in the transformation process in crown gall. *Growth* **16**(2): 65-74.

Braun, A. C. and Mandle, R. J. (1948). Studies on theinactivation of the tumor inducing principle in crown gall. *Growth* **12**(4): 255-269.

Brencic, A. and Winans, S. C. (2005). Detection of and response to signals involved in host-microbe interactions by plant-associated bacteria. *Microbiol Mol Biol R* **69**(1): 155-+.

Bundock, P., Dendulkras, A., Beijersbergen, A. and Hooykaas, P. J. J. (1995). Transkingdom T-DNA transfer from *Agrobacterium tumefaciens* to *Saccharomyces cerevisiae*. *EMBO J* **14**(13): 3206-3214.

Cabantous, S., Terwilliger, T. C. and Waldo, G. S. (2005). Protein tagging and detection with engineered self-assembling fragments of green fluorescent protein. *Nat Biotechnol* **23**(1): 102-107.

Chen, C. Y., Wang, L. and Winans, S. C. (1991). Characterization of the supervirulent *virG* gene of the *Agrobacterium tumefaciens* plasmid pTiBo542. *Mol Gen Genet* **230**(1-2): 302-309.

Chen, P. Y., Wang, C. K., Soong, S. C. and To, K. Y. (2003). Complete sequence of the binary vector pBI121 and its application in cloning T-DNA insertion from transgenic plants. *Mol Breeding* **11**(4): 287-293.

Chilton, M. D., Drummond, M. H., Merlo, D. J., Sciaky, D., Montoya, A. L., Gordon, M. P. and Nester, E. W. (1977). Stable incorporation of plasmid DNA into higher plant cells: molecular basis of crown gall tumorigenesis. *Cell* **11**(2): 263-271.

Christie, P. J. (2004). Type IV secretion: the *Agrobacterium* VirB/D4 and related conjugation systems. *Bba-Mol Cell Res* **1694**(1-3): 219-234.

Christie, P. J. and Cascales, E. (2005). Structural and dynamic properties of bacterial Type IV secretion systems. *Mol Membr Biol* **22**(1-2): 51-61.

Christie, P. J., Ward, J. E., Winans, S. C. and Nester, E. W. (1988). The *Agrobacterium tumefaciens* VirE2 gene product Is a single-stranded-DNA-binding protein that associates with T-DNA. *J Bacteriol* **170**(6): 2659-2667.

Citovsky, V., Devos, G. and Zambryski, P. (1988). Single-stranded-DNA binding-protein encoded by the *virE* locus of *Agrobacterium tumefaciens*. *Science* **240**(4851): 501-504.

Citovsky, V., Guralnick, B., Simon, M. N. and Wall, J. S. (1997). The molecular structure of agrobacterium VirE2-single stranded DNA complexes involved in nuclear import. *J Mol Biol* **271**(5): 718-727.

Citovsky, V., Lee, L. Y., Vyas, S., Glick, E., Chen, M. H., Vainstein, A., *et al.* (2006). Subcellular localization of interacting proteins by bimolecular fluorescence complementation in planta. *J Mol Biol* **362**(5): 1120-1131.

Citovsky, V., Warnick, D. and Zambryski, P. (1994). Nuclear import of *Agrobacterium* VirD2 and VirE2 proteins in maize and tobacco. *Proc Natl Acad Sci U S A* **91**(8): 3210-3214.

Citovsky, V., Zupan, J., Warnick, D. and Zambryski, P. (1992). Nuclear localization of *Agrobacterium* VirE2 protein in plant cells. *Science* **256**(5065): 1802-1805.

Dahout-Gonzalez, C., Nury, H., Trezeguet, V., Lauquin, G. J. M., Pebay-Peyroula, E. and Brandolini, G. (2006). Molecular, functional, and pathological aspects of the mitochondrial ADP/ATP carrier. *Physiology* **21**: 242-249.

Deng, W., Chen, L., Wood, D. W., Metcalfe, T., Liang, X., Gordon, M. P., *et al.* (1998). *Agrobacterium* VirD2 protein interacts with plant host cyclophilins. *Proc Natl Acad Sci U S A* **95**(12): 7040-7045.

Deng, W. Y., Chen, L. S., Peng, W. T., Liang, X. Y., Sekiguchi, S., Gordon, M. P., *et al.* (1999). VirE1 is a specific molecular chaperone for the exported single-stranded-DNA-binding protein VirE2 in *Agrobacterium*. *Mol Microbiol* **31**(6): 1795-1807.

Djamei, A., Pitzschke, A., Nakagami, H., Rajh, I. and Hirt, H. (2007). Trojan horse strategy in *Agrobacterium transformation*: Abusing MAPK defense signaling. *Science* **318**(5849): 453-456.

Douglas, C. J., Halperin, W. and Nester, E. W. (1982). *Agrobacterium tumefaciens* mutants affected in attachment to plant cells. *J Bacteriol* **152**(3): 1265-1275.

Duckely, M., Oomen, C., Axthelm, F., Van Gelder, P., Waksman, G. and Engel, A. (2005). The VirE1VirE2 complex of *Agrobacterium*

tumefaciens interacts with single-stranded DNA and forms channels. *Mol Microbiol* **58**(4): 1130-1142.

Dumont, M. D., Mathews, A. J., Nall, B. T., Baim, S. B., Eustice, D. C. and Sherman, F. (1990). Differential stability of two apo-isocytochromes c in the yeast *Saccharomyces cerevisiae*. *J Biol Chem* **265**(5): 2733-2739.

Dym, O., Albeck, S., Unger, T., Jacobovitch, J., Brainzburg, A., Michael, Y., *et al.* (2008). Crystal structure of the *Agrobacterium virulence* complex VirE1-VirE2 reveals a flexible protein that can accommodate different partners. *Proc Natl Acad Sci U S A* **105**(32): 11170-11175.

Engstrom, P., Zambryski, P., Van Montagu, M. and Stachel, S. (1987). Characterization of *Agrobacterium tumefaciens* virulence proteins induced by the plant factor acetosyringone. *J Mol Biol* **197**(4): 635-645.

Escudero, J. and Hohn, B. (1997). Transfer and integration of T-DNA without cell injury in the host plant. *Plant Cell* **9**(12): 2135-2142.

Filichkin, S. A. and Gelvin, S. B. (1993). Formation of a putative relaxation intermediate during T-DNA processing directed by the *Agrobacterium tumefaciens* VirD1,D2 endonuclease. *Mol Microbiol* **8**(5): 915-926.

Fraley, R. T., Rogers, S. G., Horsch, R. B., Sanders, P. R., Flick, J. S., Adams, S. P., *et al.* (1983). Expression of bacterial genes in plant cells. *Proc Natl Acad Sci U S A* **80**(15): 4803-4807.

Friesner, J. and Britt, A. B. (2003). Ku80- and DNA ligase IV-deficient plants are sensitive to ionizing radiation and defective in T-DNA integration. *Plant J* **34**(4): 427-440.

Gallois, P. and Marinho, P. (1995). Leaf disk transformation using *Agrobacterium tumefaciens*-expression of heterologous genes in tobacco. *Methods Mol Biol* **49**: 39-48.

Galloway, B. T. (1902). Applied botany, retrospective and prospective. *Science* **16**: 49-59.

Garfinkel, D. J. and Nester, E. W. (1980). *Agrobacterium tumefaciens* mutants affected in crown gall tumorigenesis and octopine catabolism. *J Bacteriol* **144**(2): 732-743.

Gelvin, S. B. (1998). *Agrobacterium* VirE2 proteins can form a complex with T strands in the plant cytoplasm. *J Bacteriol* **180**(16): 4300-4302.

Gelvin, S. B. (2003). *Agobacterium*-mediated plant transformation: The biology behind the "gene-Jockeying" tool. *Microbiol Mol Biol R* **67**(1): 16-+.

Gelvin, S. B. (2009). *Agrobacterium* in the Genomics Age. *Plant Physiol* **150**(4): 1665-1676.

Gelvin, S. B. (2010). Finding a way to the nucleus. *Curr Opin Microbiol* **13**(1): 53-58.

Gietz, R. D. and Schiestl, R. H. (2007). High-efficiency yeast transformation using the LiAc/SS carrier DNA/PEG method. *Nat Protoc* **2**(1): 31-34.

Gietz, R. D. and Woods, R. A. (2001). Genetic transformation of yeast. *Biotechniques* **30**(4): 816-+.

Grange, W., Duckely, M., Husale, S., Jacob, S., Engel, A. and Hegner, M. (2008). VirE2: a unique ssDNA-compacting molecular machine. *PLoS Biol* **6**(2): e44.

Green, D. R. (1998). Apoptotic pathways: The roads to ruin. *Cell* **94**(6): 695-698.

Guo, M. L., Hou, Q. M., Hew, C. L. and Pan, S. Q. (2007). *Agrobacterium* VirD2-binding protein is involved in tumorigenesis and redundantly encoded in conjugative transfer gene clusters. *Mol Plant Microbe In* **20**(10): 1201-1212.

Guralnick, B., Thomsen, G. and Citovsky, V. (1996). Transport of DNA into the nuclei of xenopus oocytes by a modified VirE2 protein of *Agrobacterium*. *Plant Cell* **8**(3): 363-373.

Gyorgy, H., Gyrogy, C., Das, S., Garcia-Perez, C., Saotome, M., Roy, S. S. and Yi, M. Q. (2006). Mitochondrial calcium signalling and cell death: Approaches for assessing the role of mitochondrial Ca2+ uptake in apoptosis. *Cell Calcium* **40**(5-6): 553-560.

Hamilton, R. H. and Fall, M. Z. (1971). The loss of tumor-initiating ability in *Agrobacterium tumefaciens* by incubation at high temperature. *Experientia* **27**(2): 229-230.

Henze, K. and Martin, W. (2003). Evolutionary biology: Essence of mitochondria. *Nature* **426**(6963): 127-128.

Hoang, T. T., Karkhoff-Schweizer, R. R., Kutchma, A. J. and Schweizer, H. P. (1998). A broad-host-range Flp-FRT recombination system for site-specific excision of chromosomally-located DNA sequences: application for isolation of unmarked *Pseudomonas aeruginosa* mutants. *Gene* **212**(1): 77-86.

Hoekema, A. (1983). A binary plant vector strategy based on separation of *vir*- and T-region of the *Agrobacterium tumefaciens* Ti-plasmid. *Nature* **303**: 179 - 180.

Hooykaas, P. J. J. and Beijersbergen, A. G. M. (1994). The virulence system of *Agrobacterium tumefaciens*. *Annu Rev Phytopathol* **32**: 157-179.

Horsch, R. B., Fraley, R. T., Rogers, S. G., Sanders, P. R., Lloyd, A. and Hoffmann, N. (1984). Inheritance of functional foreign genes in plants. *Science* **223**(4635): 496-498.

Howard, E. A., Zupan, J. R., Citovsky, V. and Zambryski, P. C. (1992). The VirD2 Protein of *A. tumefaciens* contains a C-terminal bipartite

nuclear localization signal: implications for nuclear uptake of DNA in plant cells. *Cell* **68**(1): 109-118.

Hunte, C., Palsdottir, H. and Trumpower, B. L. (2003). Protonmotive pathways and mechanisms in the cytochrome bc1 complex. *FEBS Lett* **545**(1): 39-46.

Ito, H., Fukuda, Y., Murata, K. and Kimura, A. (1983). Transformation of intact yeast cells treated with alkali cations. *J Bacteriol* **153**(1): 163-168.

Kado, C. I. (1994). Promiscuous DNA transfer system of *Agrobacterium tumefaciens*: role of the *virB* operon in sex pilus assembly and synthesis. *Mol Microbiol* **12**(1): 17-22.

Karaoglu, D., Kelleher, D. J. and Gilmore, R. (1995). Functional characterization of Ost3p : Loss of the 34-kd subunit of the *Saccharomyces cerevisiae* oligosaccharyltransferase results in biased underglycosylation of acceptor substrates. *J Cell Biol* **130**(3): 567-577.

Kerr, A. (1969). Transfer of virulence between isolates of *Agrobacterium*. *Nature* **223**(5211): 1175-&.

Klee, H. J., White, F. F., Iyer, V. N., Gordon, M. P. and Nester, E. W. (1983). Mutational analysis of the virulence region of an *Agrobacterium tumefaciens* Ti Plasmid. *J Bacteriol* **153**(2): 878-883.

Knauer, R. and Lehle, L. (1999). The oligosaccharyltransferase complex

from *Saccharomyces cerevisiae* : isolation of the *OST6* gene, its synthetic interaction with *OST3*, and analysis of the native complex. *J Biol Chem* **274**(24): 17249-17256.

Kroemer, G., Dallaporta, B. and Resche-Rigon, M. (1998). The mitochondrial death/life regulator in apoptosis and necrosis. *Annu Rev Physiol* **60**: 619-642.

Lacroix, B., Tzfira, T., Vainstein, A. and Citovsky, V. (2006). A case of promiscuity: *Agrobacterium*'s endless hunt for new partners. *Trends Genet* **22**(1): 29-37.

Lacroix, B., Vaidya, M., Tzfira, T. and Citovsky, V. (2005). The VirE3 protein of *Agrobacterium* mimics a host cell function required for plant genetic transformation. *EMBO J* **24**(2): 428-437.

Laemmli, U. K. (1970). Cleavage of structural proteins during assembly of head of Bacteriophage: T4. *Nature* **227**(5259): 680-&.

Lee, L. Y., Wu, F. H., Hsu, C. T., Shen, S. C., Yeh, H. Y., Liao, D. C., *et al.* (2012). Screening a cDNA Library for protein-protein interactions directly *in planta*. *Plant Cell* **24**(5): 1746-1759.

Lee, S. Y., Raha, S., Nagar, B. and Robinson, B. H. (2001). The functional role of conserved acidic residues of the Qcr7 protein of the cytochrome bc(1) complex in *Saccharomyces cerevisiae*. *Arch Biochem Biophys* **393**(2): 207-214.

Lin, J. J. (1994). Optimization of the transformation efficiency of *Agrobacterium tumefaciens* cells using electroporation. *Plant Sci* **101**(1): 11-15.

Lioret, C. (1956). Sur la mise en evidence d'un acide amine non identifie particulier aux tissus de 'crown-gall'. *Bull Soc Fr Physiol Veg* **2**: 76.

Lippincott, B. B., Whatley, M. H. and Lippincott, J. A. (1977). Tumor induction by agrobacterium involves attachment of the bacterium to a site on the host plant cell wall. *Plant Physiol* **59**(3): 388-390.

Liu, Y. K., Kong, X. P., Pan, J. W. and Li, D. Q. (2010). VIP1: linking *Agrobacterium*-mediated transformation to plant immunity? *Plant Cell Rep* **29**(8): 805-812.

Looke, M., Kristjuhan, K. and Kristjuhan, A. (2011). Extraction of genomic DNA from yeasts for PCR-based applications. *Biotechniques* **50**(5): 325-+.

Mao, J., Zhang, Y. C., Sang, Y., Li, Q. H. and Yang, H. Q. (2005). A role for *Arabidopsis* cryptochromes and COP1 in the regulation of stomatal opening. *Proc Natl Acad Sci U S A* **102**(34): 12270-12275.

McCullen, C. A. and Binns, A. N. (2006). *Agrobacterium tumefaciens* and plant cell interactions and activities required for interkingdom macromolecular transfer. *Annu Rev Cell Dev Bi* **22**: 101-127.

Mitchell, P. (1961). Chemiosmotic coupling in oxidative and photosynthetic phosphorylation. *Biochem J* **79**(3): P23-&.

Moore, L. W., Chilton, W. S. and Canfield, M. L. (1997). Diversity of opines and opine-catabolizing bacteria isolated from naturally occurring crown gall tumors. *Appl Environ Microbiol* **63**(1): 201-207.

Murray, R. K. and AccessMedicine (Online service) (2003). Harper's illustrated biochemistry. New York, NY, *Lange Medical Books ; McGraw-Hill***:** v.

Mysore, K. S., Nam, J. and Gelvin, S. B. (2000). An *Arabidopsis* histone H2A mutant is deficient in *Agrobacterium* T-DNA integration. *Proc Natl Acad Sci U S A* **97**(2): 948-953.

Nam, J., Matthysse, A. G. and Gelvin, S. B. (1997). Differences in susceptibility of *Arabidopsis* ecotypes to crown gall disease may result from a deficiency in T-DNA integration. *Plant Cell* **9**(3): 317-333.

Narasimhulu, S. B., Deng, X., Sarria, R. and Gelvin, S. B. (1996). Early transcription of *Agrobacterium* T-DNA genes in tobacco and maize. *Plant Cell* **8**(5): 873-886.

Neff, N. T. and Binns, A. N. (1985). *Agrobacterium tumefaciens* interaction with suspension cultured tomato cells. *Plant Physiol* **77**(1): 35-42.

Nester, E. W. and Verma, D. P. S. (1993). Advances in molecular

genetics of plant-microbe interactions : proceedings of the 6th International Symposium on Molecular Plant-Microbe Interactions, Seattle, Washington, U.S.A., July 1992. Dordrecht ; Boston, *: Kluwer Academic*.

Neupert, W. (1997). Protein import into mitochondria. *Annu Rev Biochem* **66**: 863-917.

Offringa, R., Degroot, M. J. A., Haagsman, H. J., Does, M. P., Vandenelzen, P. J. M. and Hooykaas, P. J. J. (1990). Extrachromosomal gomologous recombination and gene targeting in plant cells after *Agrobacterium* mediated transformation. *EMBO J* **9**(10): 3077-3084.

Ohta, A. and Nishiyama, Y. (2011). Mitochondria and viruses. *Mitochondrion* **11**(1): 1-12.

Palmer, A. G., Gao, R., Maresh, J., Erbil, W. K. and Lynn, D. G. (2004). Chemical biology of multi-host/pathogen interactions: chemical perception and metabolic complementation. *Annu Rev Phytopathol* **42**: 439-464.

Pansegrau, W., Schoumacher, F., Hohn, B. and Lanka, E. (1993). Site-specific cleavage and joining of single-stranded-DNA by VirD2 protein of *Agrobacterium tumefaciens* Ti plasmids: analogy to bacterial conjugation. *Proc Natl Acad Sci U S A* **90**(24): 11538-11542.

Pedelacq, J. D., Cabantous, S., Tran, T., Terwilliger, T. C. and Waldo, G. S. (2006). Engineering and characterization of a superfolder green

fluorescent protein. *Nat Biotechnol* **24**(1): 79-88.

Pelczar, P., Kalck, V., Gomez, D. and Hohn, B. (2004). *Agrobacterium* proteins VirD2 and VirE2 mediate precise integration of synthetic T-DNA complexes in mammalian cells. *Embo Rep* **5**(6): 632-637.

Pelicic, V., Reyrat, J. M. and Gicquel, B. (1996). Expression of the *Bacillus subtilis sacB* gene confers sucrose sensitivity on mycobacteria. *J Bacteriol* **178**(4): 1197-1199.

Piers, K. L., Heath, J. D., Liang, X. Y., Stephens, K. M. and Nester, E. W. (1996). *Agrobacterium tumefaciens*-mediated transformation of yeast. *Proc Natl Acad Sci U S A* **93**(4): 1613-1618.

Pitzschke, A. and Hirt, H. (2010). Mechanism of MAPK-targeted gene expression unraveled in plants. *Cell Cycle* **9**(1): 18-19.

Pruss, G. J., Nester, E. W. and Vance, V. (2008). Infiltration with *Agrobacterium tumefaciens* induces host defense and development-dependent responses in the infiltrated zone. *Mol Plant Microbe In* **21**(12): 1528-1538.

Rhee, Y., Gurel, F., Gafni, Y., Dingwall, C. and Citovsky, V. (2000). A genetic system for detection of protein nuclear import and export. *Nat Biotechnol* **18**(4): 433-437.

Rico, A., Bennett, M. H., Forcat, S., Huang, W. E. and Preston, G. M. (2010). Agroinfiltration reduces ABA levels and suppresses

Pseudomonas syringae-elicited salicylic acid production in *Nicotiana tabacum*. *Plos One* **5**(1).

Risseeuw, E., FrankevanDijk, M. E. I. and Hooykaas, P. J. J. (1996). Integration of an insertion-type transferred DNA vector from *Agrobacterium tumefaciens* into the *Saccharomyces cerevisiae* genome by gap repair. *Mol Cell Biol* **16**(10): 5924-5932.

Robinette, D. and Matthysse, A. G. (1990). Inhibition by *Agrobacterium tumefaciens* and *Pseudomonas savastanoi* of development of the hypersensitive response elicited by *Pseudomonas syringae* pv. phaseolicola. *J Bacteriol* **172**(10): 5742-5749.

Rossi, L., Hohn, B. and Tinland, B. (1993). The VirD2 protein of *Agrobacterium tumefaciens* carries nuclear localization signals important for transfer of T-DNA to plants. *Mol Gen Genet* **239**(3): 345-353.

Rossi, L., Hohn, B. and Tinland, B. (1996). Integration of complete transferred DNA units is dependent on the activity of virulence E2 protein of *Agrobacterium tumefaciens*. *Proc Natl Acad Sci U S A* **93**(1): 126-130.

Rudel, T., Kepp, O. and Kozjak-Pavlovic, V. (2010). Interactions between bacterial pathogens and mitochondrial cell death pathways. *Nat Rev Microbiol* **8**(10): 693-705.

Salman, H., Abu-Arish, A., Oliel, S., Loyter, A., Klafter, J., Granek, R.

and Elbaum, M. (2005). Nuclear localization signal peptides induce molecular delivery along microtubules. *Biophys J* **89**(3): 2134-2145.

Sauer, B. (1987). Functional expression of the Cre-Lox Site-specific recombination system in the yeast *Saccharomyces cerevisiae*. *Mol Cell Biol* **7**(6): 2087-2096.

Scheiffele, P., Pansegrau, W. and Lanka, E. (1995). Initiation of *Agrobacterium tumefaciens* T-DNA processing : Purified proteins VirD1 and VirD2 catalyze site-specific and strand-specific cleavage of superhelical T-Border DNA *in vitro*. *J Biol Chem* **270**(3): 1269-1276.

Schoppink, P. J., Berden, J. A. and Grivell, L. A. (1989). Inactivation of the gene encoding the 14-kDa subunit VII of yeast ubiquinol-cytochrome c oxidoreductase and analysis of the resulting mutant. *Eur J Biochem* **181**(2): 475-483.

Schrammeijer, B., den Dulk-Ras, A., Vergunst, A. C., Jacome, E. J. and Hooykaas, P. J. J. (2003). Analysis of Vir protein translocation from *Agrobacterium tumefaciens* using *Saccharomyces cerevisiae* as a model: evidence for transport of a novel effector protein VirE3. *Nucleic Acids Res* **31**(3): 860-868.

Schroder, G. and Lanka, E. (2005). The mating pair formation system of conjugative plasmids - A versatile secretion machinery for transfer of proteins and DNA. *Plasmid* **54**(1): 1-25.

Sciaky, D., Montoya, A. L. and Chilton, M. D. (1978). Fingerprints of

Agrobacterium Ti plasmids. *Plasmid* **1**(2): 238-253.

Shimoda, N., Toyodayamamoto, A., Nagamine, J., Usami, S., Katayama, M., Sakagami, Y. and Machida, Y. (1990). Control of expression of *Agrobacterium Vir* genes by synergistic actions of phenolic signal molecules and monosaccharides. *Proc Natl Acad Sci U S A* **87**(17): 6684-6688.

Simone, M., McCullen, C. A., Stahl, L. E. and Binns, A. N. (2001). The carboxy-terminus of VirE2 from *Agrobacterium tumefaciens* is required for its transport to host cells by the *virB*-encoded type IV transport system. *Mol Microbiol* **41**(6): 1283-1293.

Smith, E. F. and Townsend, C. O. (1907). A plant tumor of bacterial origin. *Science* **25**: 671-673.

Soltani, J. (2009). Host genes involved in *Agrobacterium* mediated transformation. *Leiden University.*

Soltani, J., van Heusden, G. P. and Hooykaas, P. J. (2009). Deletion of host histone acetyltransferases and deacetylases strongly affects *Agrobacterium*-mediated transformation of *Saccharomyces cerevisiae*. *Fems Microbiology Letters* **298**(2): 228-233.

Stachel, S. E., Messens, E., Vanmontagu, M. and Zambryski, P. (1985). Identification of the signal molecules produced by wounded plant cells that activate T-DNA transfer in *Agrobacterium tumefaciens*. *Nature* **318**(6047): 624-629.

Stachel, S. E. and Nester, E. W. (1986). The genetic and transcriptional organization of the *Vir* region of the A6-Ti plasmid of *Agrobacterium tumefaciens*. *EMBO J* **5**(7): 1445-1454.

Tao, Y., Rao, P. K., Bhattacharjee, S. and Gelvin, S. B. (2004). Expression of plant protein phosphatase 2C interferes with nuclear import of the *Agrobacterium* T-complex protein VirD2. *Proc Natl Acad Sci U S A* **101**(14): 5164-5169.

Tinland, B., Schoumacher, F., Gloeckler, V., Bravo-Angel, A. M. and Hohn, B. (1995). The *Agrobacterium tumefaciens* virulence D2 protein is responsible for precise integration of T-DNA into the plant genome. *EMBO J* **14**(14): 3585-3595.

Tu, H. (2010). A global profile of yeast genes involved in *Agrobacterium*-yeast gene transfer. *National University of Singapore.*

Tymms, M. J. and Kola, I. (2001). Gene knockout protocols. Totowa, NJ, *Humana Press*.

Tzfira, T. and Citovsky, V. (2001). Comparison between nuclear localization of nopaline- and octopine-specific *Agrobacterium* VirE2 proteins in plant, yeast and mammalian cells. *Mol Plant Pathol* **2**(3): 171-176.

Tzfira, T., Rhee, Y., Chen, M. H., Kunik, T. and Citovsky, V. (2000). Nucleic acid transport in plant-microbe interactions: the molecules that

walk through the walls. *Annu Rev Microbiol* **54**: 187-219.

Tzfira, T., Vaidya, M. and Citovsky, V. (2001). VIP1, an *Arabidopsis* protein that interacts with *Agrobacterium* VirE2, is involved in VirE2 nuclear import and *Agrobacterium* infectivity. *EMBO J* **20**(13): 3596-3607.

Tzfira, T., Vaidya, M. and Citovsky, V. (2002). Increasing plant susceptibility to *Agrobacterium* infection by overexpression of the *Arabidopsis* nuclear protein VIP1. *Proc Natl Acad Sci U S A* **99**(16): 10435-10440.

Tzfira, T., Vaidya, M. and Citovsky, V. (2004). Involvement of targeted proteolysis in plant genetic transformation by *Agrobacterium*. *Nature* **431**(7004): 87-92.

van Attikum, H., Bundock, P. and Hooykaas, P. J. J. (2001). Non-homologous end-joining proteins are required for *Agrobacterium* T-DNA integration. *EMBO J* **20**(22): 6550-6558.

van Attikum, H. and Hooykaas, P. J. (2003). Genetic requirements for the targeted integration of *Agrobacterium* T-DNA in *Saccharomyces cerevisiae*. *Nucleic Acids Res* **31**(3): 826-832.

Vanlareb.N, Engler, G., Holsters, M., Vandenel.S, Zaenen, I., Schilper.Ra and Schell, J. (1974). Large plasmid in *Agrobacterium tumefaciens* essential for crown gall-inducing ability. *Nature* **252**(5479): 169-170.

Vergunst, A. C., Schrammeijer, B., den Dulk-Ras, A., de Vlaam, C. M., Regensburg-Tuink, T. J. and Hooykaas, P. J. (2000). VirB/D4-dependent protein translocation from *Agrobacterium* into plant cells. *Science* **290**(5493): 979-982.

Vergunst, A. C., van Lier, M. C., den Dulk-Ras, A. and Hooykaas, P. J. (2003). Recognition of the *Agrobacterium tumefaciens* VirE2 translocation signal by the VirB/D4 transport system does not require VirE1. *Plant Physiol* **133**(3): 978-988.

Vergunst, A. C., van Lier, M. C. M., den Dulk-Ras, A., Stuve, T. A. G., Ouwehand, A. and Hooykaas, P. J. J. (2005). Positive charge is an important feature of the C-terminal transport signal of the VirB/D4-translocated proteins of *Agrobacterium*. *Proc Natl Acad Sci U S A* **102**(3): 832-837.

Voet, D., Voet, J. G. and Pratt, C. W. (2006). Fundamentals of biochemistry : life at the molecular level. Hoboken, N.J., *Wiley*.

Waldo, G. S., Standish, B. M., Berendzen, J. and Terwilliger, T. C. (1999). Rapid protein-folding assay using green fluorescent protein. *Nat Biotechnol* **17**(7): 691-695.

Ward, D. V. and Zambryski, P. C. (2001). The six functions of *Agrobacterium* VirE2. *Proc Natl Acad Sci U S A* **98**(2): 385-386.

Wilson, T. E. (2002). A genomics-based screen for yeast mutants with an altered recombination/end joining repair ratio. *Genetics* **162**(2):

677-688.

Winans, S. C., Kerstetter, R. A. and Nester, E. W. (1988). Transcriptional regulation of the *virA* gene and *virG* gene of *Agrobacterium tumefaciens*. *J Bacteriol* **170**(9): 4047-4054.

Wolanin, P. M., Thomason, P. A. and Stock, J. B. (2002). Histidine protein kinases: key signal transducers outside the animal kingdom. *Genome Biol* **3**(10).

Xiang, C. B., Han, P., Lutziger, I., Wang, K. and Oliver, D. J. (1999). A mini binary vector series for plant transformation. *Plant Mol Biol* **40**(4): 711-717.

Yi, Z. L., Cao, S. Y., Wang, L., Chu, C. C., Li, X., He, S. J., *et al.* (2001). Improvement of transformation frequency of rice mediated by *Agrobacterium*. *Yi Chuan Xue Bao* **28**(4): 352-358.

Zaenen, I., Vanlareb.N, Teuchy, H., Vanmonta.M and Schell, J. (1974). Supercoiled circular DNA in crown-gall inducing *Agrobacterium* strains. *J Mol Biol* **86**(1): 109-&.

Zaltsman, A., Krichevsky, A., Kozlovsky, S. V., Yasmin, F. and Citovsky, V. (2010). Plant defense pathways subverted by *Agrobacterium* for genetic transformation. *Plant Signal Behav* **5**(10).

Zambryski, P., Joos, H., Genetello, C., Leemans, J., Montagu, M. V. and Schell, J. (1983). Ti plasmid vector for the introduction of DNA into

plant cells without alteration of their normal regeneration capacity. *EMBO J* **2**(12): 2143-2150.

Zhao, F. X., Chen, L. H., Perl, A. H., Chen, S. W. and Ma, H. Q. (2011). Proteomic changes in grape embryogenic callus in response to *Agrobacterium tumefaciens*-mediated transformation. *Plant Sci* **181**(4): 485-495.

Zhou, X. R. and Christie, P. J. (1999). Mutagenesis of the *Agrobacterium* VirE2 single-stranded DNA-binding protein identifies regions required for self-association and interaction with VirE1 and a permissive site for hybrid protein construction. *J Bacteriol* **181**(14): 4342-4352.

Zhu, Y. M., Nam, J., Humara, J. M., Mysore, K. S., Lee, L. Y., Cao, H. B., *et al.* (2003). Identification of *Arabidopsis* rat mutants. *Plant Physiol* **132**(2): 494-505.

Ziemienowicz, A., Merkle, T., Schoumacher, F., Hohn, B. and Rossi, L. (2001). Import of *Agrobacterium* T-DNA into plant nuclei: Two distinct functions of VirD2 and VirE2 proteins. *Plant Cell* **13**(2): 369-383.

Zupan, J. R., Citovsky, V. and Zambryski, P. (1996). *Agrobacterium* VirE2 protein mediates nuclear uptake of single-stranded DNA in plant cells. *Proc Natl Acad Sci U S A* **93**(6): 2392-2397.